NPS-MR-98-001

NAVAL POSTGRADUATE SCHOOL
Monterey, California

Southern Hemisphere Application of the Systematic Approach to Tropical Cyclone Track Forecasting. Part I: Environmental Structure Characteristics

by

Anthony J. Bannister
Mark A. Boothe
Lester E. Carr, III
Russell L. Elsberry

December 1997

Prepared for: Space and Naval Warfare Systems Command
PMW 185 San Diego, CA 92110-3127

Naval Postgraduate School
Monterey, California 93943-5000

Rear Admiral M. J. Evans
Superintendent

Richard Elster
Provost

This report was prepared for the Space and Naval Warfare Command (PMW 185) under Program Element 0604 207N entitled: "Systematic Approach Tropical Cyclone Forecast Techniques." The technique is intended for application at the Joint Typhoon Warning Center (JTWC) at the Naval Pacific Meteorology and Oceanography Center (NPMOC) West, Guam and for the Alternate JTWC at NPMOC, Pearl Harbor, Hawaii.

This report was prepared by:

Anthony J. Bannister
Bureau of Meteorology
Perth, Australia

Mark A. Boothe
Meteorologist

Lester E. Carr, III
Assistant Professor of Meteorology

Russell L. Elsberry
Professor of Meteorology

Reviewed by:

Carlyle H. Wash, Chairman
Department of Meteorology

Released by:

David W. Netzer
Dean of Research

REPORT DOCUMENTATION PAGE

Form Approved
OMB No. 0704-0188

1. AGENCY USE ONLY (Leave blank)	2. REPORT DATE	3. REPORT TYPE AND DATES COVERED
	December 1997	Interim 12/97 - 11/98

4. TITLE AND SUBTITLE
Southern Hemisphere Application of the Systematic Approach to Tropical Cyclone Track Forecasting. Part I: Environmental Structure Characteristics

5. FUNDING NUMBERS
N0003998WRDF132

6. AUTHOR(S)
Anthony J. Bannister, Mark A. Boothe, Lester E. Carr, III, and Russell L. Elsberry

7. PERFORMING ORGANIZATION NAME(S) AND ADDRESS(ES)
Naval Postgraduate School
Department of Meteorology
589 Dyer Rd., Room 254
Monterey, CA 93943-5114

8. PERFORMING ORGANIZATION REPORT NUMBER

9. SPONSORING/MONITORING AGENCY NAME(S) AND ADDRESS(ES)
Space and Naval Warfare Systems Command
PMW 185 San Diego, CA 92110-3127

10. SPONSORING/MONITORING AGENCY REPORT NUMBER

11. SUPPLEMENTARY NOTES
The views expressed in this report are those of the author and do not reflect the official policy or position of the Department of Defense.

12a. DISTRIBUTION/AVAILABILITY STATEMENT
Approved for Public Release; Distribution Unlimited

12b. DISTRIBUTION CODE

13. ABSTRACT (Maximum 200 words)
The environment structure conceptual models of the Systematic Approach to Tropical Cyclone Track Forecasting technique of Carr and Elsberry are applied to all Southern Hemisphere tropical cyclones during January 1994 - June 1997. Whereas three of the four synoptic patterns from the western North Pacific could be applied with relatively small modifications, a new High (H) amplitude synoptic pattern was defined to classify the situations with large meridional penetrations of midlatitude troughs deep into the Southern Hemisphere tropics. Some changes in terminology were required to describe the synoptic regions that have characteristic track directions. All 1592 cases during the period could be described by these four synoptic patterns and 11 synoptic regions. Important track changes were found to be associated with transitions between these synoptic patterns and regions. Three binary tropical cyclone interactions defined for the Western North Pacific were adapted for use in the Southern Hemisphere with considerable success. A preliminary climatology of occurrences for the synoptic pattern/region combinations, transitions between combinations, and binary tropical cyclone interactions are calculated. Sequences of synoptic analyses related to these transitions are described to aid in the application.

14. SUBJECT TERMS
Tropical cyclone track forecasting
Tropical cyclone motion

15. NUMBER OF PAGES
96

16. PRICE CODE

17. SECURITY CLASSIFICATION OF REPORT	18. SECURITY CLASSIFICATION OF THIS PAGE	19. SECURITY CLASSIFICATION OF ABSTRACT	20. LIMITATION OF ABSTRACT
Unclassified	Unclassified	Unclassified	

TABLE OF CONTENTS

		Page
Report Documentation Page		i
Table of Contents		ii
Acknowledgements		iv
List of Figures		v
1.	Introduction	1
	a. Systematic approach framework	1
	b. Australian experience	3
	c. Objectives	3
2.	Approach	5
	a. Synoptic analyses	5
	b. TC positions and tracks	7
	c. Satelllite imagery	7
	d. Domain	7
	e. Tropical cyclone interactions	9
3.	Environment Structure Characterizations	12
	a. Standard synoptic pattern	12
	1. Conceptual model	12
	2. Analysis examples	14
	3. Tracks	16
	b. Poleward synoptic pattern	19
	1. Conceptual model	19
	2. Analysis examples	21
	3. Tracks	24
	c. High-amplitude synoptic pattern	27
	1. Conceptual model	27
	2. Analysis examples	29
	3. Tracks	35
	d. Multiple synoptic pattern	38
	1. Conceptual model	38
	2. Analysis examples	40
	3. Tracks	40
4.	Environment Structure Summary	42
5.	Tropical Cyclone Interactions	45
	a. Frequency	45
	b. ITIE illustrations	46
6.	Environment Structure Transitions	57
	a. Frequency	57
	b. Transitions within the S Pattern	60
	1. TC Beti (2396) case	60

2. TC Daryl/Agnielle (0196) case 63
c. Transitions to/from P Pattern 67
1. TC Ivy (1694) case 67
2. TC Drena (1697) case 68
3. TC Lisette (3097) case 72
4. TC Sharon (2294) case 73
d. Transition to/from the H Pattern 79
1. TCs Elvina (0996), Nicholas (1096), and Ophelia (1196) case 79
2. TC Kelli (3897) case 83
7. Conclusions 86
8. Future Work 88

References 89

Appendix 91

ACKNOWLEDGMENTS

This research has been sponsored by the Space and Naval Warfare Systems Command. The original concept of the Systematic Approach to Tropical Cyclone Track Forecasting was developed over several years with funding from the Office of Naval Research Marine Meteorology Program under the management of Robert F. Abbey, Jr. This Southern Hemisphere application of the Systematic Approach was initiated as a result of discussions with the Bureau of Meteorology, Australia. A three-month visit by Tony Bannister of the Perth, Western Australia office was arranged, with travel assistance from the Office of Naval Research Grant No. N-00014-94-I-0556 via Greg Holland in the Bureau of Meteorology Research Centre, Melbourne. Best-track tropical cyclone records were provided by the Joint Typhoon Warning Center, Guam. NOGAPS analyses were provided by the Fleet Numerical Meteorology and Oceanography Center. Mrs. Penny Jones expertly typed the manuscript.

List of Figures

page

Fig. 1. Summary of the meteorological knowledge basis of the Systematic Approach adapted for Southern Hemisphere tropical cyclones. 2
Fig. 2. (a) NOGAPS 500-mb wind analysis at 12 UTC 10 February 1997 and (b) corresponding Darwin wind analysis at 16 UTC 10 February. 6
Fig. 3. Comparison of JTWC track for Pancho/Helinda and the corresponding BM track (dashed) beginning 12 UTC 19 January. 8
Fig. 4. Summary of TC tracks from JTWC during January 1994 - June 1997. 8
Fig. 5. Schematics of three modes of TC interaction by Carr *et al.* (1997a) adapted for the Southern Hemisphere. 10
Fig. 6. Conceptual model of Standard (S) synoptic pattern for the Southern Hemisphere. 13
Fig. 7. NOGAPS 500-mb streamlines at (a) 12 UTC 8 March 1996, (b) 00 UTC 10 December 1995, and (c) 12 UTC 3 January 1997. 15
Fig. 8. Tracks while TC was in the Standard (S) pattern. 17
Fig. 9. Conceptual model for Poleward (P) synoptic pattern. 20
Fig. 10. NOGAPS 500-mb analyses at (a) 12 UTC 15 March 1997, (b) 00 UTC 6 January 1996, and (c) 12 UTC 24 February 1997. 22
Fig. 11. Satellite infrared imagery at 03 UTC 3 January 1996 and at 03 UTC 4 January. 25
Fig. 12. Tracks while the TCs are in the Poleward/Poleward-Oriented (P/PO) synoptic pattern/region. 26
Fig. 13. Conceptual model for the High-amplitude (H) synoptic pattern. 28
Fig. 14. NOGAPS 500-mb analyses for (a) 00 UTC 3 May 1996, and (b) 00 UTC 14 March 1996. 30
Fig. 15. NOGAPS 500-mb analysis for 00 UTC 24 February 1996. 32
Fig. 16. NOGAPS 500-mb analyses for (a) 00 UTC 15 December 1994, and (b) 00 UTC 16 May 1997. 33
Fig. 17. NOGAPS 500-mb analyses for (a) 12 UTC 16 February 1996, and (b) 00 UTC 18 December 1996. 34
Fig. 18. Tracks while in the High-amplitude (H) pattern. 36
Fig. 19. Conceptual model for the Multiple (M) TC synoptic pattern. 39
Fig. 20. NOGAPS 500-mb analysis for 00 UTC 7 January 1994. 39
Fig. 21. Tracks while the TCs are in the (a) M/Equatorward Flow (EF) and (b) M/Poleward Flow (PF) pattern/regions. 41
Fig. 22. Summary of the four synoptic patterns and associated synoptic regions for the Systematic Approach knowledge base in the Southern Hemisphere. 43
Fig. 23. Climatology (percent) of (a) synoptic patterns and (b) synoptic region in the SH environment structure for 1571 cases during January 1994-June 1997. 44
Fig. 24. Locations at which ITIE events were first detected during January 1994-June 1997. 47
Fig. 25. Tracks of TC 2094 (Litanne) and 2194 (Mariola) during 12 UTC 13 March to 12 UTC 17 March. 47
Fig. 26. NOGAPS 500-mb analyses at 12 UTC on (a) 14, (b) 15, (c) 16, and (d) 17 March 1994. The western (eastern) TC is Litanne (Mariola). 48
Fig. 27. Tracks of TCs 2197 (Iletta) and 1997 (Pancho/Helinda). 49

page

Fig. 28. NOGAPS 500-mb analyses at 00 UTC on (a) 26, (b) 27, (c) 28, and (d) 29 January 1997. 50
Fig. 29. Tracks of TCs 1297 (Phil) and 1597 (Rachel). 53
Fig. 30. NOGAPS 500-mb analyses at 12 UTC on (a) 30 and (b) 31 December 1996, and (c) 1, and (d) 2 January 1997. 54
Fig. 31. NOGAPS 500-mb analyses at 12 UTC on (a) 3 and (b) 4 January 1997. 55
Fig. 32. Tracks of TCs Ivy (eastern) and Hollanda (western). 55
Fig. 33. NOGAPS 500-mb analyses for 00 UTC on (a) 10, (b) 11, (c) 12, and (d) 13 February 1994. 56
Fig. 34. Environment structure transition occurrences for the 110 TCs in the SH during January 1994 to June 1997. 58
Fig. 35. Recurring environment structure transitions for (a) 37 TCs in the South Pacific Ocean separately from the (b) 77 TCs in the South Indian Ocean. 59
Fig. 36. Track of TC Beti. 61
Fig. 37. NOGAPS 500-mb analyses for 12 UTC on (a) 24, (b) 25, (c) 26, and (d) 27 March 1996. 62
Fig. 38. Track of TC Daryl/Agnielle. 64
Fig. 39. NOGAPS 500-mb analyses at 12 UTC for (a) 17, (b) 18, (c) 19, and (d) 20 November 1995. 65
Fig. 40. NOGAPS 500-mb analyses at 12 UTC for (a) 21, (b) 22, (c) 23, and (d) 24 November 1995. 66
Fig. 41. Track of TC Ivy. 68
Fig. 42. NOGAPS 500-mb analysis at 00 UTC on (a) 13, (b) 14, (c) 15, and (d) 16 February 1994. 69
Fig. 43. Track of TC Drena. 70
Fig. 44. NOGAPS 500-mb analysis at 00 UTC on (a) 3, (b) 4, (c) 5, and (d) 6 January 1997. 71
Fig. 45. Track of TC Lisette. 73
Fig. 46. NOGAPS 500-mb analyses at 00 UTC on (a) 27, (b) 28 February, and (c) 1, and (d) 2 March 1997. 74
Fig. 47. Track of TC Sharon. 75
Fig. 48. NOGAPS 500-mb analyses at 00 UTC on (a) 15, (b) 16, (c) 17, and (d) 18 March 1994. 77
Fig. 49. NOGAPS analyses at 850 mb and at 00 UTC on (a) 16 and (b) 18 March 1994. 78
Fig. 50. Infrared imagery of TC Sharon at 0300 UTC on (a) 17 and (b) 19 March 1994. 78
Fig. 51. Tracks of (a) TC Elvina and (b) TC Nicholas (eastern) and Ophelia (western). 80
Fig. 52. NOGAPS 500-mb analysisat 12 UTC on (a) 11, (b) 12, (c) 13, and (d) 14 December 1996. 81
Fig. 53. NOGAPS 500-mb analyses at 12 UTC on (a) 15 and (b) 16 December 1996. 82
Fig. 54. Track of TC Kelli. 84
Fig. 55. NOGAPS 500-mb analyses at (a) 12 UTC 8 June, (b) 00 UTC 10 June, (c) 12 UTC 11 June, and (d) 00 UTC 13 June 1997. 85

1. INTRODUCTION

a. *Systematic Approach framework*

The basic concepts of a Systematic and Integrated Approach to Tropical Cyclone (TC) Track Forecasting (hereafter the Systematic Approach) were introduced by Carr and Elsberry (1994) for the western North Pacific region. The central thesis of the Systematic Approach is that the forecaster can be equipped to formulate track forecasts that improve on the accuracy and/or consistency of the dynamical or other objective guidance if he/she is provided: (i) a meteorological knowledge base of dynamically sound conceptual models that classify various TC-environment situations; (*ii*) a knowledge base of recurring TC track forecast errors attributed to various combinations of TC structure and environment structure, and the anticipated changes; and (*iii*) an implementing methodology or strategy for applying these two knowledge bases to particular TC forecast situations.

The basic components of the meteorological knowledge base in the Systematic Approach is given in Fig. 1. Environment structure is defined in terms of synoptic patterns and synoptic regions. Synoptic patterns are classifications of the large-scale environment based on the existence and orientation of circulations such as cyclones and anticyclones. Synoptic regions are smaller regions within the synoptic patterns where certain characteristic directions of environmental steering of the TC may be expected. The TC structure is described in terms of traditional intensity categories and distinguishing between midget, small, average, and large sizes. The motivation for the size grouping, and a proposed strategy for determining operationally the size, is given by Carr and Elsberry (1997a).

A key element of the Systematic Approach is to recognize transitional mechanisms, and especially the TC-environment transformations (lower right portion of Fig. 1), that will lead to a transition in the environment structure. Because each such synoptic pattern/region transition is associated with a TC track change, it is important that the forecaster be equipped to recognize that a transition is (or will be) occurring. Equipping forecasters to recognize these changes in environment structure is a major goal of the Systematic Approach.

Carr *et al.* (1995) prepared a climatology of 12-h TC and environment structure characterizations for all TCs in the western North Pacific during 1989-1993, and this led to a refinement of the Systematic Approach. This climatology has subsequently been extended through the 1996 TC season for the western North Pacific. A similar climatology of the environment structure has been prepared in the eastern and central North Pacific (White 1995, Boothe 1997, Boothe *et al.* 1997). A preliminary climatology was also prepared for the Atlantic (Kent 1995). Although the synoptic patterns and synoptic regions that make up the environment structure vary slightly in the TC basins examined thus far, the important conclusion is that all TC scenarios have been able to be classified with only a small set of conceptual models. Furthermore, the basic Systematic Approach concepts of associating characteristic TC tracks with specific synoptic environment circulations, and identifying TC structure characteristics that may lead to an

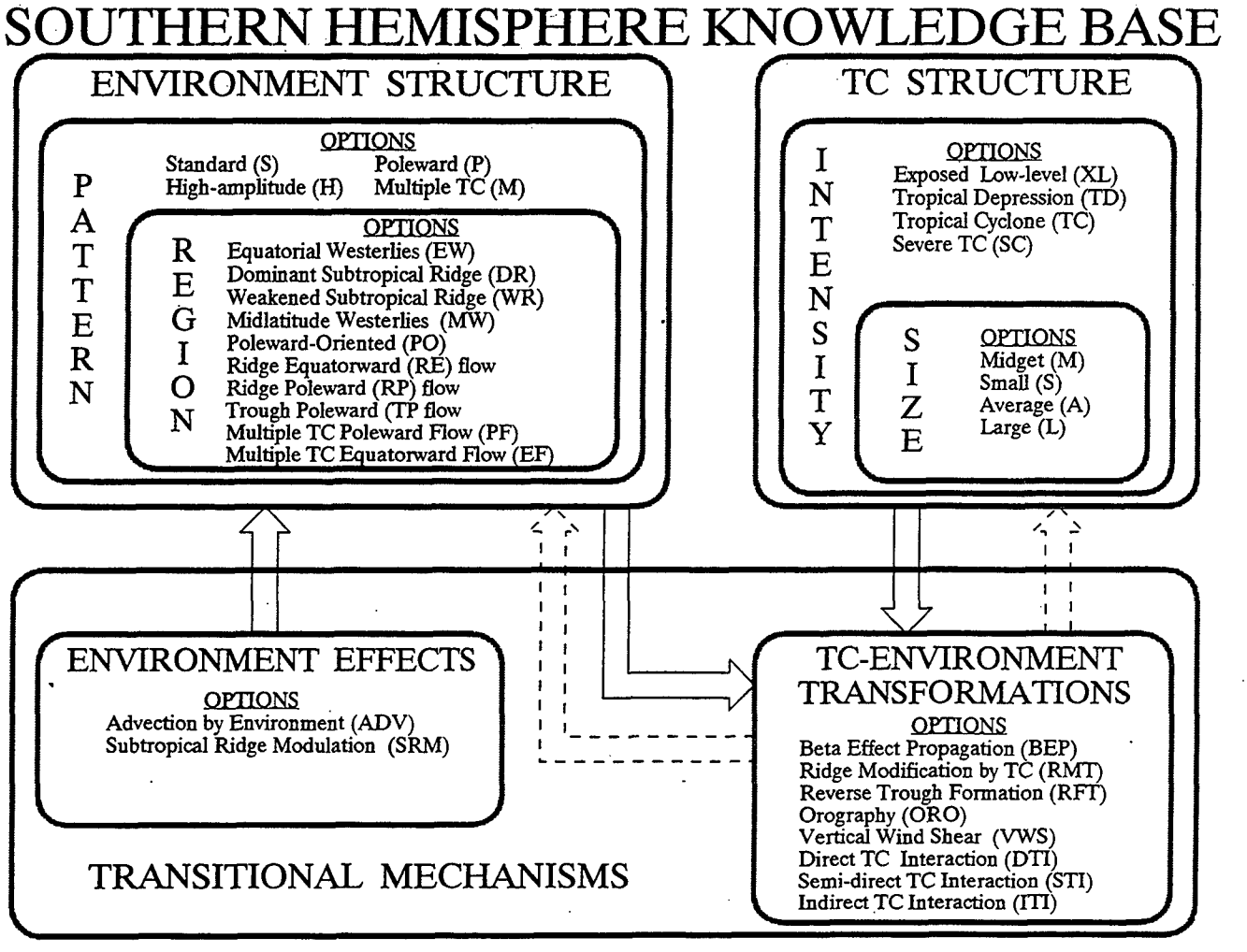

Figure 1. Summary of the meteorological knowledge basis of the Systematic Approach adapted for Southern Hemisphere tropical cyclones. See text for definitions and descriptions of these components.

environment structure change, have been demonstrated to be valid. Making allowance that the specific transformation mechanisms do vary among the TC basins examined thus far, a (retrospective) explanation for all significant track changes has been possible in terms of only a small set of transitional mechanisms.

The Joint Typhoon Warning Center (JTWC), Guam, forecasters have utilized the environment structure aspect of the Systematic Approach for several seasons. The second knowledge base of recurring track forecast errors continues to be developed for western North Pacific TCs, and preliminary versions have been introduced to JTWC forecasters. The third aspect of an implementing methodology is still in development.

b. *Australian experience*

As several Australian forecasters became aware of the Systematic Approach conceptual models, it became evident that similar ideas had been developed for TCs in the region of Australia. For example, Alan Sharp and Barry Hanstrum of the Bureau of Meteorology in Perth, Western Australia, had distinguished recurving from straight-moving TCs based on the adjacent synoptic flow represented by local rawinsondes along the Northwest Australian coast. The location of the box relative to these TCs falls in a key region of the Systematic Approach conceptual model of a transformation from a straight-moving to a recurving track. A similar forecast technique by Jeff Callaghan in the Brisbane, Queensland, office associates the movement of TCs with synoptic observations along the east coast of Australia. Again, a consistent relationship was noted between one of the Systematic Approach conceptual synoptic models and the key location of observations used in this forecast rule.

Based on these apparent consistencies between Australian forecaster practice and experience with ideas being incorporated in the Systematic Approach, an exchange visit of a Bureau of Meteorology forecaster (T. Bannister) was arranged.

c. *Objectives*

The primary objective of this study was to examine the possible adaptation of the Systematic Approach meteorological knowledge base to Southern Hemisphere (SH) TCs. Just as in the extensions of the original Systematic Approach from the western North Pacific to other NH basins, it was expected that some modifications would be necessary. However, the apparent consistency with some Australian forecast rules was an indicator of likely success.

The specific objectives were to: (*i*) Examine a large number of SH cases to determine whether conceptual synoptic models from the Northern Hemisphere (NH) Systematic Approach could be applied; (*ii*) Develop new synoptic models of the TC-environment structure as needed; (*iii*) Determine if the conceptual models of transitional mechanisms leading to synoptic pattern/region transitions for NH storms could be applied; and (*iv*) Develop a short-term climatology of environment structure characterizations and transitions. The goal is that each TC track may be described in terms of a small set of easily recognized synoptic patterns and regions,

as in the other TC basins for which the Systematic Approach has been applied.

2. APPROACH

a. *Synoptic analyses*

The Systematic Approach environment structure conceptual models have been developed based on the U. S. Navy Operational Global Atmospheric Prediction System (NOGAPS) analyses from the Fleet Numerical Meteorology and Oceanography Center (FNMOC), Monterey, California. Beginning in June 1990, synthetic observations have been included in the NOGAPS analyses to improve the TC location and structure representation. These synthetic observations for SH TCs have been based on the JTWC warning messages. Since October 1994, the synthetic observations have included an adjustment to make the average flow in the region of the TC agree with the recent 12-h motion of the storm as contained in the JTWC warnings. The synthetic observations, any rawinsondes or other observations, and a 6-h NOGAPS forecast are blended in the data assimilation system to provide the initial conditions for the global model forecast. Although the 500-mb analyses are typically used to characterize the synoptic pattern/region that determines the steering flow, analyses at 700 mb or lower may be used when the TC is weak or vertical wind shear has affected the upper-tropospheric structure. An archive of NOGAPS analyses and forecasts each 12 h is maintained at the Naval Postgraduate School.

Another source of synoptic analyses in the Australian region (generally 70°E to 180°E) is available from the Bureau of Meteorology (BM). The Darwin BM office Tropical Area Wind Analyses were available in digital form for the 1995-96 and 1996-97 seasons. These analyses also include synthetic TC observations whenever the TC is above 33 kt based on warnings from any of the three BM forecast offices. Hand-drawn analyses at 500 and 700 mb from the Darwin BM office were available for 1983-85.

The NOGAPS and Darwin 500 mb wind analyses were compared for a limited set of four cyclones. As indicated in Fig. 2, the circulation features such as adjacent troughs and ridge lines were typically similar in both analyses. Slight differences were noted near TCs if one analysis included synthetic observations and the other did not. For example, JTWC may report a Tropical Storm (TS) of 34 kt (based on 1-minute average winds) and thus trigger a full set of synthetic observations in the NOGAPS analysis, while the BM may not make a TS designation based on 10-minute average winds. Other differences in the two analyses were noted for weak synoptic systems and for precise positions of cols between circulation systems.

The conclusion is thus that either the NOGAPS or the BM analyses would be suitable for determining the synoptic patterns and regions in the Systematic Approach. Although the Australian forecasters have real-time access to the Australia, UK Meteorological Office, and European Center for Medium-range Weather Forecasats (ECMWF) global model analyses, these analyses were not available for this study. Only the UKMO model includes synthetic TC observations, so the applicability of the Systematic Approach with the other analyses may be more uncertain.

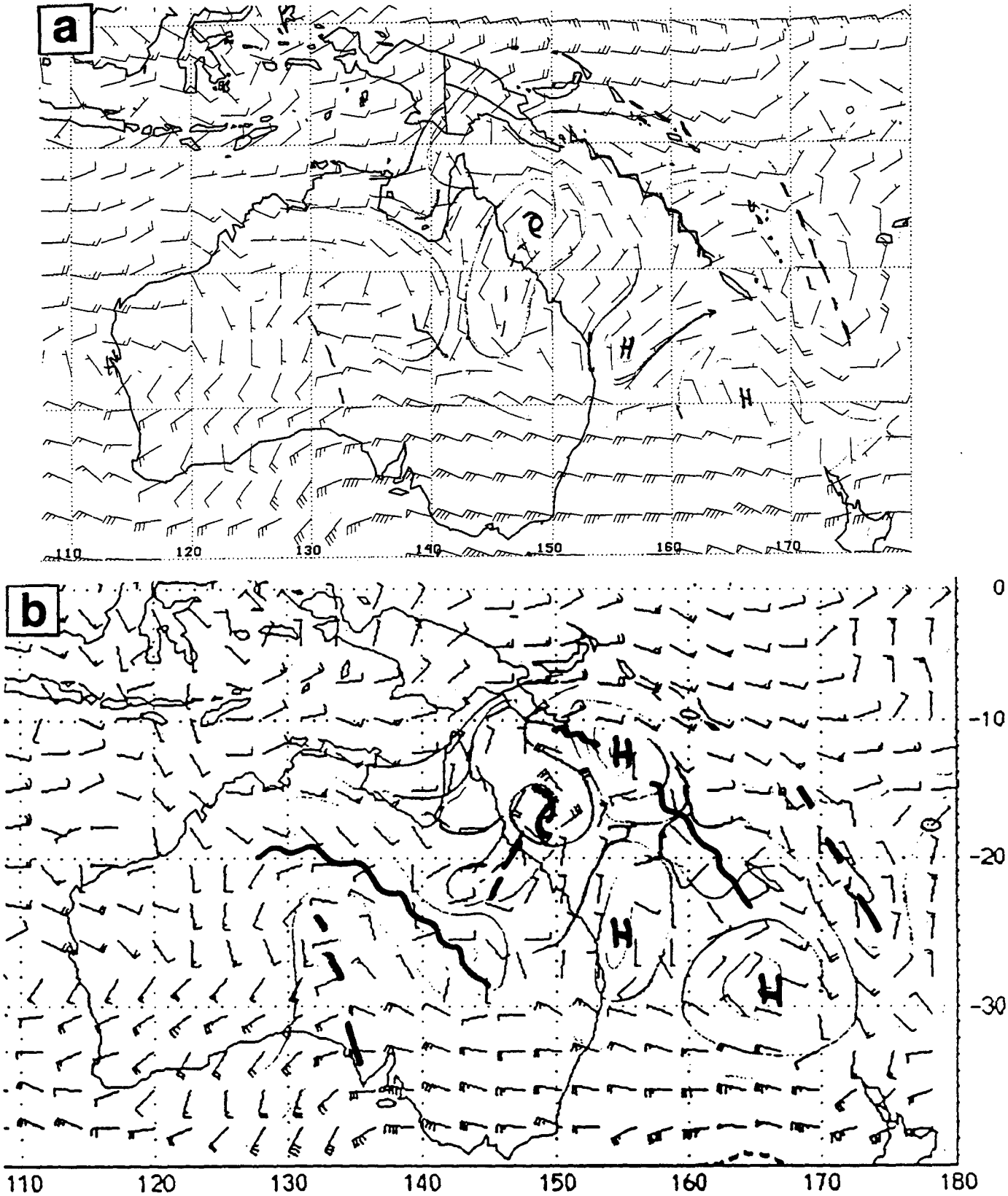

Figure 2. (a) NOGAPS 500-mb wind analysis at 12 UTC 10 February 1997 and (b) corresponding Darwin wind analysis at 16 UTC 10 February. Long (short) wind barb indicates 10 (5) kt or 5 (2.5) m s^{-1}.

b. *TC positions and tracks*

Intercomparisons of TC positions from various warning centers often reveal differences of about 25 n mi (40 km). Thus, the JTWC best-track (post-storm analysis) positions and the corresponding Australian best tracks were compared for all cyclones during the 1989-90 through 1996-97 seasons. Only one Australian cyclone was not included in the JTWC data base, and neither the BM nor the Fiji center named one TS to the east of Australia for which JTWC issued warnings. However, seven cyclones in the Australian region and six cyclones in the Fiji region during January 1994 -- June 1997 had only a Guam designator, which indicates Guam picks up more tropical depressions. In general, the JTWC data records for each TC are expected to be longer based on the 1-minute average winds versus the 10-minute average used in Australia. As shown in Fig. 3, the JTWC and BM sets of best tracks are very similar when the TC is at the TS stage or stronger. Differences are noted for weaker systems, as it is often difficult to establish a circulation center for tropical depressions.

The conclusion is that either the JTWC or the BM best tracks may be used in examining the applicability of the Systematic Approach for Australian region TCs. Some of the small-scale variability in the tracks is smoothed by a 12-h centered difference calculation of the storm motion over $\pm$ 6 h.

c. *Satellite imagery*

Monthly catalogues of Geostationary Meteorological Satellite (GMS) full disk visible and infrared imagery were available once a day at 03 UTC. After October 1995, a GMS water vapor image was also included in the catalogues. While these images are rather small, they are useful for noting the size and organization of the TC and the adjacent cloud systems. Unfortunately, some of the central Indian Ocean TCs are often on the edge of the GMS image and thus are not well resolved. No Meteosat (geostationary) imagery was available for the Indian Ocean TCs.

d. *Domain*

Choice of the domain for this study is complicated by a number of different constituency interests. The BM has separate offices in Perth, Western Australia; Darwin, Northern Territory, and Brisbane, Queensland, to forecast TCs in the adjacent regions. The JTWC just distinguishes between the South Pacific and the South Indian Ocean, with a dividing line of 135°E. Thus, JTWC has forecast responsibilities to the west of the forecast domain of Perth, and to the east of the Brisbane forecast domain.

No scientific basis exists for distinguishing between TCs in the western and eastern South Indian Ocean, or throughout the western South Pacific region. Similar tracks (Fig. 4) are found throughout the South Indian Ocean, and in the western South Pacific. *As it is expected that similar environment structures will be found throughout the South Pacific Ocean, all TCs west of Cape York (142°E) will be examined in this study and referred to as the South Pacific (SP).*

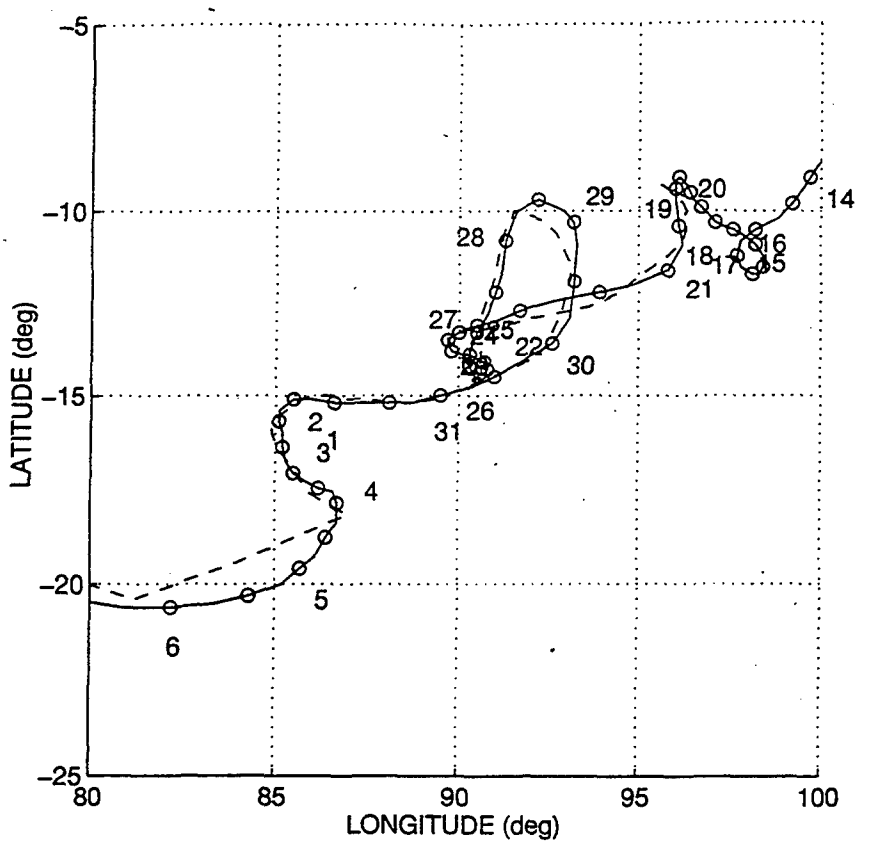

Figure 3. Comparison of JTWC track (solid, with circles indicating 12-h positions) for Pancho/Helinda from 00 UTC 14 January through 00 UTC 6 February 1997 and the corresponding BM track (dashed) beginning 12 UTC 19 January.

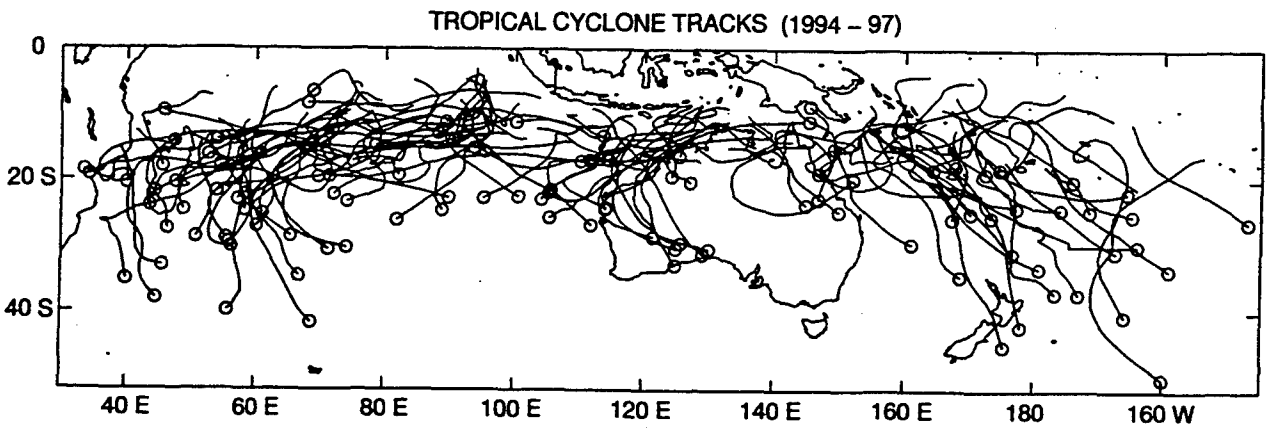

Figure 4. Summary of TC tracks from JTWC during January 1994 -- June 1997. The ending position is indicated with a circle.

Similarly, all TCs in the South Indian Ocean including the Gulf of Carpentaria, Arafura or Timor Seas, will be examined and referred to as the Indian Ocean (IO). Recall that no satellite imagery is available in the area west of about 70°E, which is a limitation for this study. Some special cases in the Darwin, Northern Territory, area of responsibility will also be highlighted.

The decision to examine all SH tropical cyclones dictated that the NOGAPS analyses and the JTWC best tracks be utilized rather than the longitudinally limited BM analyses and Australian best tracks. A longer record of TCs is also available from the NOGAPS archive. The TC positions at +12, 00, -12, -24, and -36 h are plotted on the NOGAPS analyses to indicate the track orientation relative to the synoptic circulations.

e. *Tropical cyclone interactions*

The original discussion by Carr and Elsberry (1994) about TC interactions (TCI) has been clarified in a recent paper (Carr *et al.* 1997a). Three primary TCIs are defined: Direct (DTI); Semi-direct (STI); and Indirect (ITI). Southern Hemisphere adaptations of these conceptual models are given in Fig. 5.

The DTI is analogous to the frequently described Fujiwhara type in which the primary environmental steering for one TC is the circulation of an adjacent TC. This may be a one-way interaction (Fig. 5a) in which a smaller TC is embedded in, and moves cyclonically around, a larger TC circulation. Clearly this situation only occurs for smaller separation distances. Whereas the smaller TC may have a large cyclonic rotation rate relative to the larger TC, the larger TC may not experience a very large deflection.

By definition, the separation distance for the two TCs in a STI is sufficiently large (about 10° latitude in NH) that their circulations do not overlap, and yet is not so large that an anticyclone is present between them. A more rapid than normal poleward deflection of the eastern TC (Fig. 5b) will occur if the two TCs are aligned east-west with an anticyclone farther to the east. That is, the low (high) pressure of the western TC (eastern anticyclone) establishes a poleward steering flow across the eastern TC, which is then termed a STIE. Similarly, an equatorward deflection of the western TC (Fig. 5b) will occur if the two TCs are aligned east-west with an anticyclone farther to the west. In this STIW case, the low (high) pressure of the eastern TC (western anticyclone) establishes an equatorward steering flow across the western TC that tends to inhibit recurvature.

A key feature of the ITI (Fig. 5c) is a larger separation distance so that an anticyclone exists between the two TCs. The origin of this anticyclone is from the Rossby wave dispersion associated with a relatively large western TC. Development of this peripheral anticyclone results in a poleward steering flow across the western TC (see Carr and Elsberry 1995, 1997a). As the eastern TC approaches the peripheral anticyclone of the western TC, and equatorward steering current will be imposed, and the eastern TC in the SH may be deflected to an unusual north of west track (Fig. 5c), which is called an ITIE. Notice that a poleward (equatorward) deflection of

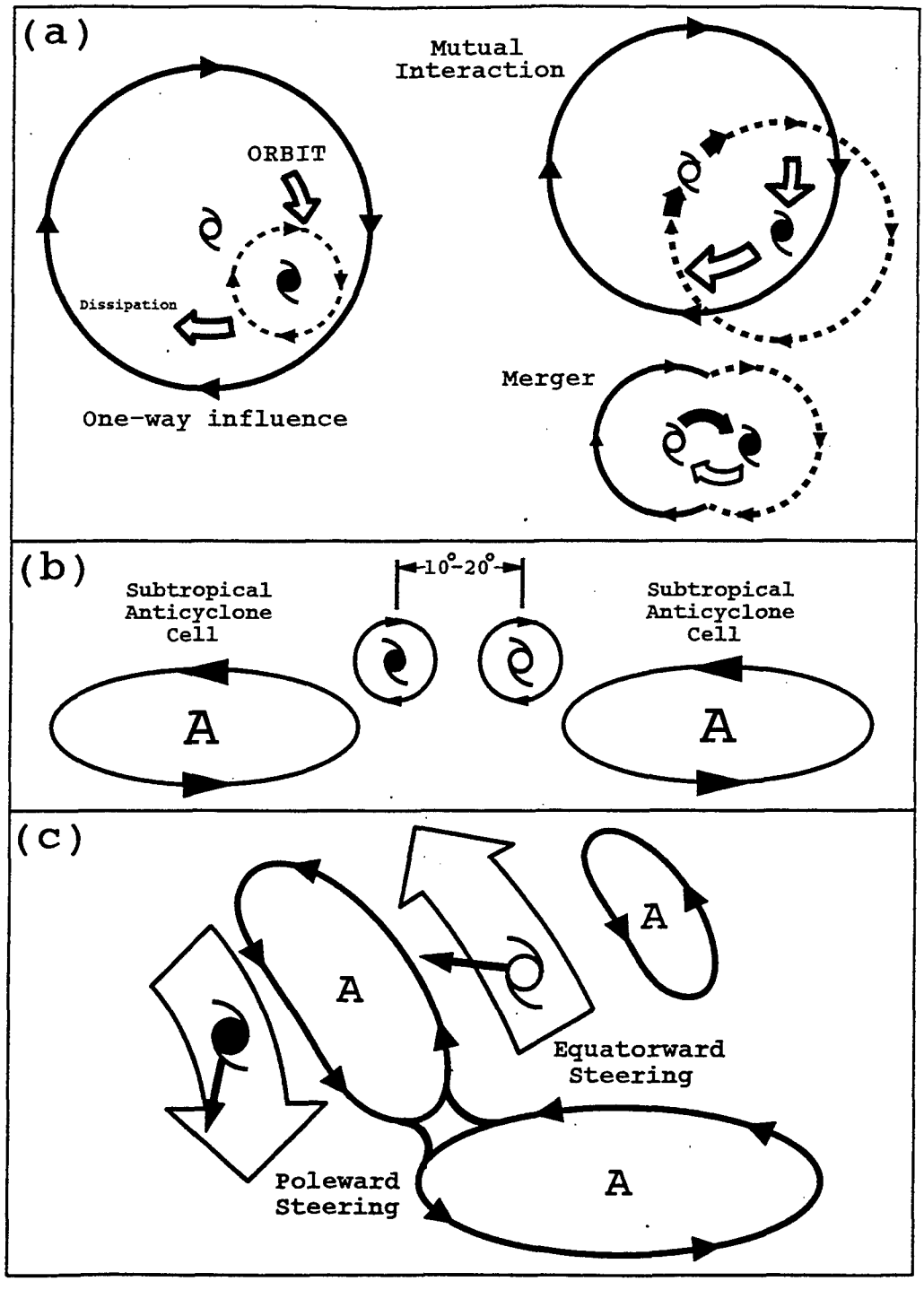

Figure 5. Schematics of three modes of TC interaction by Carr *et al.* (1997a) adapted for the Southern Hemisphere.

the western (eastern) TC by the intervening peripheral anticyclone will cause an anticyclonic rotation about the centroid between the two TCs. This anticyclonic rotation distinguishes the ITI from the DTI and STI, both of which have a cyclonic rotation rate.

Carr and Elsberry (1997b) have recently developed an objective technique for detecting DTI, STIE, STIW, and ITIE events in the western North Pacific. They calculated the separation distances and rotation rates for all TCs with 30° latitude. Because overlaps exist between the separation distances and rotation rates for DTI and STI events, somewhat arbitrary dividing lines had to be established, and the forecaster must evaluate all cases near the dividing lines. In addition, some other environmental conditions that may cause similar apparent rotation rates had to be defined to reduce the number of false alarms.

As an experiment, the separation distances and rotation rates were calculated in a similar manner for all SH TCS within 30° latitude. The objective criteria for detecting DTI, STIW, SITE, and ITIE in the western North Pacific (Carr and Elsberry 1997b) were reflected across the equator and provided as guidance during the synoptic pattern and region characterization process. It was clearly indicated that this information was to be used as a "flag," and independent judgement should be exercised as to whether the TCIs were actually occurring as in Fig. 5.

3. ENVIRONMENT STRUCTURE CHARACTERIZATIONS

Each of the synoptic pattern/region combinations that were found to apply in the SH will be described first as a conceptual model. Examples of NOGAPS analyses with the JTWC positions will also be given. Although the streamlines in the conceptual models below ideally represent the deep-layer steering flow appropriate for the present TC intensity (shallower for weaker storms), 500-mb NOGAPS analyses are normally used for convenience. Since the environmental steering by definition excludes the TC circulation, the forecaster must qualitatively infer the streamline flow after mentally removing the TC circulation. The goal here is only synoptic map typing, and not to derive *quantitative* estimates of steering, which would require more precise vertical layer choices and an explicit decomposition of the vortex and environment.

a. *Standard synoptic pattern*

1. Conceptual model. In the standard (S) synoptic pattern (Fig. 6), the axis of the subtropical anticyclone is approximately east-west, although it may be slightly tilted longitudinally. The arrows adjacent to the subtropical anticyclone cells on either side indicate the mobility of these SH circulations relative to the more "anchored" circulations in the western North Pacific region. Although a "break" in the subtropical anticyclone may be present in association with a passing midlatitude trough, the distinguishing characteristic is the essentially zonal (as opposed to meridional orientation -- see below) character of the subtropical anticyclone. A zonally oriented monsoon trough is also included in the S synoptic pattern, with equatorial westerlies between the Equator and the monsoon trough, and trade easterlies between this trough and the subtropical anticyclone.

Four synoptic regions are defined in the S pattern (Fig. 6). A TC that forms in the Equatorial Westerlies (EW) region will initially have a west-to-east track. Superposition of the clockwise TC circulation in such a westerly flow will lead to an isotach maximum on the equatorward side in the EW region. A TC that forms or moves into the Dominant Ridge (DR) region will have basically an east-to-west track in the easterly trade flow, so that the isotach maximum will then be on the poleward side. If the subtropical anticyclone has a significant tilt away from a zonal orientation, the track of the TC in the DR region will have a similar deflection from an east-to-west orientation. The clockwise turning track at the western end of the DR region indicates it is possible for a TC in a monsoon trough cell to rotate into the EW region and thus move from west to east. If a TC in the DR region moves into the break between the subtropical anticyclonic cells, the translation speed will decrease, and the track will turn poleward in response to the northeasterly-to-northerly environmental steering. Concurrently, the isotach maximum will rotate to be southeast and then east of the TC center. This is defined to be the Weakened Ridge (WR) synoptic region in the S pattern (Fig. 6).

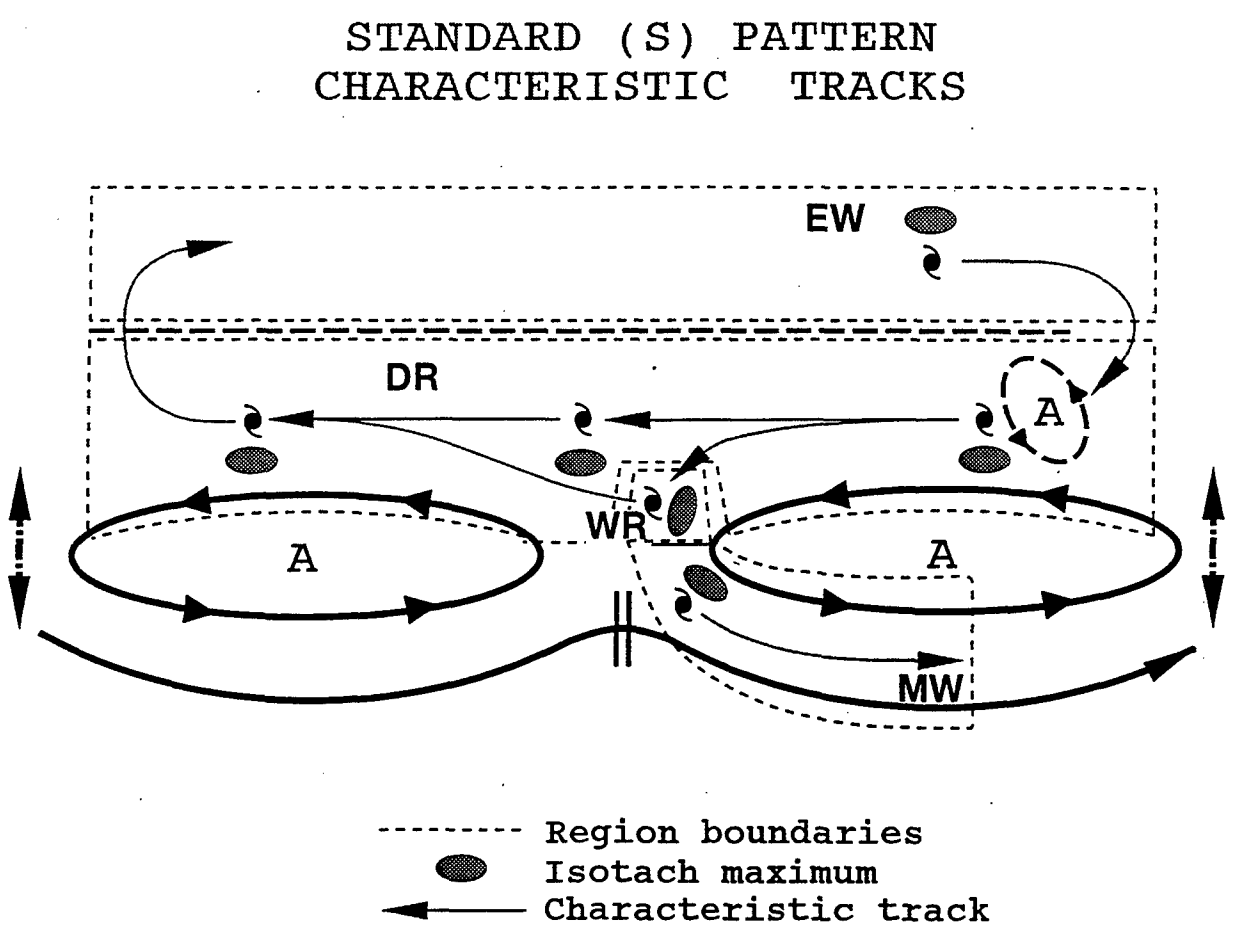

Figure 6. Conceptual model of Standard (S) synoptic pattern for the Southern Hemisphere. Thick solid streamlines represent the 500-mb environmental flow after removal of the TC circulation. Vertical arrows on the left and right indicate the possible meridional positions of the subtropical anticyclone. The heavy dashed line in upper portion represents the monsoon trough. Light solid lines with arrows illustrate characteristic TC tracks. Isotach maxima relative to the TC positions are indicated by elliptical regions. Light dashed lines enclose the Equatorial Westerlies (EW), Dominant Ridge (DR), Weakened Ridge (WR), and Midlatitude Westerlies (MW) synoptic regions. A trailing anticyclone (A) to the east and north of the eastern most TC in the DR region illustrates a Rossby wave dispersion effect (see text for description).

In a typical recurvature sequence, the TC in the WR region will move poleward through the subtropical anticyclone axis and then have an eastward translation component in the Midlatitude Westerlies (MW) synoptic region (Fig. 6). Although the environmental steering governing the TC motion in the MW is still considered to be the subtropical anticyclone, the translation speed and direction will be strongly influenced by the presence and orientation of a trough in the midlatitude westerlies. Notice that the isotach maximum will be to the northeast (and later to the north) as the TC motion is southeastward (and then eastward). If a TC in the WR region fails to recurve through the subtropical anticyclone axis, it will return to the DR region -- first with a north-of-west track and then westward, which is sometimes called a stairstep track.

2. Analysis examples. Representative NOGAPS streamline and isotach analyses for a TC in the Standard/ Equatorial Westerlies (S/EW) pattern/region combination are shown in Fig. 7a. The central TC at 15°S, 140°E in the Gulf of Carpenteria has been moving eastward in the equatorial westerlies on the equatorward side of the monsoon trough across northeast Australia. Notice the 30-kt isotach on the equatorward side is consistent with the eastward track in the EW synoptic region conceptual model (Fig. 6). The eastern TC at 15°S, 158°E is a weak (20-kt) system drifting southeastward in the monsoon trough, which is tilted NW-SE in this region. Although the synoptic pattern/region is not classified until the Tropical Depression (TD) stage is achieved, this is an example of how the conceptual model in Fig. 6 may have to be adjusted when the circulations are not zonally oriented. The western TC at 16°S, 120°E is moving westward. Notice also the 20-kt isotach to the south that is consistent with such a motion, and is another indication that this TC is in the Standard/Dominant Ridge (S/DR) pattern/region just poleward of the monsoon trough in the S pattern conceptual model of Fig. 6.

An Indian Ocean example (Fig. 7b) of a S/EW case is the TC at 10°S, 96°E that is tracking eastward. An extensive 20-kt isotach is found equatorward of the TC, which indicates strong equatorial westerlies even though a prominent monsoon trough is evidently not depicted well in this analysis. The eastern TC near 20°S, 115°E in Fig. 7b is in a synoptic pattern/region (to be defined below) called High-amplitude/Ridge Poleward (H/RP) and is approaching the subtropical anticyclone axis. Notice the 30-kt isotach to the east is consistent with the southward track

An example of three TCs in the S/DR pattern/region is given in Fig. 7c. Notice the extensive subtropical anticyclone and the 30-kt isotach south-southeast of the TC near 15°S, 164°E. Although this TC has been moving southwestward, the equatorward tilt of the subtropical anticyclone farther west would indicate a more westward steering in the future. At 12 UTC 4 January 1997 (not shown), the 12-h averaged motion was 265° at 6 kt. A second TC near 13°S, 128°E has also been tracking southwestward. However, this TC is approaching a region of west-northwest steering flow that is quite strong (notice the 30-kt isotach). Although a closed trailing anticyclone as with the easternmost TC in the DR region of Fig. 6 is not present here, a distinct ridge is building to the east and north of this TC, and this circulation contributes to a more poleward steering flow across this cyclone. Thus, this situation has some of the characteristics of the Poleward synoptic pattern to be discussed below. Finally, the third TC near 18°S, 102°E in Fig. 7c is also moving westward in the S/DR pattern. This TC has not moved into the Weakened

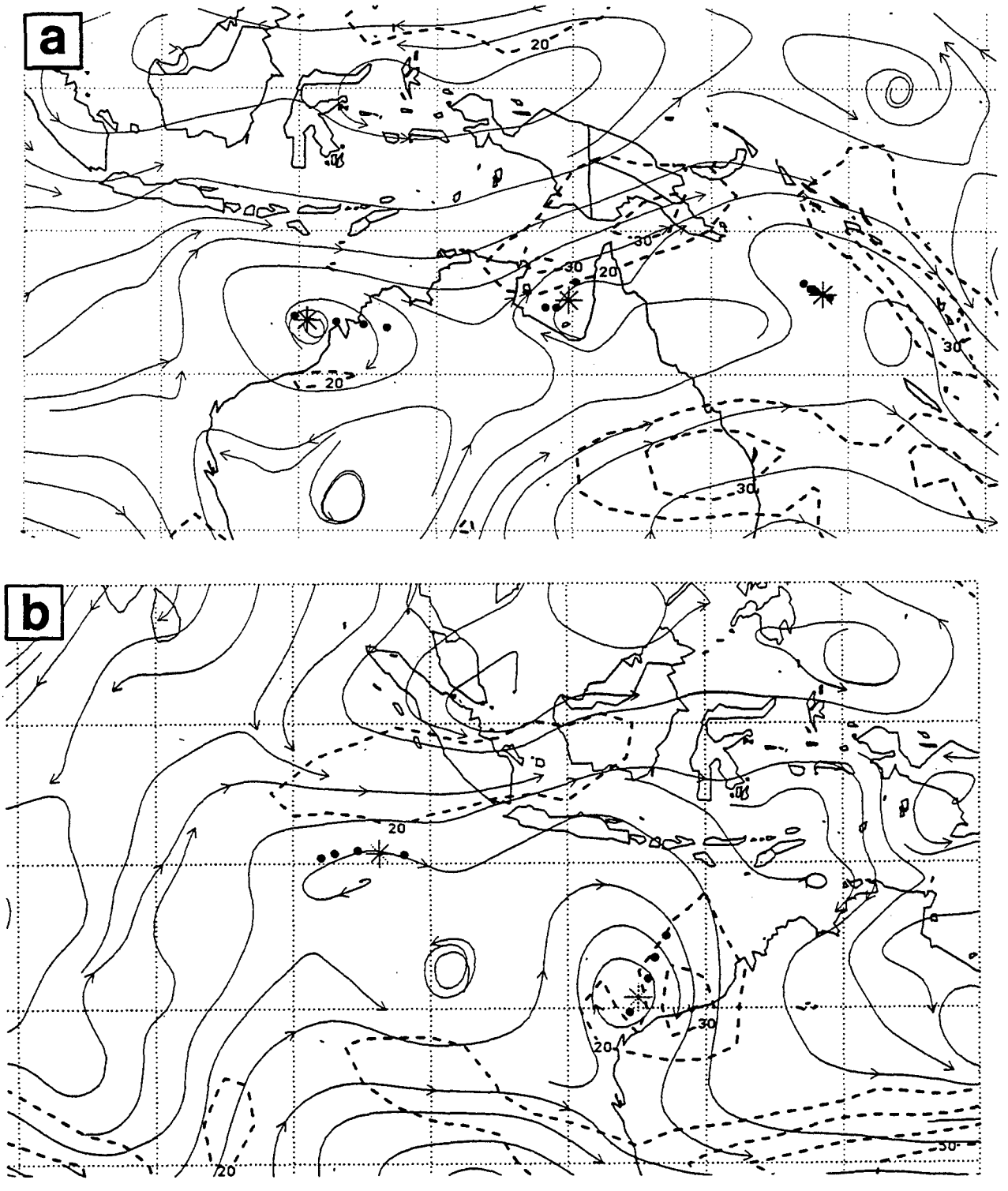

Figure 7. NOGAPS 500-mb streamlines (thin solid) and isotachs (thick dashed) at 10-kt intervals beginning at 20 kt at (a) 12 UTC 8 March 1996, (b) 00 UTC 10 December 1995, and (c) 12 UTC 3 January 1997. The current TC position is indicated by a large asterisk and the prior -36, -24, and -12 h and future + 12 h positions are given as dots.

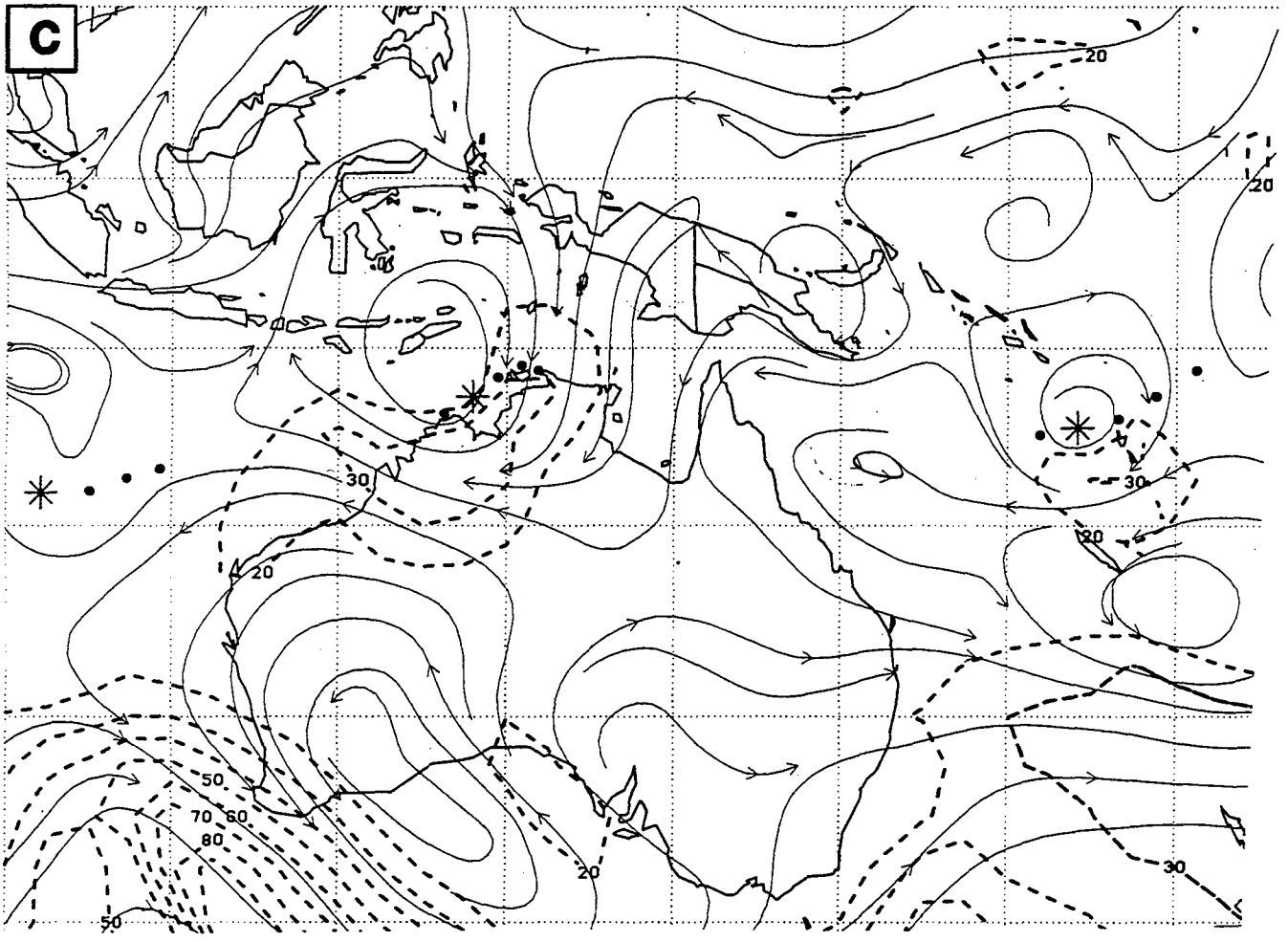

Figure 7c. (continued).

Ridge (WR) region near the break in the subtropical anticyclone farther to the south. Evidence that the TC is not in the WR region is that the translation speed has not decreased and the track has not turned southward.

3. Tracks. All tracks while TCs were in the S/EW pattern/region combination during 1994-97 are shown in Fig. 8a. Notice that most of these tracks are between about 10°S-15°S because the equatorial westerlies are on the equatorward side of the monsoon trough. Some of the TCs persisted in S/EW relatively short periods, and thus had only short eastward tracks. Other TCs remained in the S/EW pattern/region for some time and had longer tracks. The longest track, which is actually toward the southeast and extends to about 17°S near the dateline, is associated with the South Pacific Convergence Zone so that the equatorial westerlies are tilted away from a zonal orientation. This is another example of how the forecaster must adapt the idealized circulations in the conceptual model (Fig. 6) to fit the existing scenario.

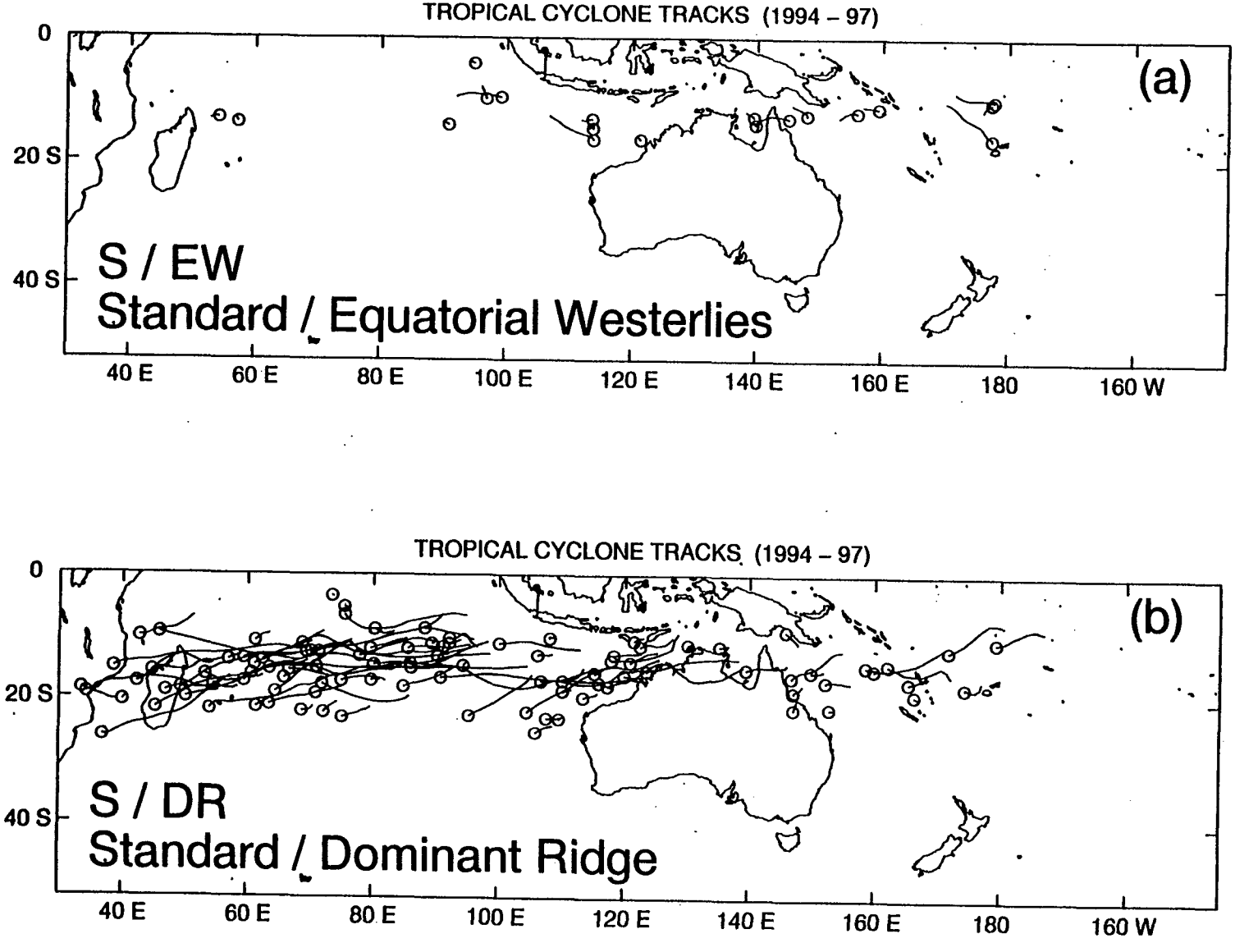

Figure 8. Tracks as in Fig. 4, except only while TC was in the Standard (S) pattern and (a) Equatorward Westerlies (EW) or (b) Dominant Ridge (DR) regions.

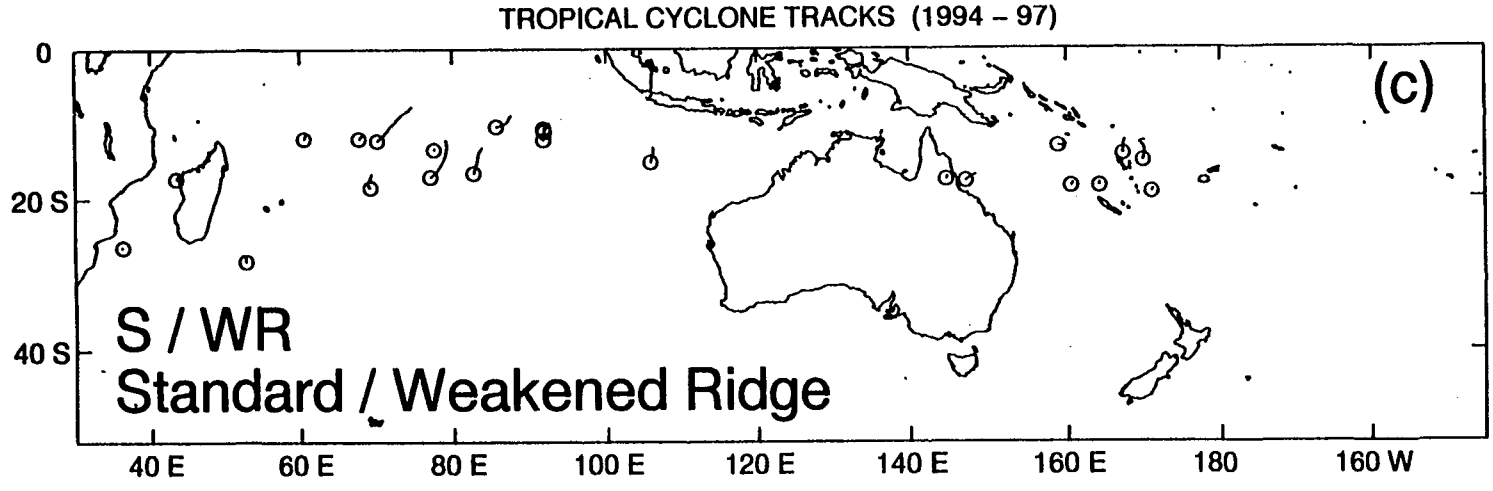

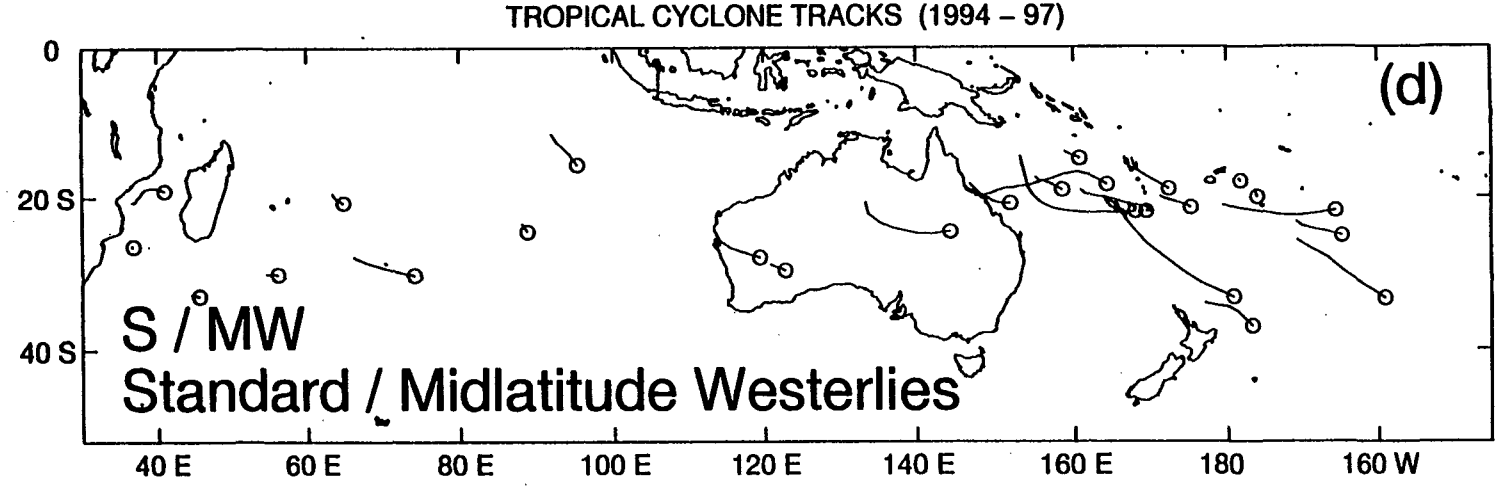

Figure 8. (continued) Tracks in S pattern and (c) Weakened Ridge (WR) and (d) Midlatitude Westerlies (MW) regions.

Representative tracks while the TCs are in the S/DR pattern/region are provided in Fig. 8b. Most of these tracks are between 10°S and 22°S as these TCS are embedded in the tradewind easterlies. Many more S/DR cases are found in the Indian Ocean (IO) than in the South Pacific, and the IO tracks are generally longer, which means the TCs persist longer in the S/DR pattern/region in the IO. This persistence in turn is related to the more zonal and more persistent subtropical anticyclones in the IO. As will be demonstrated below, more extensive meridional excursions at 500 mb occur in the western South Pacific, which makes the subtropical anticyclone circulation more transient

Tracks while the TCs are in the S/WR pattern/region (Fig. 8c) are generally quite short and toward the south-southwest. These aspects are consistent with the small S/WR domain, and the steering flow in the conceptual model (Fig. 6). Except for a case along the east coast of Africa, these S/WR cases are equatorward of 20°S.

Finally, the TC tracks in the S/Midlatitude Westerlies (S/MW) are illustrated in Fig. 8d. By definition, these tracks must have an eastward component on the poleward side of the subtropical anticyclone. Some of the S/MW tracks are quite short, which indicates the TC probably dissipates. Other tracks are considerably longer, especially in the South Pacific. Notice that some of the TCs maintain at least 25-kt intensities while crossing Australia. Another anomalous S/MW track occurs in the Mozambique Channel (in which the TC had a period with equatorward (and eastward) motion.

In summary, distinctly different paths are found to be associated with each of the four synoptic regions in the S pattern. Although the translation speeds along these paths, and the times that the TC remains in the synoptic region, do vary, these characteristic tracks demonstrate that this environment structure aspect can be applied to SH TCs as was the case for the NH TCs.

b. *Poleward synoptic pattern*

1. Conceptual model. In the Poleward (P) synoptic pattern (Fig. 9), the environment structure usually has a significant break in the subtropical anticyclone poleward of the TC, and a prominent, primarily poleward-oriented anticyclone to the east that extends equatorward of the TC. A climatologically favored SH region for such a P pattern is the South Pacific Convergence Zone (SPCZ), which is a favored region for TC development and serves as a poleward steering flow. A key TC-environment transformation (Fig. 1, lower right) in the Systematic Approach (Carr and Elsberry 1994, 1997a) called the Ridge Modification by the TC (RMT) results in a P pattern. In this transformation, a peripheral anticyclone is formed to the north and east (Southern Hemisphere) of larger TCs as a result of Rossby wave dispersion. Consequently, the motion of the TC acquires a poleward component with an isotach maximum to the east-northeast (Fig. 9). When two TCs are present and the eastern TC is poleward of the western TC, the Rossby wave dispersion of each TC may act in concert to form an extensive peripheral anticyclone to the northeast. The environmental steering may then cause a nearly simultaneous transition of both TCs into the P pattern. This transitional mechanism is termed Reverse Trough Formation (RTF)

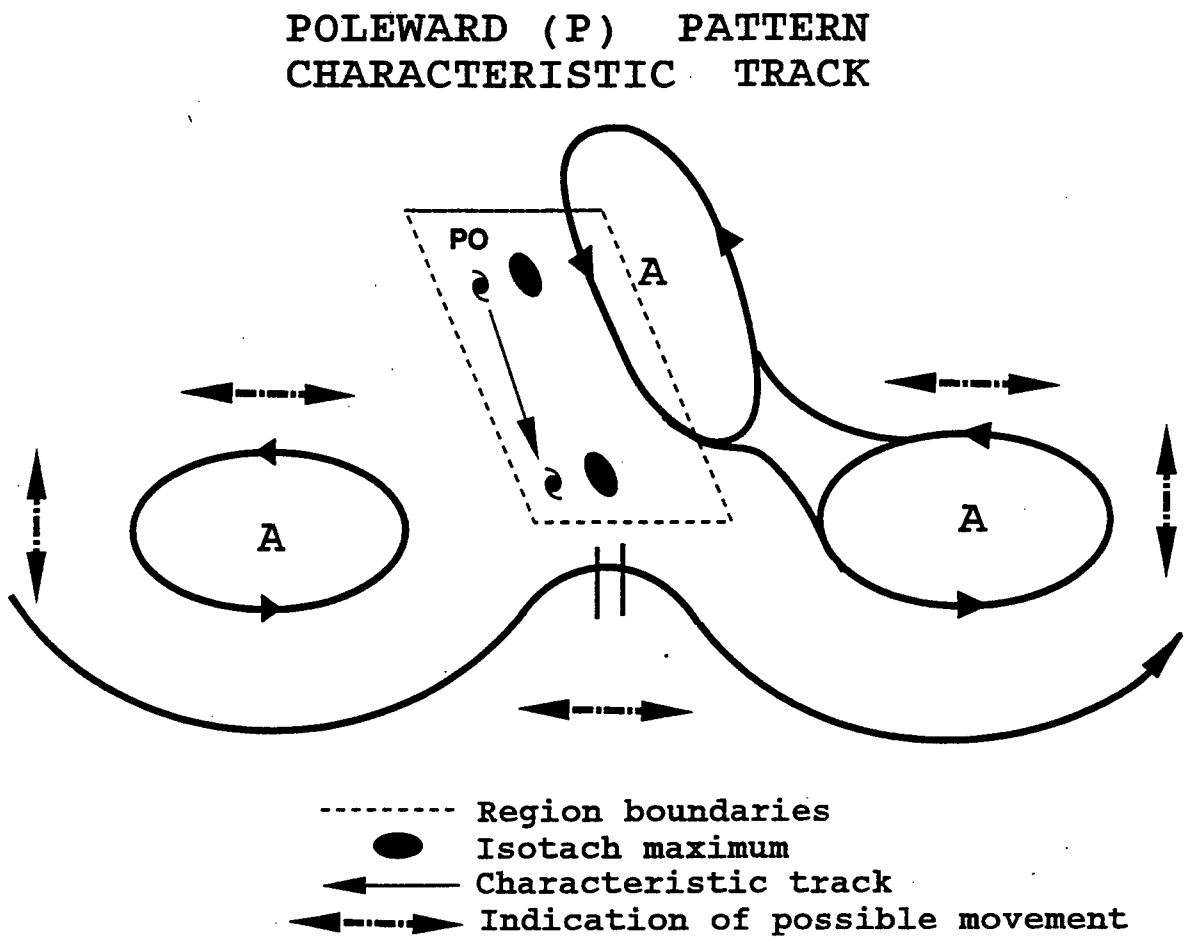

Figure 9. Conceptual models as in Fig. 6, except for Poleward (P) synoptic pattern and Poleward-Oriented (PO) synoptic region.

in Fig. 1, and is basically a variation of the RMT mechanism except that it involves more than one TC (see Carr *et al.* 1997a). The region from where the TC turns poleward to the axis of the subtropical anticyclone is called the Poleward-Oriented (PO) synoptic region (Fig. 9). After the TC passes through the subtropical anticyclone axis, the environment structure is considered to change to the Standard (S)/Midlatitude Westerlies (MW) synoptic pattern/region, as described in section 3a.

As illustrated by Carr and Elsberry (1994, 1997a), the amplitude of the Rossby wave dispersion (peripheral anticyclone) is greater for TCs with stronger outer winds (larger TCs). As the Rossby wave dispersion pattern translates with the TC, the peripheral anticyclone may also appear to translate poleward, and thus delay recurvature (passage through subtropical anticyclone axis). The most important signal that a TC is in the P/PO pattern/region in the SH is the

peripheral anticyclone to the northeast. Poleward of the TC may be a strong subtropical anticyclone or a trough in the westerlies may be found to the southwest, south or southeast. Especially in the South Pacific, a wide trough will often split the two subtropical anticyclone cells in Fig. 9, and with an enhanced trough to the west of the TC, the poleward steering flow is increased across the TC. This scenario will favor a more rapid recurvature. However, passage of a midlatitude anticyclone may establish a continuous ridge to the south of the TC. This is called a Subtropical Ridge Modulation, and is considered to be a transitional mechanism (Fig. 1, lower left) that is external to the TC and its immediate environment. If a continuous ridge is established to the south of the TC via the SRMR mechanism, and this becomes the dominant steering flow, the isotach maximum will be to the south of the TC, and the motion will be westward. Thus, the TC will be in the S/DR pattern/region rather than P/PO.

2. Analysis examples. Some NOGAPS analyses of TCs in the P/PO pattern/region are provided in Fig. 10. A TC case in the SPCZ with a weak trough to the west is shown in Fig. 10a. Notice the extensive anticyclone to the east of the eastern TC that extends from the Equator to 30°S. The 40-kt isotach maximum to the northeast of the TC is consistent with the rapid translation to the south-southeast. This streamline/istoach pattern indicates that it is the steering flow associated with the anticyclone to the east that is controlling the TC motion. However, the presence of the trough to the west is favorable for a strong steering flow. Notice also that the western TC in Fig. 10a is moving eastward on the equatorward side of the monsoon trough, and thus is in the S/EW pattern/region.

Another example with a well-defined peripheral anticyclone to the northeast is given in Fig. 10b. Although a 30-kt isotach maximum is analyzed to the northeast, the translation speed is much less than in Fig. 10a. The explanation for the slower translation probably lies in the presence of an opposing steering flow just to the southwest of the TC. That is, the TC is located between two opposing steering flows, and the translation will be governed by the stronger flow, which is indicated by the 30-kt isotach to the northeast.

An Indian Ocean example of a P/PO case with an extensive meridional anticyclone to the east is illustrated in Fig. 10c. The sequence of -36 h through +12 h storm positions indicates an accelerating poleward translation. The maximum isotach of 40 kt to the east-southeast (rather than east-northeast as in the conceptual model in Fig. 9) is consistent with a continued motion acceleration in the next 12 h. This isotach maximum reflects the presence of an encroaching midlatitude trough that is tightening the pressure gradient, and increasing the environmental steering flow between the trough and the anticyclone to the east. This is an example of the TC-transitional mechanism in Fig. 1 (lower left) called Subtropical Ridge Modulation (SRM) by a midlatitude trough. Notice that the midlatitude ridge is also phased properly with the anticyclone to the east of the TC to contribute to the extensive meridional anticyclone. If this phasing with the midlatitude trough-ridge system continues (rather than be a transient event as the progressive midlatitude system translates eastward), the TC will continue to experience a poleward-oriented environmental steering in this P/PO synoptic pattern/region. However, the TC is already at 30°S, and the interaction with the midlatitude trough may also result in a vertical wind shear across the

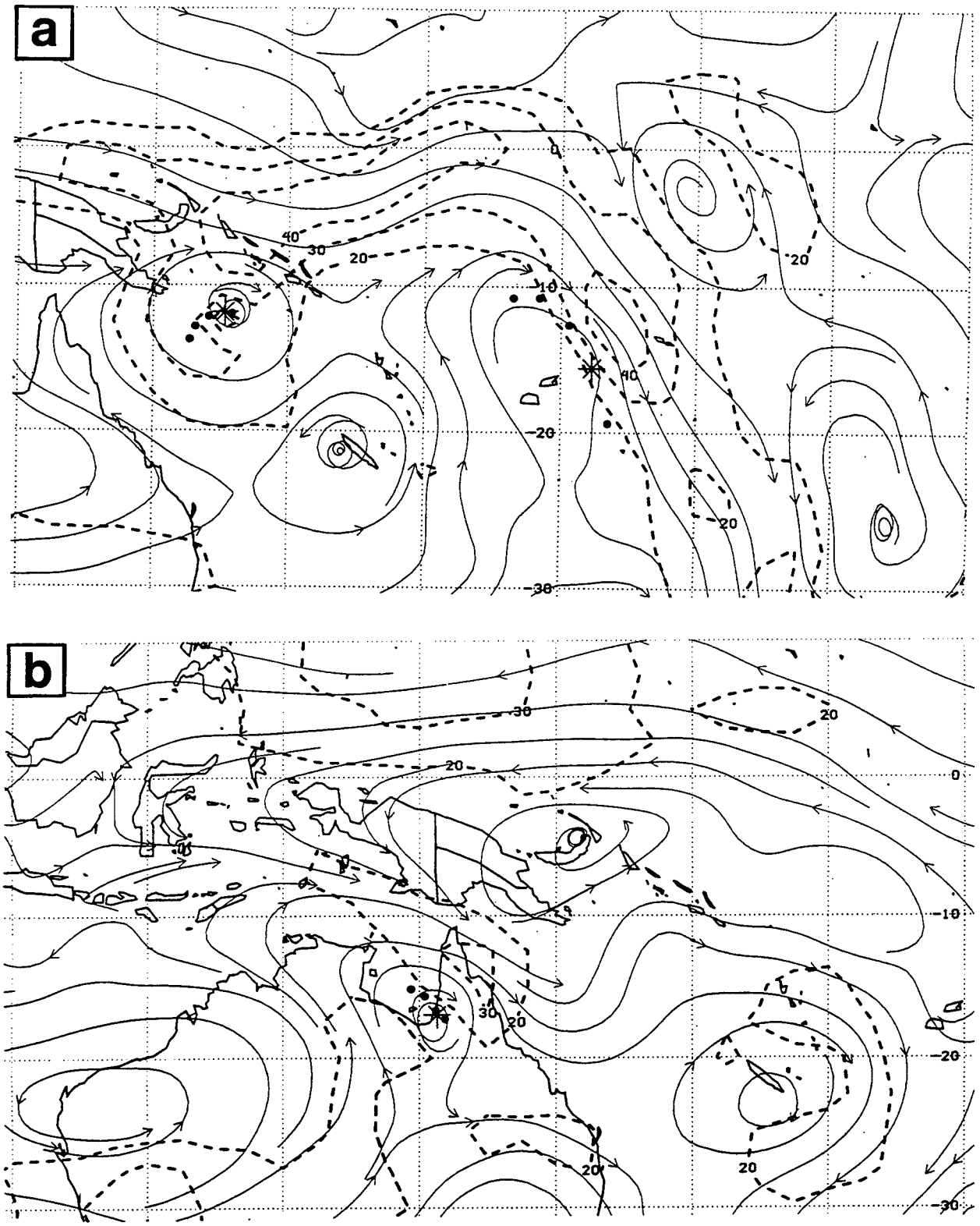

Figure 10. NOGAPS 500-mb analyses as in Fig. 7, except at (a) 12 UTC 15 March 1997, (b) 00 UTC 6 January 1996, and (c) 12 UTC 24 February 1997.

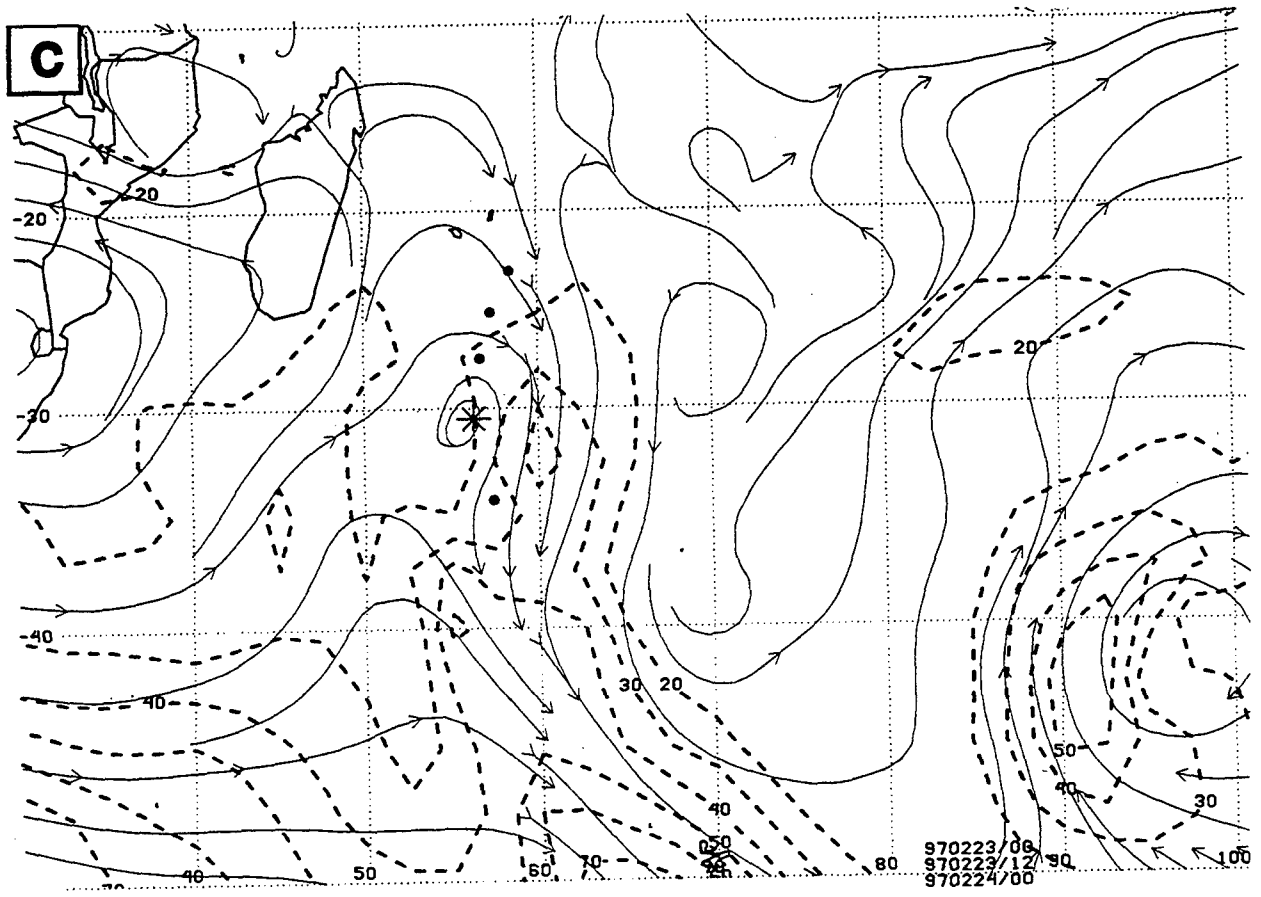

Figure 10c. (continued).

TC that will disrupt the circulation. A rapid decrease in intensity will then occur and the appropriate steering level will be at 700 mb, or even 850 mb, instead of 500 mb.

This process of Vertical Wind Shear (VWS) changing the level of the environmental steering is considered to be another TC-environmental transformation in the lower-right box of Fig. 1. An asymmetry in convection with subsidence clearing upshear and deep convection only on the downshear side was illustrated in the well-documented cyclone Kerry case (Holland and Black 1995). In the Kerry case, the TC circulation structure remained vertically coherent, i.e., Kerry was able to "fight off" the potential shearing off of the upper-tropospheric warm core. In other cases, the vertical wind shear does decouple the TC circulation and advect the warm core downstream, so that the remnants of the TC will then be advected by a lower layer in the troposphere, which may change the track direction and speed considerably. The remaining TC circulation is still dangerous to maritime activity and should continue to be followed. Tracking the remnants is usually easy from the spiraling cumulus lines in the visible satellite imagery after the cirrus cloud shield has been advected downshear. Unfortunately, no Meteosat imagery was available for this study to illustrate the process in this western South Indian Ocean case.

An important aid in diagnosing the onset of a peripheral anticyclone associated with Rossby wave dispersion is the infrared and visible satellite imagery. When the TC forms in the monsoon trough as in most SH cases, the cloud signature of the TC is typically embedded in a zonally oriented band of convection. As described above (Carr and Elsberry 1994, 1997a), the Rossby wave dispersion produces an anticyclone equatorward and to the east, especially for larger TC circulations. This peripheral anticyclone is a region of upper-tropospheric subsidence, which tends to suppress deep convection as the anticyclone develops. This subsidence is evident in the satellite imagery by a progressive clearing of the cloudiness to the northeast of a SH TC. This confirmation from satellite imagery of the peripheral anticyclone development is often important because the global model analyses may only indicate a weak ridge to the northeast of the TC until the outer wind strength in the TC circulation is better represented. Consequently, the explanation for a slowing of the westward TC translation and the beginning of a poleward turn may not be so evident in just the global model analyses. However, confirmation from the satellite imagery of the development of a peripheral anticyclone can verify that the RMT transformation is occurring. Whether the TC steering flow changes from being dominated by the subtropical anticyclone (and thus a westward track) to being dominated by the peripheral anticyclone depends on the relative strength of the peripheral and subtropical anticyclone cells. In the P/PO pattern/region (Fig. 9), the peripheral anticyclone is dominant and a poleward track results. One difference noted in this sample versus the western North Pacific sample used to develop the Systematic Approach is the weaker and more transient subtropical anticyclone in the SH, which is indicated by the vertical arrows along the sides of Fig. 9. Consequently, the peripheral anticyclone development associated with relatively smaller SH, TC circulations can still trigger a RMT transformation, the transition to a P/PO pattern/region, and a change to a poleward TC track.

An example of the infrared satellite image evolution at an earlier stage of the case in Fig. 10b is shown in Fig. 11. This TC formed on the poleward side of an active monsoon trough. Notice the convection at 03 UTC 3 January 1996 (Fig. 11a) to the north and east of the TC that is forming in the Gulf of Carpenteria. By 03 UTC 4 January 1996 (Fig. 11b), a distinct clearing of the upper-level cloudiness has occurred to the north and east, including the region of Papua New Guinea. This is generally the region of the peripheral anticyclone in the analyses at 00 UTC 6 January (Fig. 10b). The prior 36 h TC positions in Fig. 10b indicate a slow translation and a more poleward track than might have been expected for a TC forming in the equatorial westerlies of a zonally-oriented monsoon trough. In this case, the east of south track, the isotach maximum to the northeast (Fig. 10b), the anticyclone to the northeast, and the confirming presence of subsidence clearing of the high clouds to the northeast during the previous days (Fig. 11b) indicate that this TC had a transition from S/EW to P/PO, rather than passing through the S/DR pattern/region.

3. Tracks. A summary of all tracks during January 1994 - June 1997 while the TCs were in the P/PO pattern/region is given in Fig. 12. By definition, all of the tracks are poleward-oriented. Although a few P/PO tracks originate equatorward of 10°S, most of these TCs turn poleward between 10°S and 20°S. Many of these tracks have a sinuous nature. While many tracks have cyclonic curvature during the early portion of the P/PO period, the curvature becomes

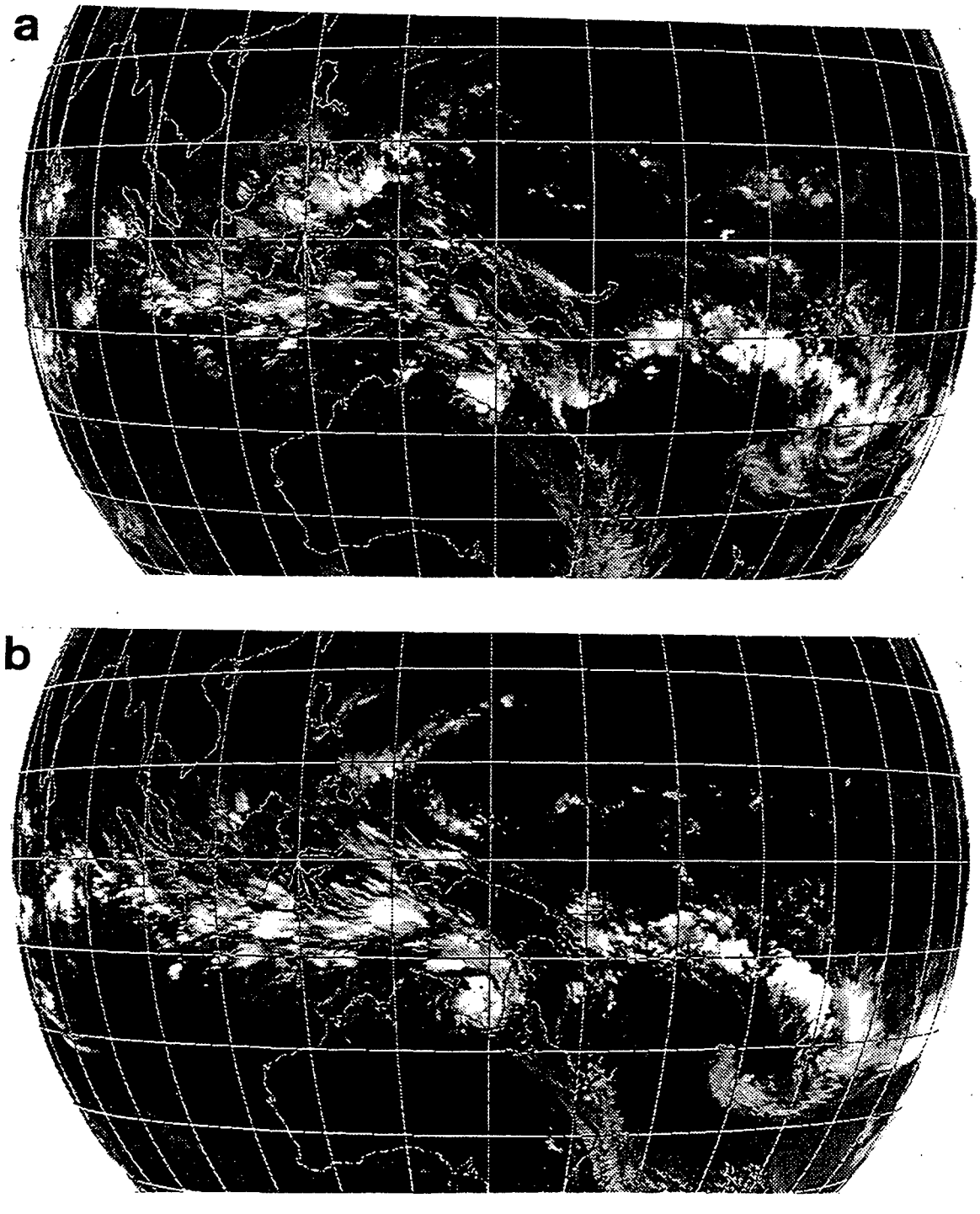

Figure 11. Satellite infrared imagery illustrating (a) the nearly continuous cloud band associated with the monsoon trough at 03 UTC 3 January 1996 and (b) the clearing of the convection to the east and north of the developing TC at 03 UTC 4 January in the region of the peripheral anticyclone in Fig. 10b.

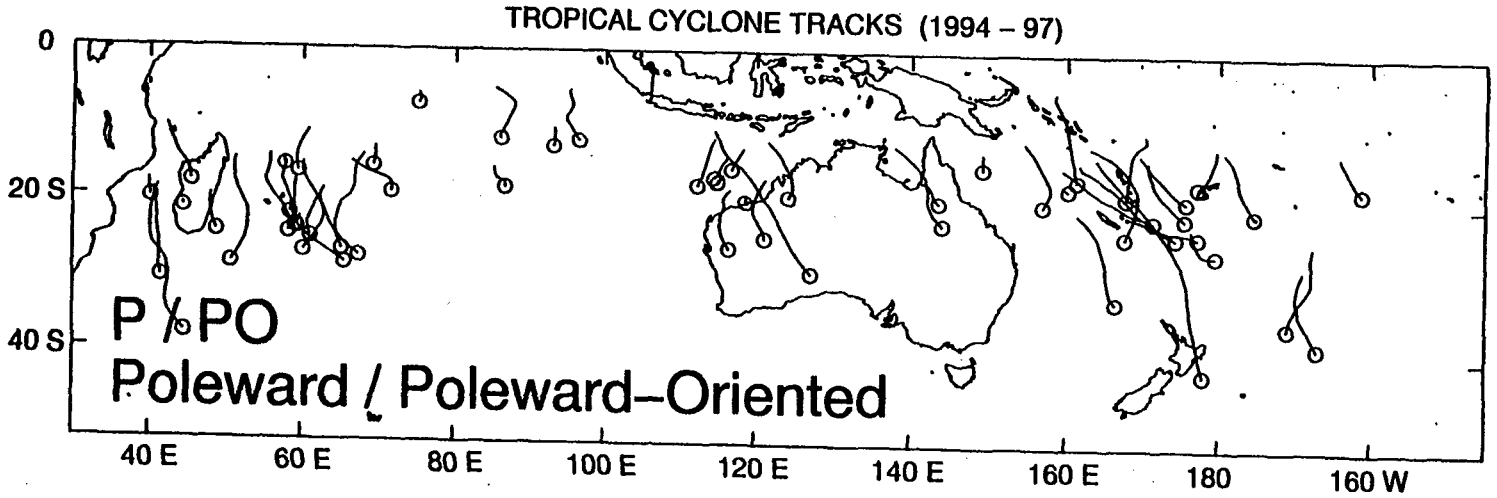

Figure 12. Tracks as in Fig. 4, except only while the TCs are in the Poleward/Poleward-Oriented (P/PO) synoptic pattern/region

anticyclonic near the end of the track. Such variability in track directions contributes to lower forecast accuracy with persistence-type techniques. As described in the previous subsection, the translation speed in the P/PO pattern/region is governed by the strength of the pressure gradient between the peripheral anticyclone and the trough in which the TC is embedded. Transients in either circulation feature, and especially enhanced troughing from the midlatitudes in the SH, causes accelerations/decelerations in translation speed. Variability in translation speeds is not well handled by persistence-type forecasts, or by climatological techniques.

Whereas a few P/PO tracks are short, many are quite long, especially in the region of the SPCZ. Other regions with long poleward tracks are off Africa between 40° and 60°E and over Western Australia. Comparison of the P/PO tracks in these three regions with the overall track summary in Fig. 4 indicates that the P/PO tracks represent a considerable fraction of all TCs in the SH that are sustained south of 30°S. As described in the previous subsection, these long-lasting TCs evidently do not experience vertical wind shear while in the P/PO pattern/region.

c. *High-amplitude synoptic pattern.*

The most important difference in the environment structure of SH TCs from the western North Pacific TCs addressed in the original Systematic Approach application arises from the more vigorous intrusions of midlatitude trough/ridge systems deep into the SH tropics. In the western North Pacific, the subtropical anticyclone is steady, zonally oriented, and broad, especially during the primary TC season. By contrast, the subtropical anticyclone from the coast of Africa to the central South Pacific is highly transient, often has more circular cells, is frequently disrupted by midlatitude trough/ridge systems that are usually tilted NW-SE, and is comparatively weak. The Standard (S) synoptic pattern (section 3a) is used when the TC exists during periods with zonally oriented subtropical anticyclones. However, it was clear that another synoptic pattern was necessary to describe the more meridionally oriented SH subtropical anticyclone events and the intervening periods of TCs. The new High-amplitude (H) synoptic pattern (Fig. 13) serves that purpose

1. Conceptual model. This H synoptic pattern brings together two inherently linked components of a meridionally oriented trough/ridge system: (i) a meridional subtropical anticyclone with adjacent meridional troughs to the east and the west; and (ii) a deep incursion of a midlatitude trough toward the Equator with adjacent meridional anticyclones to the east and the west. The two components are linked because a meridional anticyclone (trough) does not generally exist in isolation, i.e., a meridional trough (anticyclone) is usually present on at least one side. Notice that such meridional subtropical anticyclones and deeply penetrating midlatitude troughs can be present without necessarily affecting a TC in the deep tropics. However, the H pattern applies when the TC is embedded in an environmental steering that is primarily determined by either the meridional subtropical anticyclone or the penetrating midlatitude trough. The TCs do not exist in the *middle* of either of these circulations; rather, the TC is considered to exist on the "shoulder" of one or the other of these two circulations.

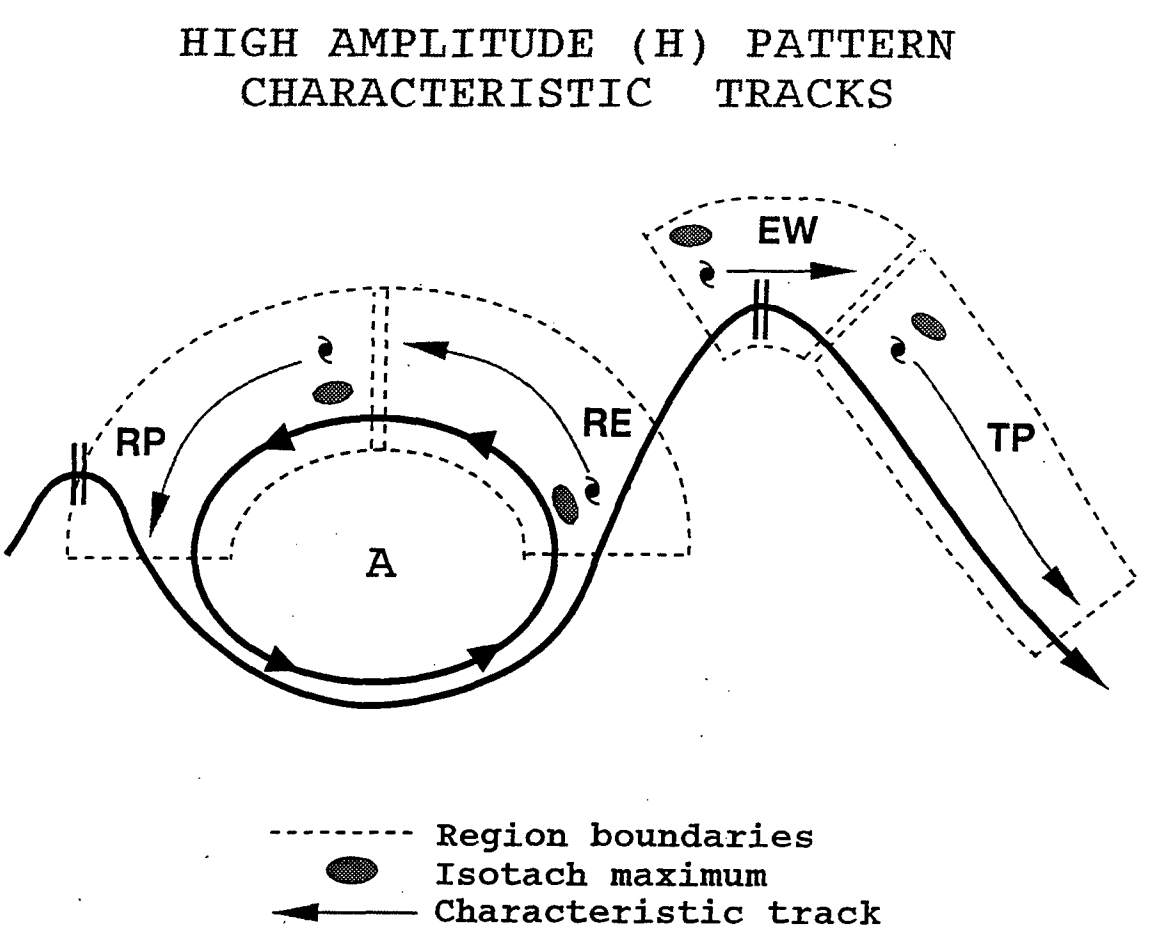

Figure 13. Conceptual model as in Fig. 6, except for the High-amplitude (H) synoptic pattern, which includes the Ridge Poleward (RP), Ridge Equatorward (RE), Equatorial Westerlies (EW), and Trough Poleward (TP) synoptic patterns.

Three synoptic regions in Fig. 13 are defined to indicate whether the environmental steering determining the meridional motion of the TC is primarily associated with the meridional subtropical anticyclone cell or the penetrating midlatitude trough. Whereas the orientation and magnitude of the TC track vectors in the Ridge Poleward (RP) flow and Ridge Equatorial (RE) flow synoptic regions are primarily determined by the meridional subtropical anticyclone (ridge), the amplitude of the trough to the west or to the east, respectively, is also important. Similarly, the environmental steering vector of the TC in the Trough Poleward (TP) flow synoptic region is primarily determined by the deeply penetrating midlatitude trough circulation. However, it is the

pressure gradient between this trough and the subtropical anticyclonic cell to the east that determines the environmental steering of the TC. In most cases, it is clear from the relative amplitudes of the anticyclone and the trough, and from the past storm-motion vector, which circulation is primarily determining the environmental steering, and thus whether RP or PO is the appropriate synoptic region. Although the isotach maxima in the RP and TP regions in Fig. 13 are both on the eastern side of the TC, the orientation will rotate as the environment steering changes direction when the TC moves poleward. A TC in the RE synoptic region is quite rare, and appears to exist when the subtropical anticyclone builds eastward poleward of a low-latitude TC and causes an environmental steering that is equatorward of west.

As in the S pattern (Fig. 6), an Equatorial Westerlies (EW) synoptic region is included in the H pattern conceptual model (Fig. 13). This region is at the equatorward end of a deeply penetrating midlatitude trough that often exist in the SH. Although EW is usually reserved for the monsoon trough, this terminology is applied here because the environment steering is from the west at latitudes rather close to the Equator. Consequently, the isotach maximum will be on the equatorward side of the TC in a proper analysis. As the TC moves cyclonically around the equatorward side of the trough in the EW region, it may move into the H/TP pattern/region and continue to be primarily influenced by the trough circulation. If the trough weakens, and the meridional anticyclone to the east becomes the dominant environmental steering, a transition to the P/PO pattern/region will have occurred. In this case, the peripheral anticyclone may have arisen from the Rossby wave dispersion from the midlatitude trough as it weakens and propagates eastward. The basic Rossby wave dynamics are similar to the NH monsoon gyre developing an anticyclone on the equatorward-east side (Carr and Elsberry 1995).

Notice that the Midlatitude Westerlies (MW) synoptic region in Fig. 13 is poleward of a subtropical anticyclone with a considerable zonal extent. Because this MW region is considered to have similar characteristics as in the Standard (S) pattern in Fig. 6, it thus is not considered to be a separate synoptic region in the H pattern. It is conceivable that a TC might move into the midlatitude westerlies at the poleward end of the H/TP pattern/region. However, this was not observed in this sample because the TCs either dissipated over a cold ocean or became vertically sheared, decreased in intensity, and were advected by an environmental steering at a lower level.

2. Analysis examples. Some analyses while the TC is in a High-amplitude (H)/Ridge Poleward (RP) flow synoptic pattern/region are given in Fig. 14. A subtropical anticyclone (center near 19°S, 106°E) analyzed on 00 UTC 3 May 1996 (Fig. 14a) has relatively high amplitude compared to the more zonally oriented subtropical anticyclone in Fig. 6b. Although midlatitude westerlies have flattened the poleward side of the anticyclone, the trade easterlies on the equatorward side extend to and across the Equator. Even though the TC near 90°S, 92°E clearly has a poleward steering flow between the subtropical anticyclone and an equatorial trough cell, the isotach maximum to the southeast of the TC is not particularly well-defined as in the conceptual model in Fig. 13. The $\pm$ 12 h positions do not indicate any slowing of translation speed as would be expected for a TC in a S/DR pattern/region turning poleward into a S/WR pattern/region. Rather, the image is that the TC is moving poleward on the northwestern

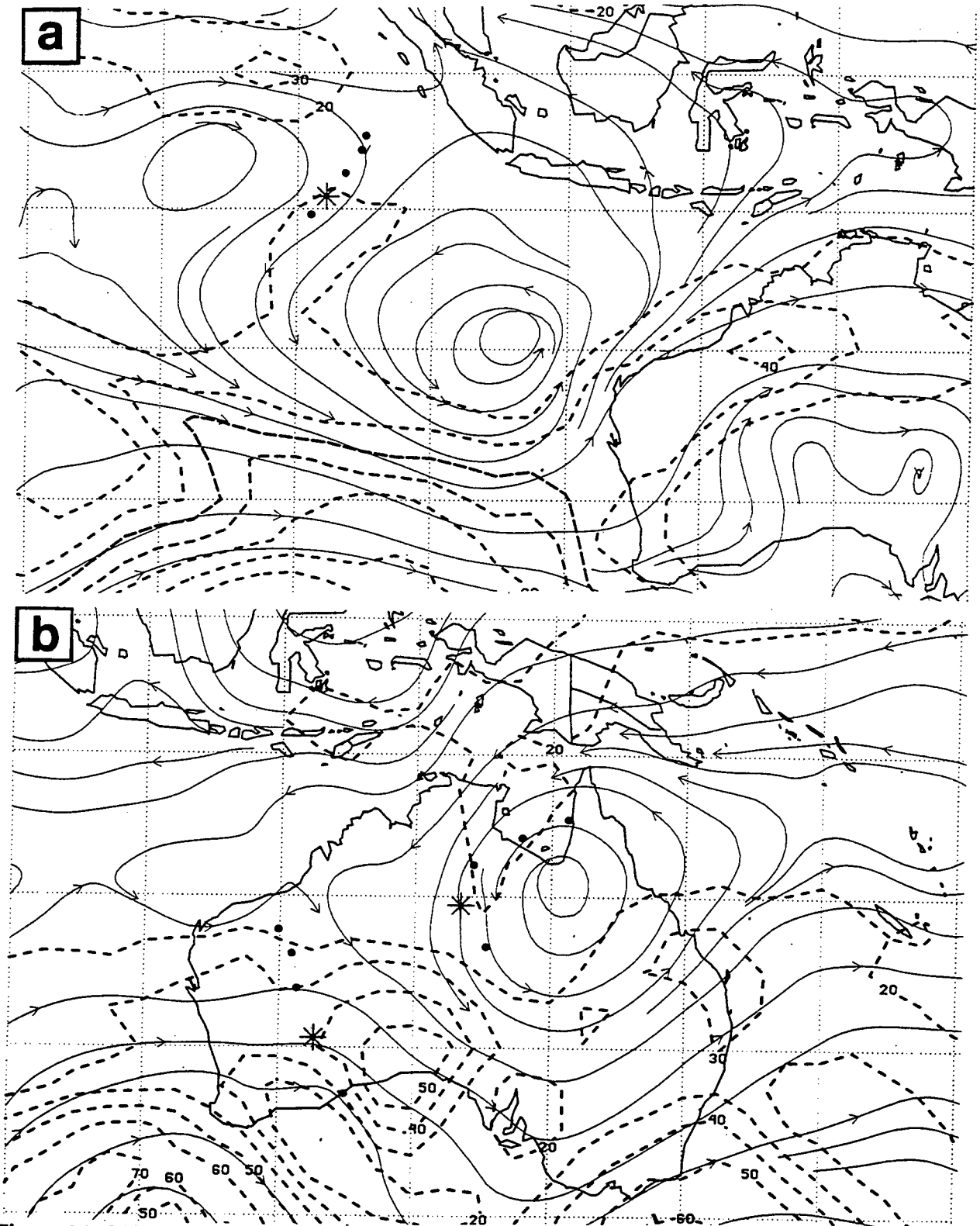

Figure 14. NOGAPS 500-mb analyses as in Fig. 7, except for (a) 00 UTC 3 May 1996, and (b) 00 UTC 14 March 1996.

shoulder of a meridional subtropical anticyclone cell.

Another example of a meridional subtropical anticyclone cell leading to a poleward environmental steering flow is shown in Fig. 14b. Even though the TC near 20°S, 133°E has moved rapidly out of the Gulf of Carpenteria during the past 24 h, the isotach maximum is displaced somewhat to the north of the position indicated in the H/RP conceptual model in Fig. 13. By 00 UTC 14 March 1996 (Fig. 14b), the 12-h average motion is toward 174° at 15 kt. Thus, the TC has undergone a transition to the S/MW pattern/region, and the translation speed has not decreased as in a normal recurvature through the subtropical anticyclone axis via the S/DR to S/WR to S/MW pattern/ region sequence.

A second TC near 30°S, 122°E in Fig. 14b is rapidly traversing Western Australia. This TC is well poleward of the subtropical anticyclone axis and has an eastward component. If the intensity of this TC had not decreased below the TD stage, it would have been classified in the S/MW pattern/region. The 50-kt isotach to the east of this TC indicates a tight pressure gradient between the meridional subtropical anticyclone over Australia and the midlatitude trough to the southwest of Australia, and is consistent with the rapid translation of this TC to the southern coast of Western Australia in the next 12 h.

As indicated above, the H/Ridge Equatorward (RE) flow synoptic pattern/region is rare. In the case in Fig. 15, a TC near 22°S, 66°E has suddenly turned equatorward after previously drifting southwestward. Even though a high-amplitude, NW-SE tilted, midlatitude trough is present to the southeast, the TC is clearly not embedded in the westerlies at the equatorial side of this trough. Rather, the extensive, similarly NW-SE tilted, subtropical anticyclone to the west is controlling the TC motion, and during the next 12 h the TC accelerates to the northwest. Thus, this TC is classified in the H/RE pattern/region. Here, the image is that the TC is on the northeastern shoulder of the meridional subtropical anticyclone as in the H conceptual model (Fig. 13).

A penetrating midlatitude trough that is an extreme example of the H pattern is given in Fig. 16. This trough extends all the way to the Equator. A TC near 13°S, 176°E is clearly embedded in an environmental flow on the northeastern shoulder of this trough, even though an extensive, highly tilted anticyclone is also present farther east. The magnitude of this 500-mb environmental flow is indicated by the 30-kt isotach to the east of the TC, and the extension southeastward to a region with a 40-kt isotach. An increase in translation speed is clearly indicated by the $\pm$ 12 h TC positions, and further acceleration would be expected if this pattern persists. Such a rapid translation at 13° latitude would certainly be unusual in any TC basin. However, the environmental flow in association with such a deep trough has not been found in the other NH basins in which the Systematic Approach application has been attempted (hence, the title "Mother of all Troughs" would be appropriate in this case).

Another extreme H synoptic pattern is given in Fig. 16b. In this South Indian Ocean example, the northern end of the midlatitude trough has split the subtropical anticyclone and

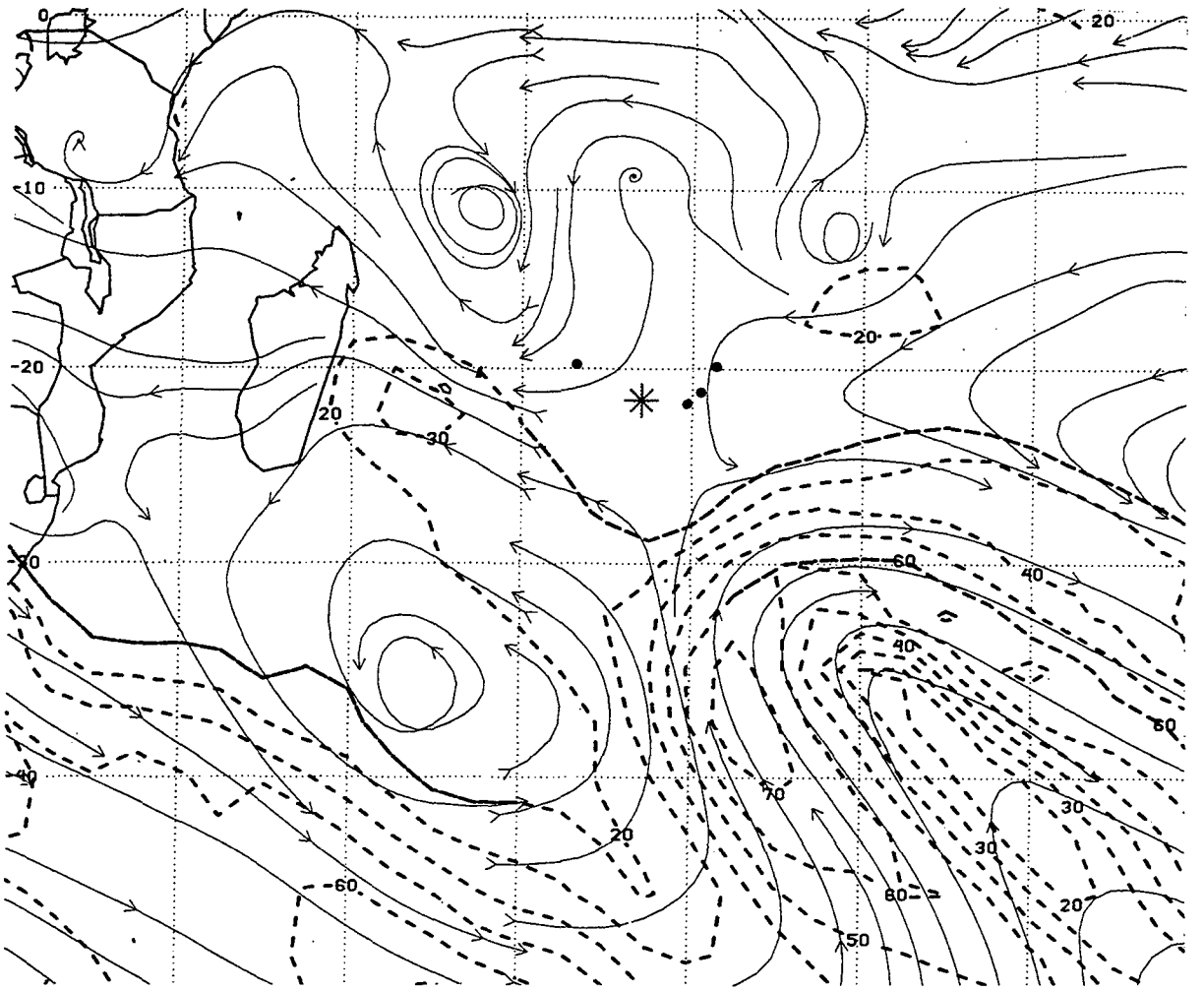

Figure 15. NOGAPS 500-mb analysis as in Fig. 7, except for 00 UTC 24 February 1996.

merged with the monsoon trough. Thus, the equatorial westerlies have a 40-kt isotach near 5°N, 90°E. The TC near 23°S, 108°E is embedded in a strong southeastward environmental flow, as indicated by the 30-kt isotach to the northeast. An increase in translation speed over the past 24 h is indicated. If TC Rhonda had not been weakened by vertical wind shear and stalled offshore, it might have been expected to produce high winds along the coast of Western Australia within the next 12-24 h.

An example of a H/EW pattern/region combination is provided in Fig. 17a. This midlatitude trough has penetrated deep into the tropics and connected with a counter-clockwise eddy on the Equator. The TC near 14°S, 147°E has been moving eastward after forming in the Gulf of Carpenteria and crossing the Cape York Peninsula. As in the H conceptual model (Fig. 13), an isotach maximum is found on the equatorward side of the TC, which is consistent with an eastward environmental steering, and is clearly associated with the trough circulation.

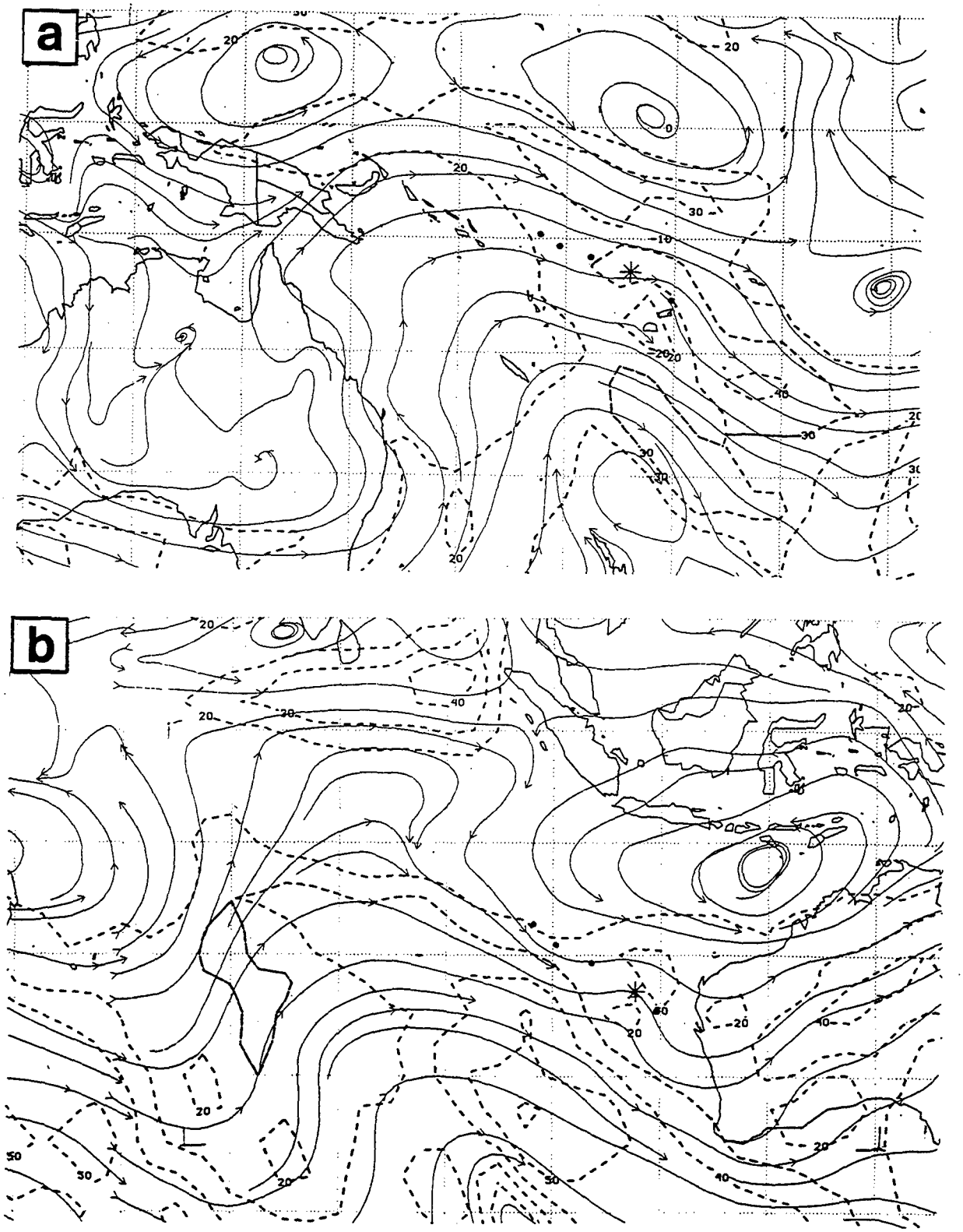

Figure 16. NOGAPS 500-mb analyses as in Fig. 7, except for (a) 00 UTC 15 December 1994, and (b) 00 UTC 16 May 1997.

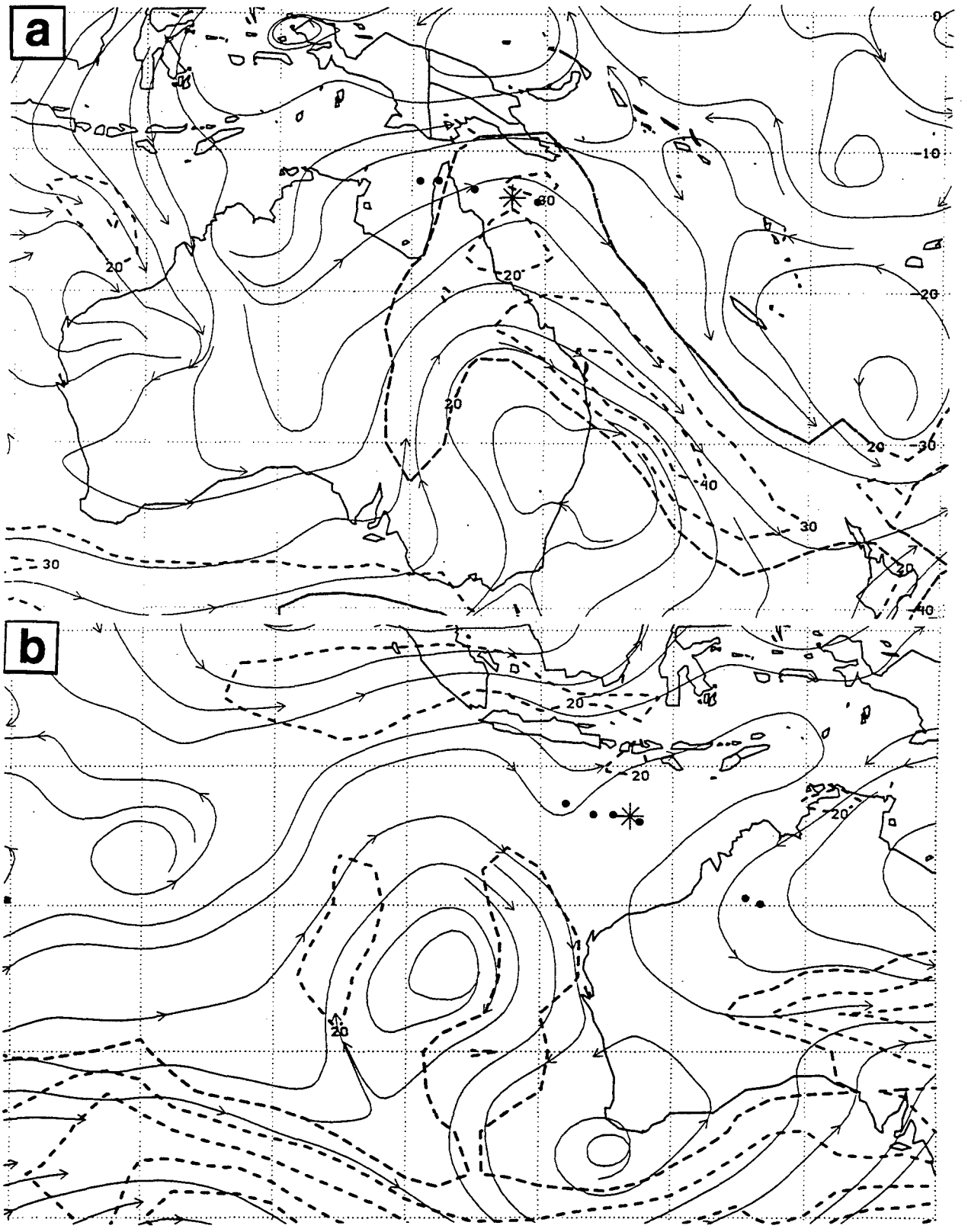

Figure 17. NOGAPS 500-mb analyses as in Fig. 7, except for (a) 12 UTC 16 February 1996, and (b) 00 UTC 18 December 1996.

A more subtle H/EW case is illustrated in Fig. 17b, in which a midlatitude trough has split the subtropical anticyclone and merged with the monsoon trough (notice the east-west oriented 20-kt isotach along 5°S in the equatorial westerly flow). Whereas the TC near 14°S, 117°E had been moving steadily eastward 24 h ago, its translation speed is decreasing at the time of this analysis. The TC is evidently moving into a weaker environmental flow and approaching a bifurcation point. If the trough weakens and drifts northwestward, the subtropical anticyclone over northern Australia will likely become re-established and penetrate westward. If this scenario occurs, the TC will gradually experience a westward environmental steering on the equatorward side of the subtropical anticyclone. That is, the synoptic pattern/region would undergo a transition from H/EW to S/DR, and the track direction would change to westward. The key to forecasting such a scenario is an accurate prediction of the relative strengths (and positions) of the trough to the southwest and the subtropical anticyclone over northern Australia. An alternate scenario is that the monsoon trough may become re-established or intensify and the environmental steering and track will continue eastward. Until one system or the other begins to dominate the environmental steering of the TC, its motion is likely to be slow with large direction changes possible.

3. Tracks. As indicated above and by the small number of H/RE tracks in Fig. 18a, these cases are rare. The short tracks in three of the five cases during January 1994-June 1997 indicate that the TC may not persist very long in this pattern region. However, the long equatorward tracks terminating near 10°S, 71°E and 10°S, 152°E provide counter-examples that are marked departures from climatological tracks.

The number of H/RP tracks (Fig. 18b) is considerably larger. Except for the TC terminating near 26°S, 62°E, these tracks are generally southwestward, as would be expected from the conceptual model in Fig. 13. That is, these TCs are on the northwestern shoulder of a meridional subtropical anticyclone and the tracks turn anticyclonically to become southward as the TC approaches the axis of the anticyclone. As noted in the NOGAPS analyses in Fig. 16, the subtropical anticyclone and the adjacent trough to the west may be tilted NW-SE, which could also lead to a more southward track.

A surprisingly large number of H/EW tracks (Fig. 18c) are found in the South Indian Ocean. Only a few cases are found in the South Pacific east of the Cape York Peninsula. Notice also that these tracks lie in the latitudinal range of 10°-20°S, which normally might be considered the tradewind easterly regime in which TCs would be moving westward. Here, the tracks are toward the east, and some are quite long. Thus, the H/EW situations have anomalous tracks and are not that infrequent. These cases again emphasize the importance of the very active upper-troposphere in the SH with midlatitude troughs that penetrate deep into the tropics. In combination with the monsoon trough and the equatorial westerly flow that establishes favorable cyclonic environmental shear and thermodynamic conditions, TC formation does occur. Clearly, this is one of the unique aspects of TC formation and movement in the SH that does not occur in the western (or eastern) North Pacific.

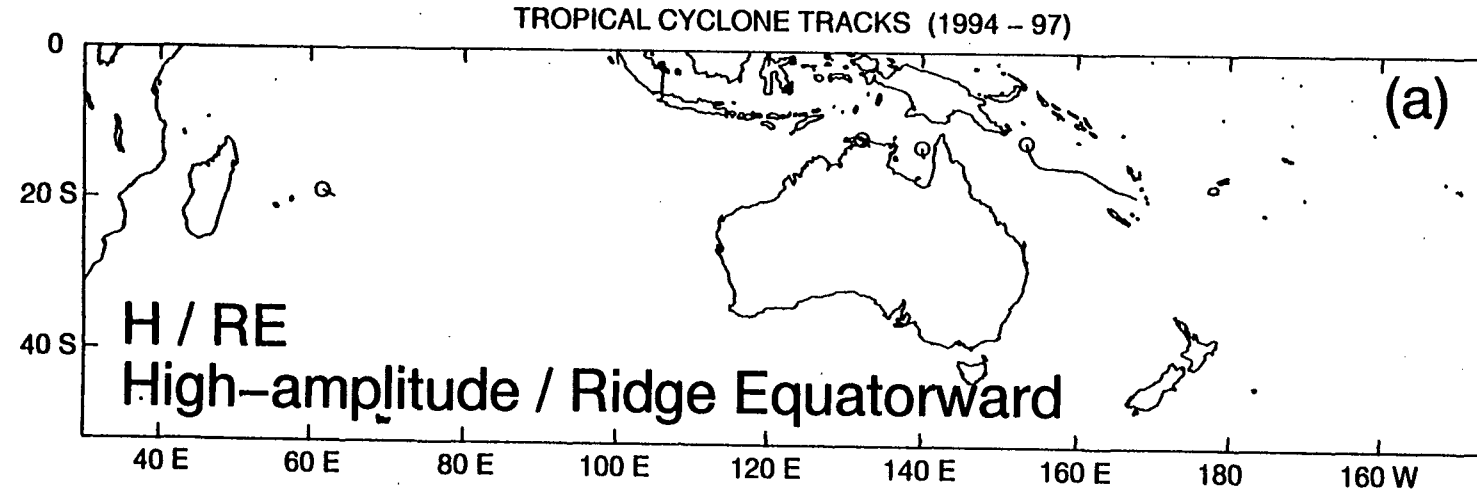

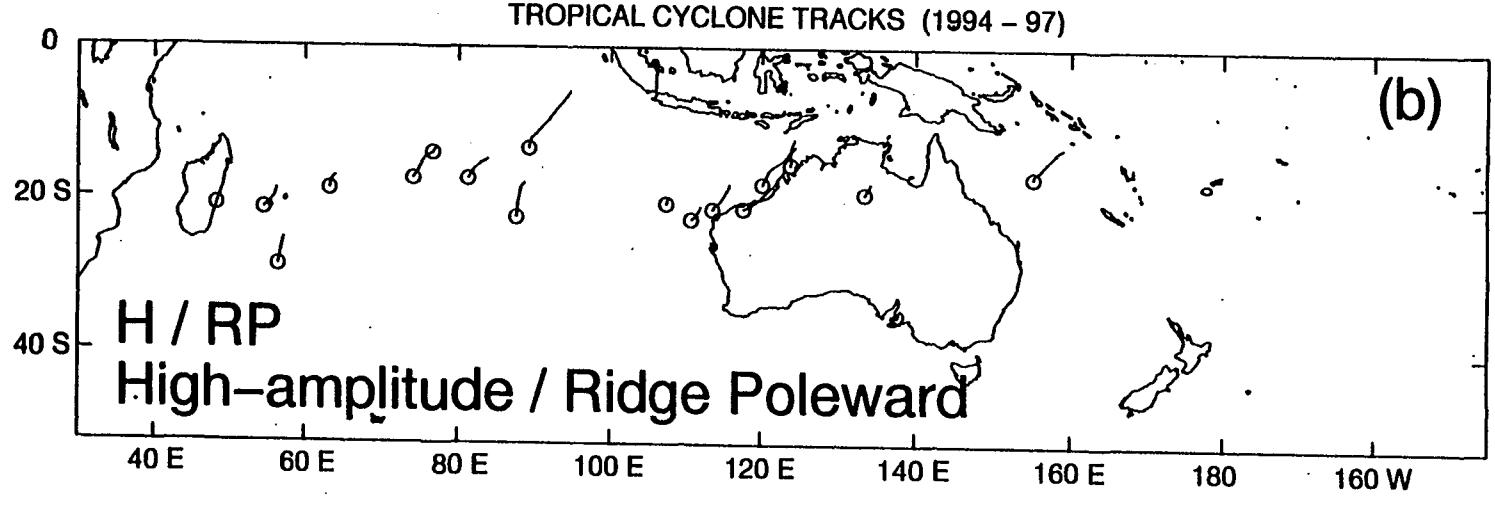

Figure 18. Tracks as in Fig. 4, except only for TCs while in the High-amplitude (H) pattern and (a) Ridge Equatorward (RE) and (b) Ridge Poleward (RP) regions.

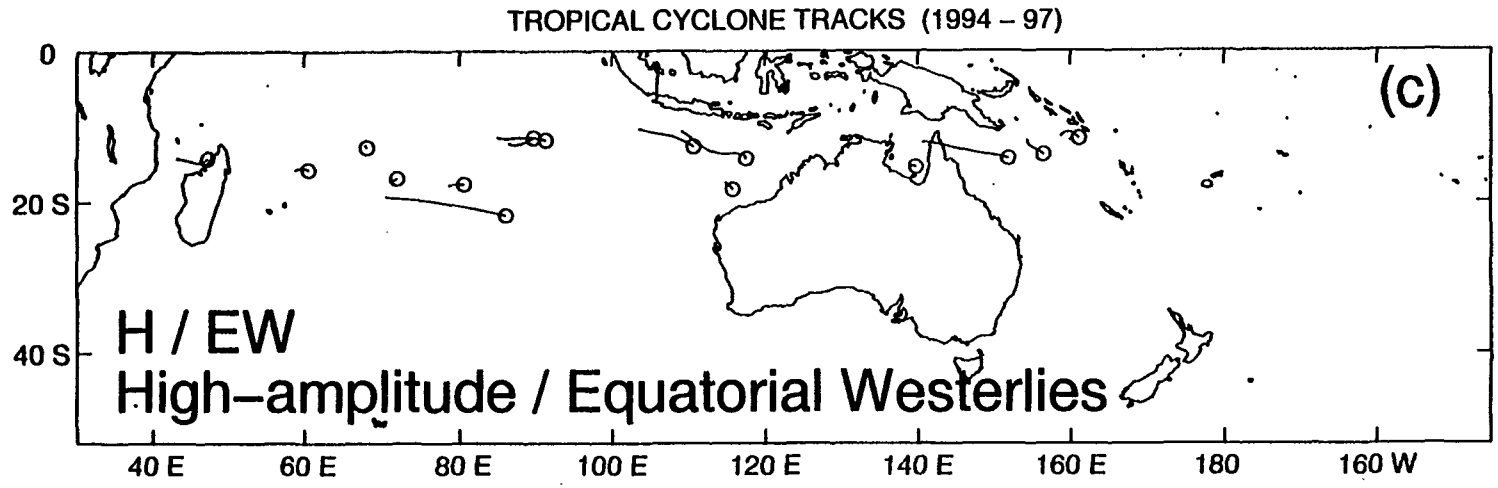

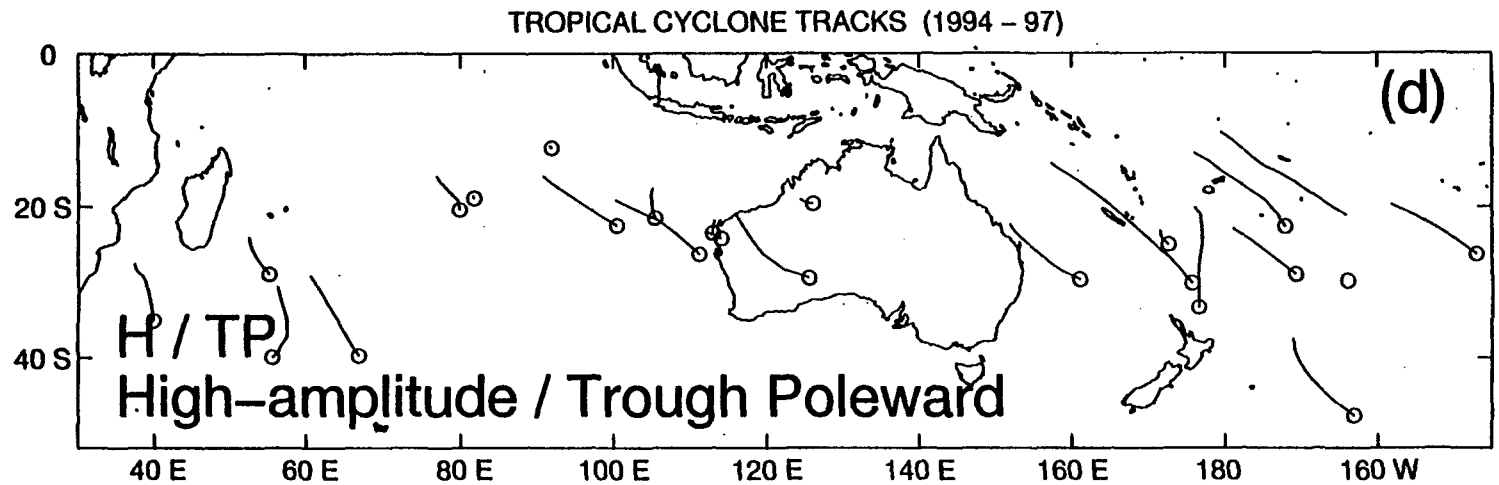

Figure 18 (continued). Tracks in H pattern for the (c) Equatorial Westerlies (EW) and (d) Trough Poleward (TP) regions.

Another unusual characteristic of SH TCs is the long poleward tracks in association with the H/TP pattern/region (Fig. 18d). In the South Pacific region, many of these tracks are southeastward throughout most of the life cycle of the TC, and thus are very anomalous from a climatological perspective. Recall that the environmental flow determining the orientation and translation speed of these H/TP storms are determined by the amplitude of the midlatitude trough in conjunction with an anticyclone to the east (see conceptual model in Fig. 13). Since both of these circulations are transient, the translation speed along the tracks in Fig. 18d are not necessarily uniform. Thus, the TC motion is quite difficult to forecast, and the western South Pacific is acknowleged to be the most difficult of all basins for TC track forecasting (Pike and Neumann 1985). However, the tracks in Fig. 18d indicate that the South Indian Ocean also has a considerable number of H/TP tracks. In the western South Indian Ocean, the tracks continue quite far poleward as in the P/PO pattern/region (Fig. 12). In the eastern South Indian Ocean, the H/TP storms threaten the Western Australia region.

d. *Multiple synoptic pattern.*

The Multiple (M) TC synoptic pattern was introduced in the original Systematic Approach (Carr and Elsberry 1994) to account for anomalous TC tracks in special conditions involving two TCS, which occurs rather frequently in the western North Pacific region. However, the M synoptic pattern is also one of the binary TC interactions defined by Carr *et al.* (1997a) -- the semi-direct TC interaction (STI) that has been adapted for the SH in Fig. 5b, and described in Section 2e.

1. Conceptual model. The conceptual model for the M pattern is given in Fig. 19. Recall from the discussion of STI that the two TCs must be separated by more than about 10° lat., oriented approximately east-west, and be at a latitude within about 10° lat. of the subtropical anticyclone axis. These geometric relationships distinguish the STI from the direct DTI, because the two TC circulations do not overlap, and establish pressure gradients with adjacent subtropical high pressure cells that result in anomalous steering currents.

Notice in Fig. 19 that the low pressure associated with the western TC and the high pressure of the eastern subtropical anticyclone cell will establish a poleward environmental steering across the eastern TC. The region in which these conditions are met is called the Poleward Flow (PF) synoptic region in the M pattern. This is also the STIE in the conceptual models (Fig. 5b) of binary TC interactions. An important track characteristic of the M/PF pattern/region is that the TC will generally move poleward toward the recurvature point without the customary deceleration of the S/DR to S/WR to S/MW recurvature sequence.

The other special arrangement in Fig. 19 is that the low pressure associated with the eastern TC and the high pressure of the western subtropical anticyclone cell may establish an Equatorward Flow (EF) environmental steering. This scenario defines the EF synoptic region in the M pattern (Fig. 19) and the STIW conceptual model in Fig. 5b. Notice that this equatorward steering flow tends to oppose the expected poleward and westward beta-effect propagation for a

MULTIPLE (M) PATTERN
CHARACTERISTIC TRACKS

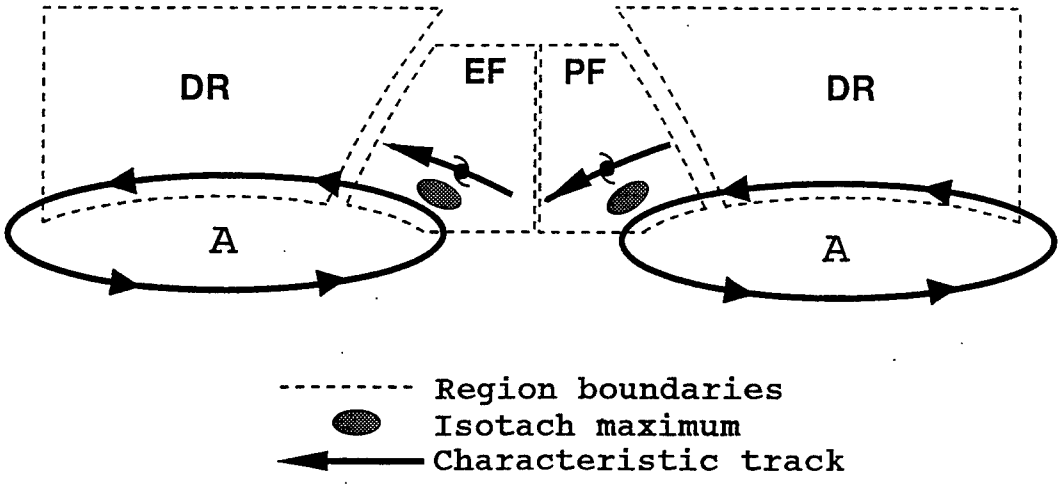

Figure 19. Conceptual model as in Fig. 6, except for the Multiple (M) TC synoptic pattern, including the Equatorward Flow (EF) and Poleward Flow (PF) synoptic regions.

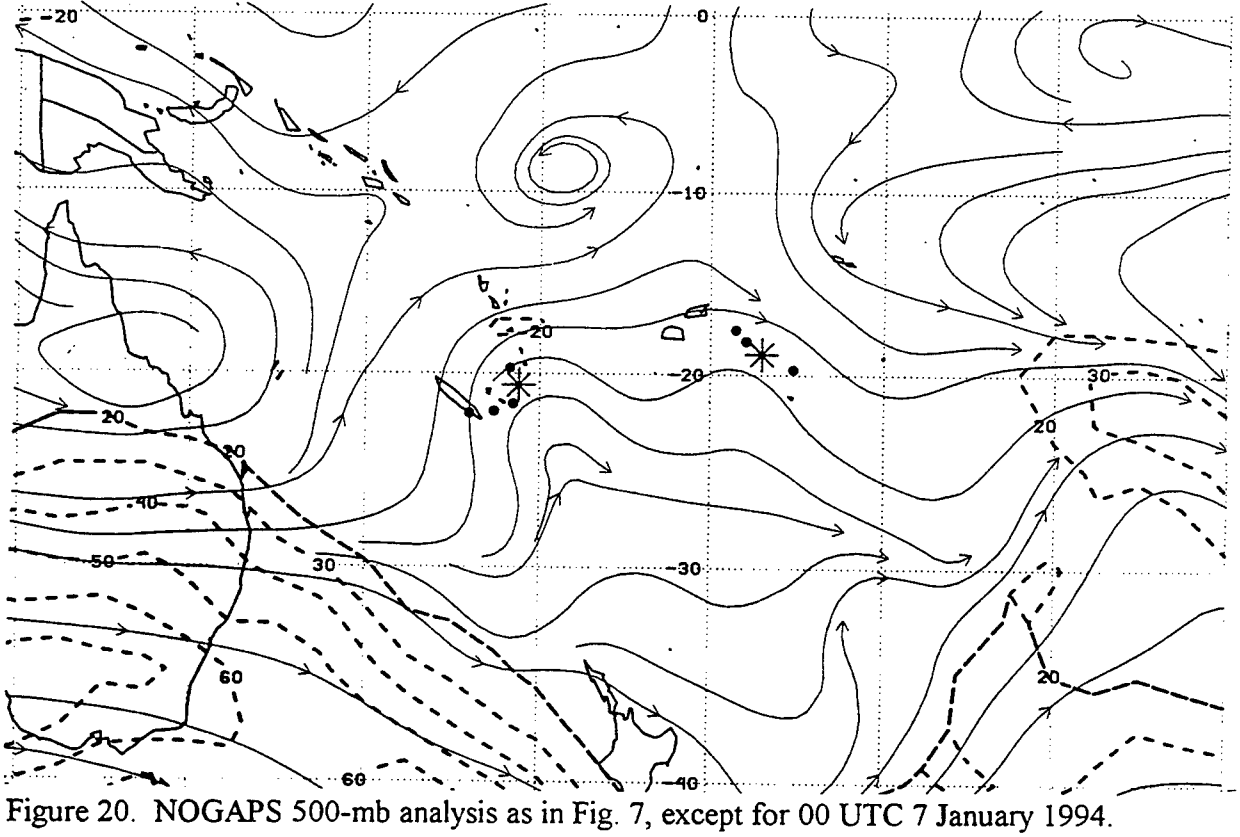

Figure 20. NOGAPS 500-mb analysis as in Fig. 7, except for 00 UTC 7 January 1994.

SH TC. Consequently, the TC in the EF region will tend to have a westward and either small poleward or small equatorward drift depending on the relative strengths of the opposing two effects. Thus, the TC in the EF region may make a transition to the Standard (S) pattern/Dominant Ridge (DR) region associated with the anticyclone to the west.

2. Analysis example. The conditions for a M pattern are illustrated in Fig. 20. The separation of these two TCs is about 15° lat., and they are oriented east-west near the subtropical anticyclone axis. Notice that the western TC Rewa (0594) has been moving equatorward and in the next 12 h will move toward the northwest. This equatorward motion is consistent with a pressure gradient between the low pressure associated with the eastern TC (0794) and the high pressure associated with the subtropical anticyclone centered near 20°S, 146°E. Meanwhile, the eastern TC near 19°S, 177°W has begun to accelerate poleward (compare the + 12-h position relative to the - 12-h position). This acceleration is consistent with a poleward pressure gradient between the western TC Rewa and the eastern subtropical anticyclone cell.

3. Tracks. These M patterns are not expected to persist very long as the special conditions regarding the separation distance and the favorable positions relative to the anticyclones to the east or west do not persist. Storm tracks in Fig. 21 confirm this expectation. In addition to the rare events of a M/EF event indicated by the few cases in Fig. 21a, the equatorward tracks are very short. This characterization is generally true also for the M/PF events in Fig. 21b. However, one case in the central South Indian Ocean did persist in the M/PF for some time and had a relatively long track toward the southwest.

The relatively rare M synoptic patterns in the SH probably is related to several factors. First, the occurrence of multiple TCs with separation distances of 10° - 20° lat. is smaller in the SH (Newmann 1993). Second, the more transient and smaller amplitudes of the subtropical anticyclone cells in the SH does not allow the establishment and maintenance of the pressure gradients implied in the conceptual model in Fig. 19.

Although the simultaneous occurrence of more than one TC in the SH is certainly notable, the infrequent occurrence may not cause the forecaster to check for a M pattern, or equivalently whether the STIE or STIW conditions are met. Thus, the experimental application of the objective diagnosis of TC interactions described in Section 2e is important. The results of this experiment will be described in Section 5 below, and examples of NOPGAPS analyses and tracks will be given.

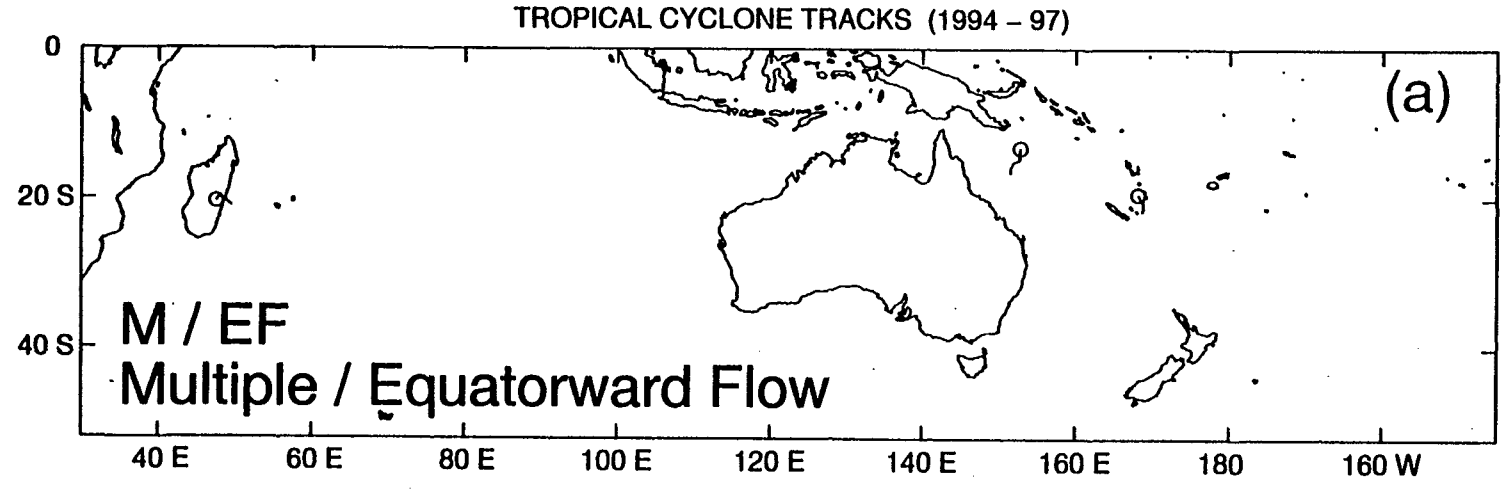

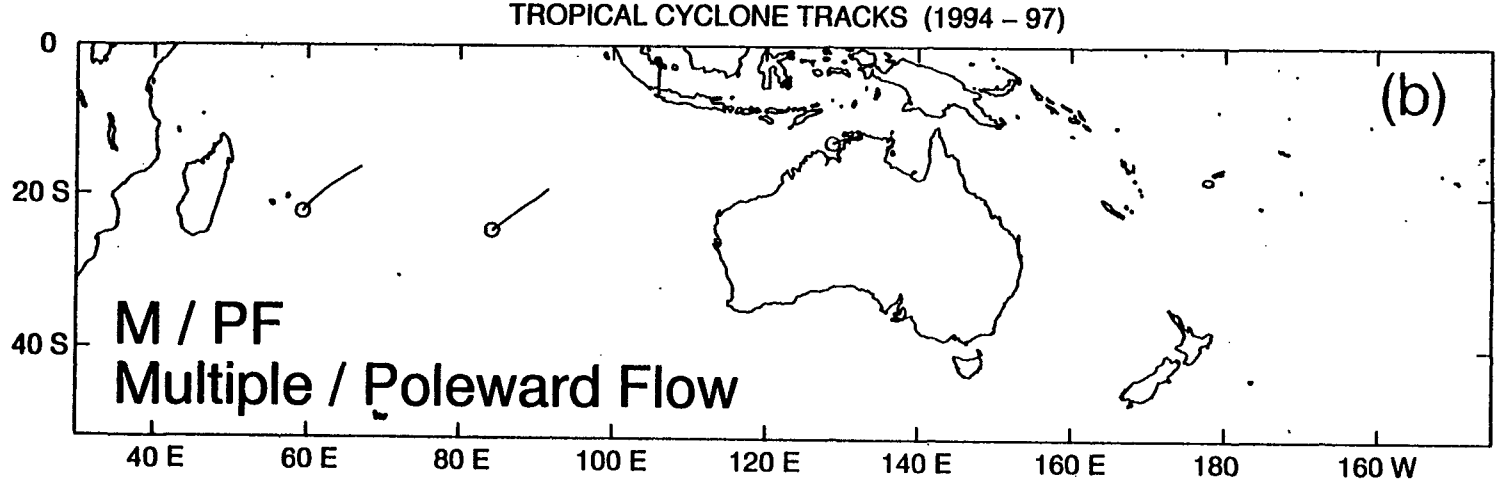

Figure 21. Tracks as in Fig. 4, except only while the TCs are in the (a) M/Equatorward Flow (EF) and (b) M/Poleward Flow (PF) pattern/regions.

4. ENVIRONMENT STRUCTURE SUMMARY

The conceptual models of the four synoptic patterns are summarized in Fig. 22. A total of 11 synoptic regions are defined within the four synoptic patterns. A short-term climatology from January 1994 through June 1997 has been prepared. Considering each TC on each 12-h NOGAPS analysis whenever the intensity was at least 25 kt (these are JTWC intensities based on one-minute average winds), a total of 1592 characterizations resulted. It is important that all of these cases could be characterized into just four patterns and 11 regions.

The synoptic pattern climatology is summarized in Fig. 23a. Notice that 61% of all SH cases are in the Standard (S) pattern, which is a slightly higher percentage than in the western North Pacific. The 22% of Poleward (P) pattern characterizations in the Southern Hemisphere is smaller to the total number in the western North Pacific, except TCs passing into the Midlatitude Westerlies (MW) are kept in the P pattern rather than being transferred to the S pattern as in these SH characterizations. The new synoptic pattern required in the SH is the High-amplitude (H) pattern, which constitutes 15% of the 1592 cases. As noted in Section 3d, the Multiple (M) pattern is relatively rare, with only 2% of all cases. Clearly some of these percentages in Fig. 23a could change with a larger sample.

The corresponding synoptic region climatology is given in Fig. 23b, with segments having the same shadings as in the synoptic pattersn in Fig. 23a. Thus, the 43% cases in the Dominant Ridge (DR) region are associated with the S pattern. Notice that 7% of these S pattern cases are in the Equatorial Westerlies (EW) region. Another 4% of the cases are in the EW region of the H pattern. These eastward-moving TCs at low latitudes thus constitute 11% of all cases. Only 5% of cases are in the Weakened Ridge (WR) region of the S pattern. This small number reflects the small size of this region (Fig. 22) and the short time that TCs typically stay in this region. Finally, only 7% of all cases are in the Midlatitude Westerlies (MW) region of the S pattern. This small percent is consistent with the short tracks in Fig. 8d.

All of the P pattern cases are in the Poleward-Oriented (PO) synoptic region, which amounts to 22% of the 1592 cases. In addition to the 4% cases in the H/EW pattern/region, the Trough Poleward (TP) and Ridge Poleward (RP) are the next-most frequent cases inthe H pattern. By definition, both of these regions will have poleward tracks. The distinction is whether the trough or the ridge circulation provides the dominant environmental steering influence (see Fig. 22). As indicated in Section 3c, the Ridge Equatorward (RE) region is rarely found, and only 1% of all cases are in this region. Also rare are the Poleward Flow (PF) and Equatorward Flow (EF) synoptic regions of the M pattern, each of which have 1% of all cases. Notice that a M pattern does not imply that both TCs are simultaneously experiencing an anomalous environmental steering. Since the M pattern also represents the Semi-direct TC Interaction (STI), these subsets of TC interactions will be described further in the next section.

SOUTHERN HEMISPHERE SYNOPTIC PATTERNS AND REGIONS

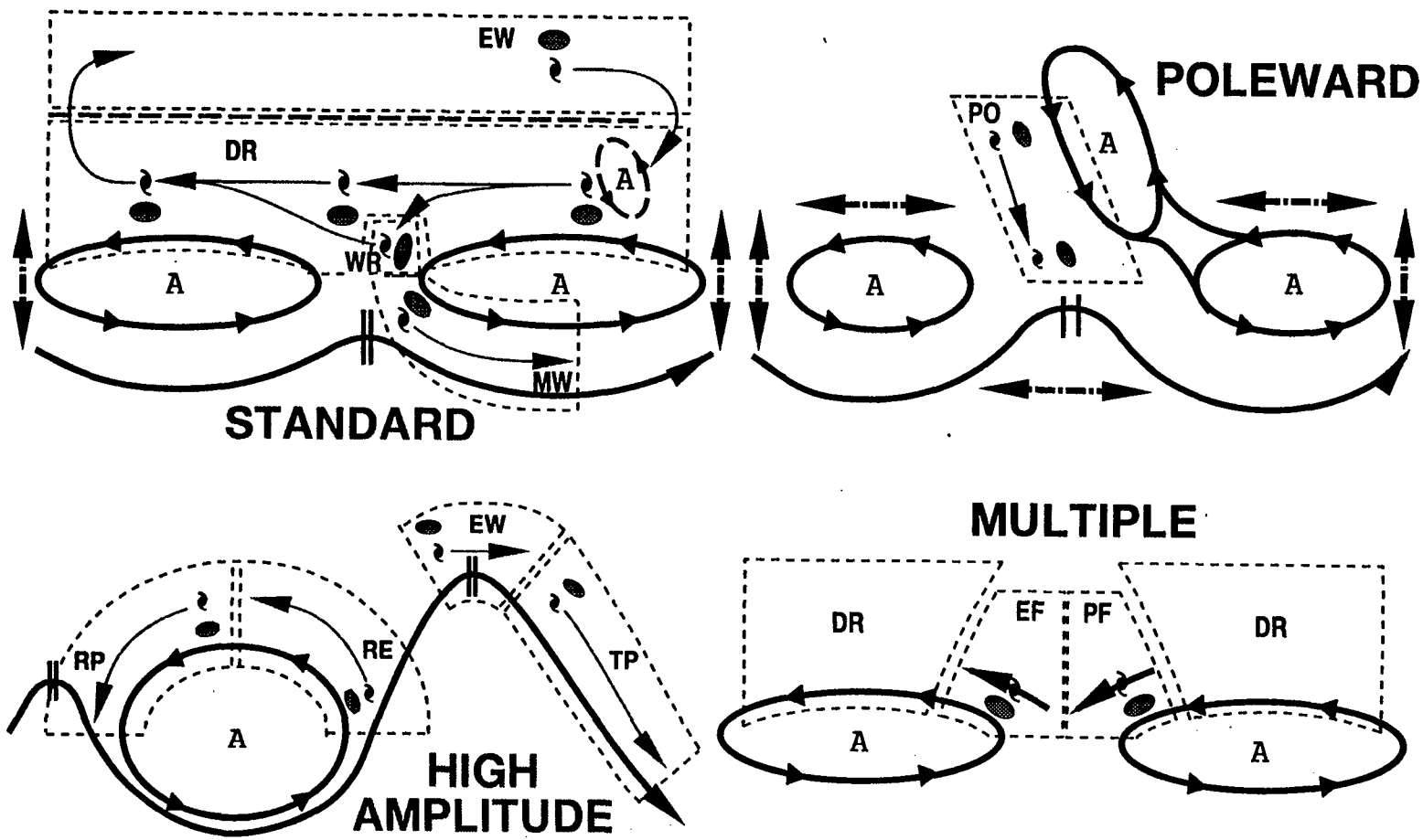

Figure 22. Summary of the four synoptic patterns and associated synoptic regions for the Systematic Approach knowledge base in the Southern Hemisphere.

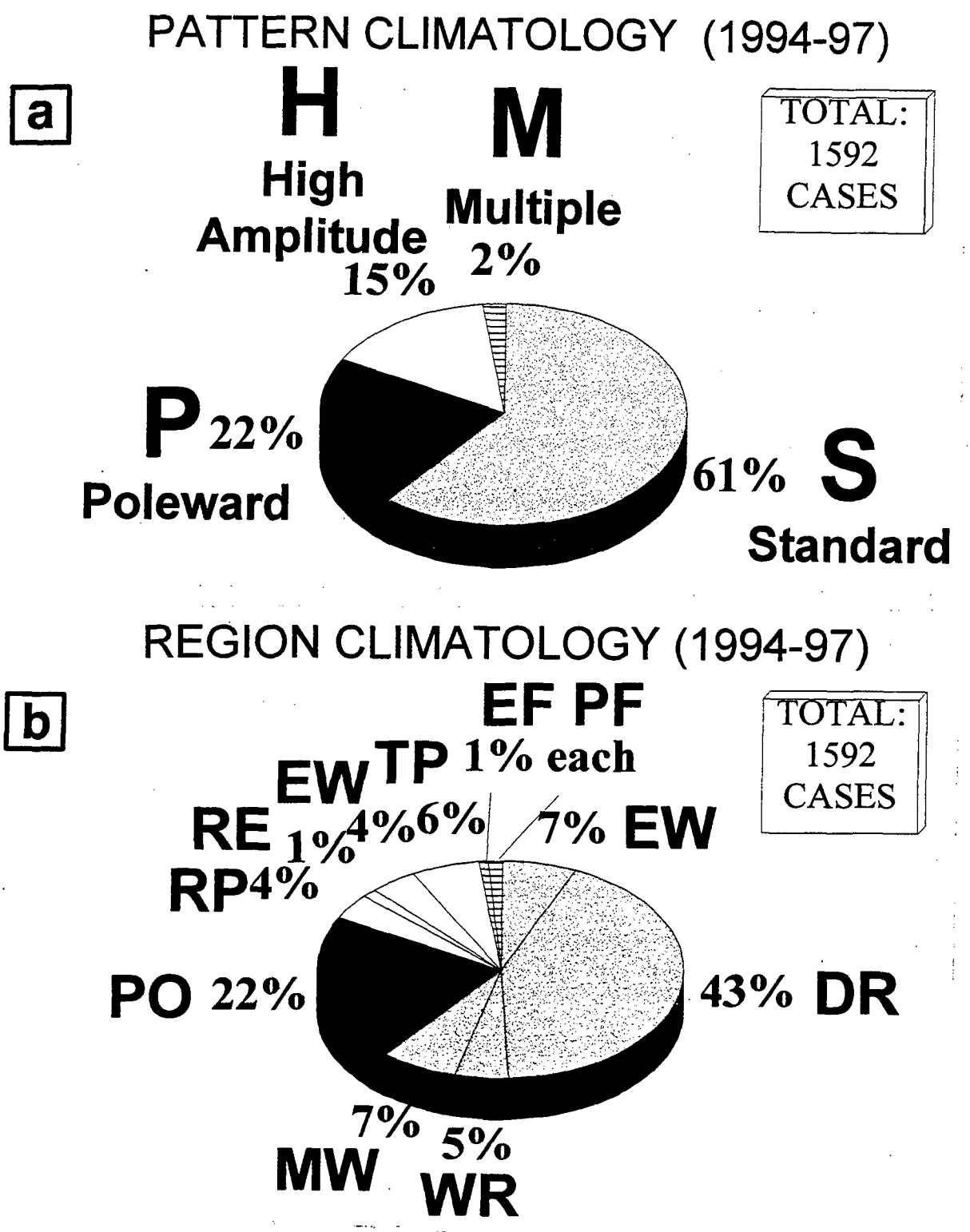

Figure 23. Climatology (percent) of (a) synoptic patterns and (b) synoptic regions in the SH environment structure for 1592 cases during January 1994-June 1997.

5. TROPICAL CYCLONE INTERACTIONS

a. *Frequency*

As mentioned in Section 2e, Carr *et al.* (1997a) have formulated conceptual models for three distinct modes of TCI (see SH adaptations in Fig. 5) based on a comparison of the observed motion of western North Pacific TCs and the structure of the environment in the vicinity of the TCs depicted in NOGAPS streamline/isotach analyses. Since these modes of TCI tend to produce unusual TC motion, it is important for the TC forecaster to be cognizant of the climatological frequency of TCI throughout his/her area of responsibility, and to have a sense of the TC motion patterns that tend to result from the various modes of TCI.

Only two pairs of TCs (0695 and 0795 and 1297 and 1897) in the four-year database of 111 TCs were influenced by mutual Direct TC Interaction (DTI), and one TC (1695) experienced one-way DTI (see Fig. 5a). Thus, on the average the occurrence of DTI is a rare phenomenon in the Southern Hemisphere. In view of this infrequent occurrence of DTI, and because the phenomenon is well-documented (e.g., Lander and Holland 1993), no further discussion is given here.

Similarly, only two TC pairs (0594 and 0794; and 1696 and 1796) were influenced by Semi-direct TC Interaction (STI; see Fig. 5b), which also corresponds to the formation of the Multiple (M) TC synoptic pattern (see Section 3d). In addition, a one-way variation of STI was invoked to explain brief periods in the tracks of six other TCs (1195; 1795; 2095; 1096; 1897; and 3297). That is, the orientation of the TCs and the adjacent subtropical anticyclone cell was such that only one TC of the pair was classified as being in the M pattern. Thus, a total of eight independent instances of STI (or two per year) were identified. However, the majority of these were marginal cases. Barring any significant variation of STI frequency over multi-year periods, it appears that STI is an infrequent and not particularly robust phenomenon in the Southern Hemisphere. This observation is consistent with prevalance of high-amplitude midlatitude wave activity in the Southern Hemisphere that tends to preclude the development of persistent, zonally oriented subtropical anticyclones that are necessary for a STI event.

Recall that Indirect TC Interaction (ITI; see Fig. 5c) has two variants: (i) ITIE, which results in a period of anomalous equatorward motion (or significantly reduced poleward motion) of the eastern TC in response to the beta-induced anticyclone that tends to form on the northeast periphery of the western TC; and (ii) ITIW, in which the eastern TC erodes the peripheral anticyclone of the western TC, which results in a decreased poleward motion of the western TC and a poleward turn by the eastern TC. Although only a few poorly defined ITIW events were observed, the tracks of 18 TCs that were of tropical depression intensity or greater were influenced by the ITIE phenomenon. In all but two of these cases a TC, or its precursor or remnant, was the source of a peripheral anticyclone that subjected the eastern TC to equatorward steering. In those other two cases, the source of the peripheral anticyclone causing the ITIE was a tropical disturbance that did not intensify sufficiently to be designated as a TC, but was clearly evident in the satellite imagery and NOGAPS analyses.

The 18 observed cases of ITIE corresponds to an average rate of about five times per year, which is larger than the three per year rate in the western North Pacific observed by Carr *et al.* (1997a) for a seven-year dataset. Owing to the comparatively small size of the Southern Hemisphere database, the difference of ITIE average frequency in the two basins is not statistically significant. Nevertheless, ITIE is clearly a frequent phenomena south of the Equator, and occurs throughout the region where Southern Hemisphere TCs form (Fig. 24). Thus, forecasters throughout the Southern Hemisphere may expect to regularly encounter ITIE events. Illustrations of ITIE are provided in the next section to give forecasters an appreciation for the type and range of track alterations that may result, and also to show that the fidelity with which NOGAPS analyses depict the intervening anticyclone between the two TCs may vary from case to case.

b. *ITIE illustrations*

From 12 UTC 14 March 1994 to 12 UTC 17 March 1994, the track of TC Mariola (2194) turns from a climatological west-southwest direction to a non-climatological west-northwest direction, and then turns back to a climatological heading (Fig. 25). The NOGAPS analyses during this period (Fig. 26a-d) depict an anticyclone between Mariola and Litanne as in the conceptual model in Fig. 5c. The period of west-northwest motion of Mariola during 12 UTC 14 March to 12 UTC 15 March in Fig. 25 results from the superposition of the equatorward steering flow on the east side of the intervening anticyclone and the generally westward steering of the subtropical anticyclone to the south. On 12 UTC 16 March (Fig. 26c), the isotach maximum east of Mariola is consistent with an equatorward steering. Mariola is moving west at this time, presumaably as a result of the equatorward steering. Given that conventional data are sparse in this region, the intervening anticyclone may be under-represented on 15 March (Fig. 26b), and over-represented on 16 March (Fig. 26c). After 12 UTC 15 March, Litanne weakens as it moves poleward along the east coast of Madagascar. Coincidentally, the equatorward motion of Mariola decreases, and then west-southwestward motion begins. The interpretation here is that the strength of the beta-induced anticyclone of Litanne decreases as the TC weakens, which then can no longer induce an equatorward steering flow across Mariola. Another factor that may play a role in the resumption of poleward motion by Mariola after 12 UTC 16 March is that the size of Mariola's circulation apparently increased considerably (compare Figs. 26a and 26d) during the period of indirect TC interaction. According to the barotropic modeling results of Carr and Elsberry (1997a), such a size increase should result in an increased southwestward propagation by Mariola, and also a development of a beta-induced ridge to the northeast that generates an additional poleward steering component.

The ITI influence via the peripheral anticyclone associated with Litanne resulted in a comparatively minor perturbation on the west-southwestward track that Mariola would otherwise have followed in response to easterly steering by the subtropical ridge. The impact of ITIE is not always so subtle. During 26-29 January 1997, the tracks (Fig. 27) of Pancho/Helinda and Iletta underwent very pronounced equatorward and poleward excursions, respectively, during an ITIE event that occurred when the influence of the subtropical ridge was weak and variable due to

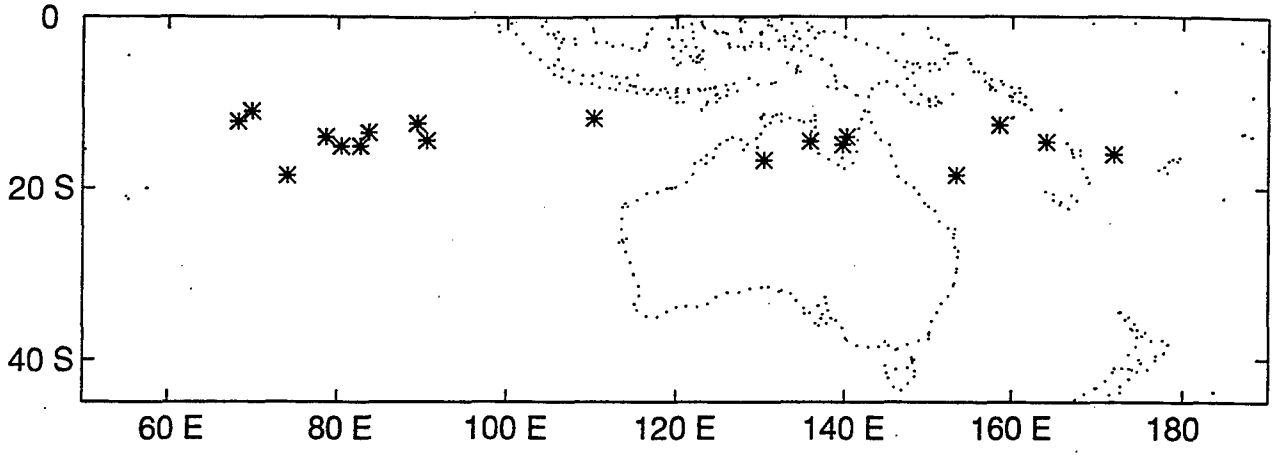

Figure 24. Locations at which ITIE events were first detected during January 1994-June 1997.

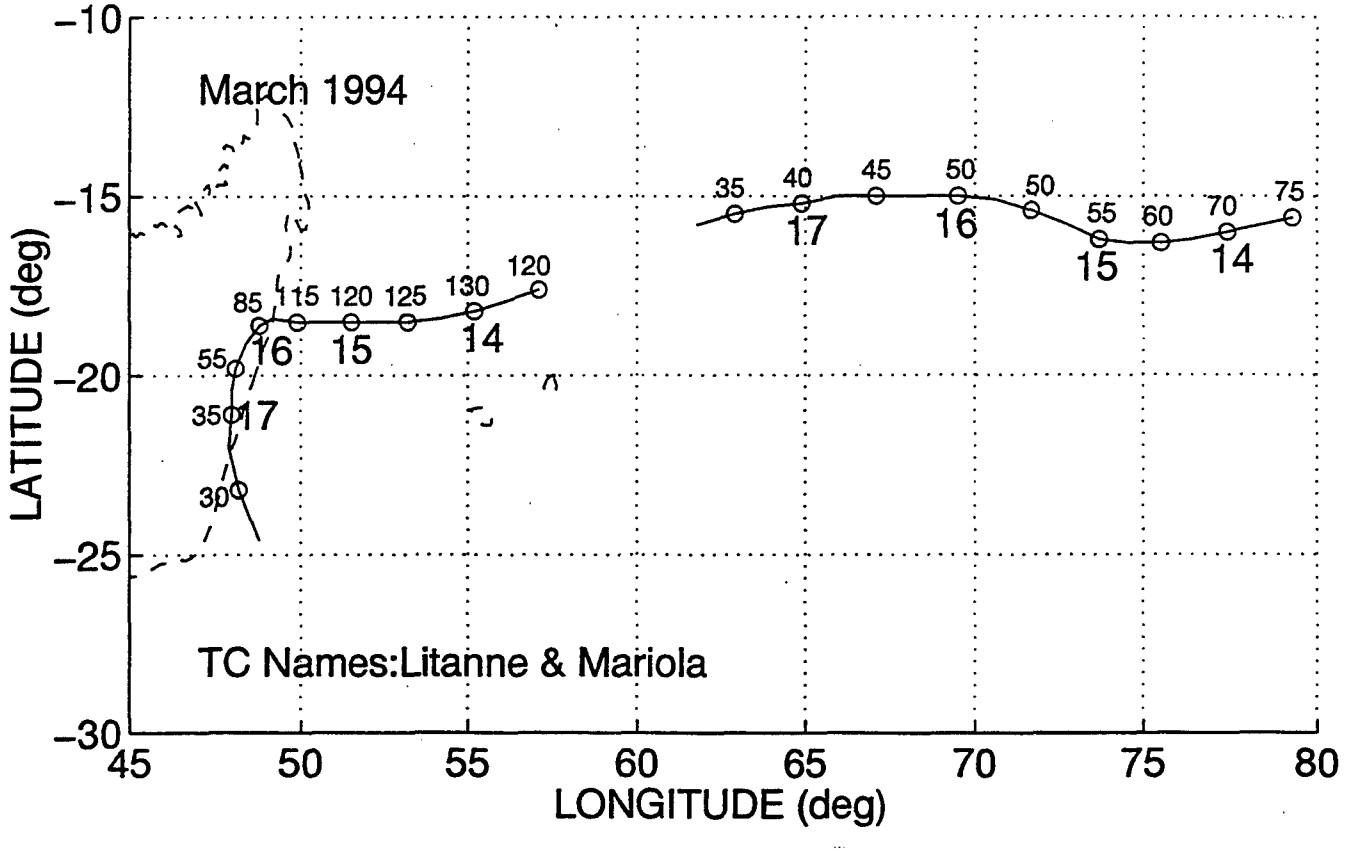

Figure 25. Tracks of TC 2094 (Litanne) and 2194 (Mariola) during 12 UTC 13 March to 12 UTC 17 March with circles each 12 h. Large numbers indicate the date and small numbers are the intensity (kt).

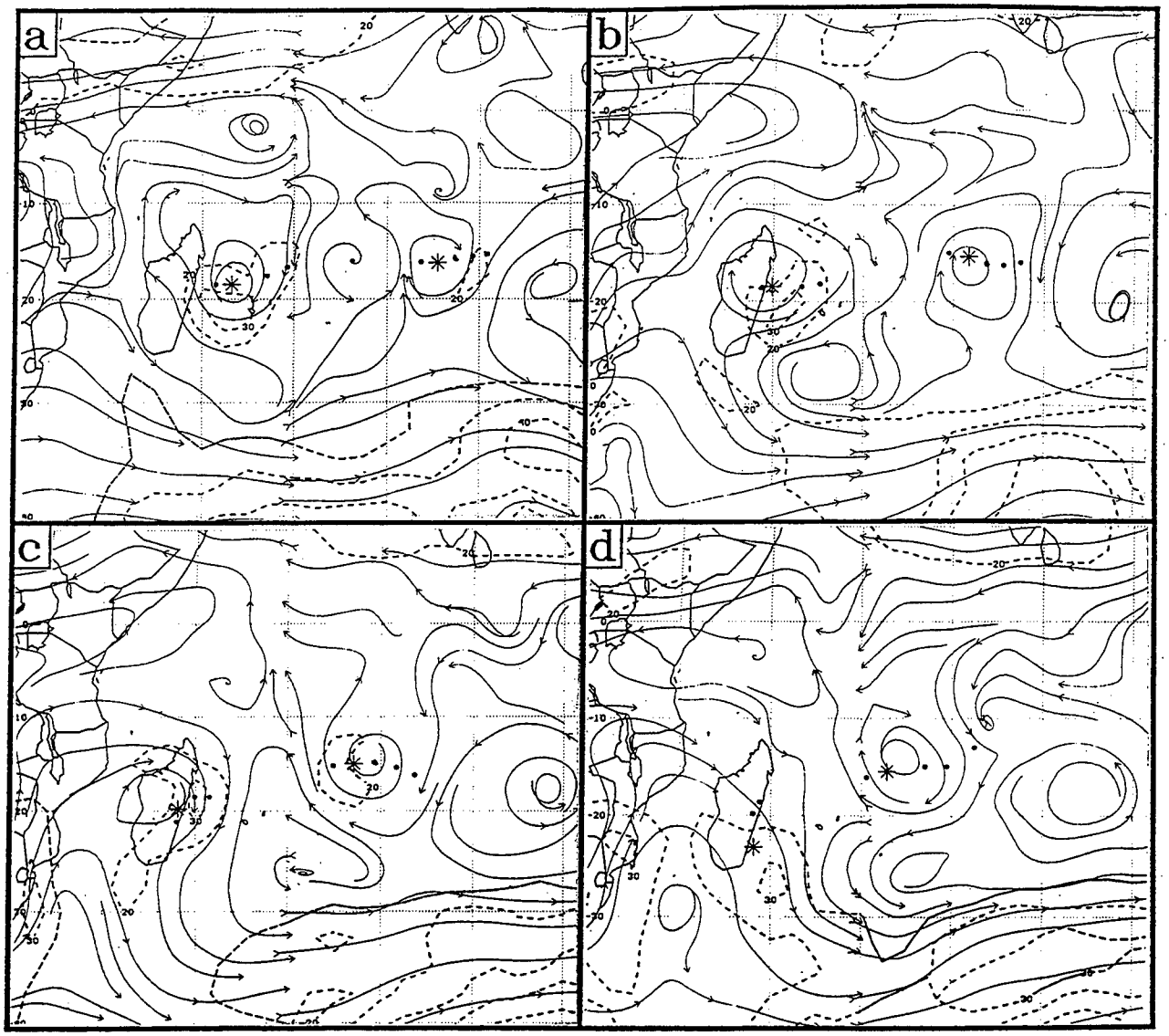

Figure 26. NOGAPS 500-mb analyses as in Fig. 7, except at 12 UTC on (a) 14, (b) 15, (c) 16, and (d) 17 March 1994. The western (eastern) TC is Litanne (Mariola).

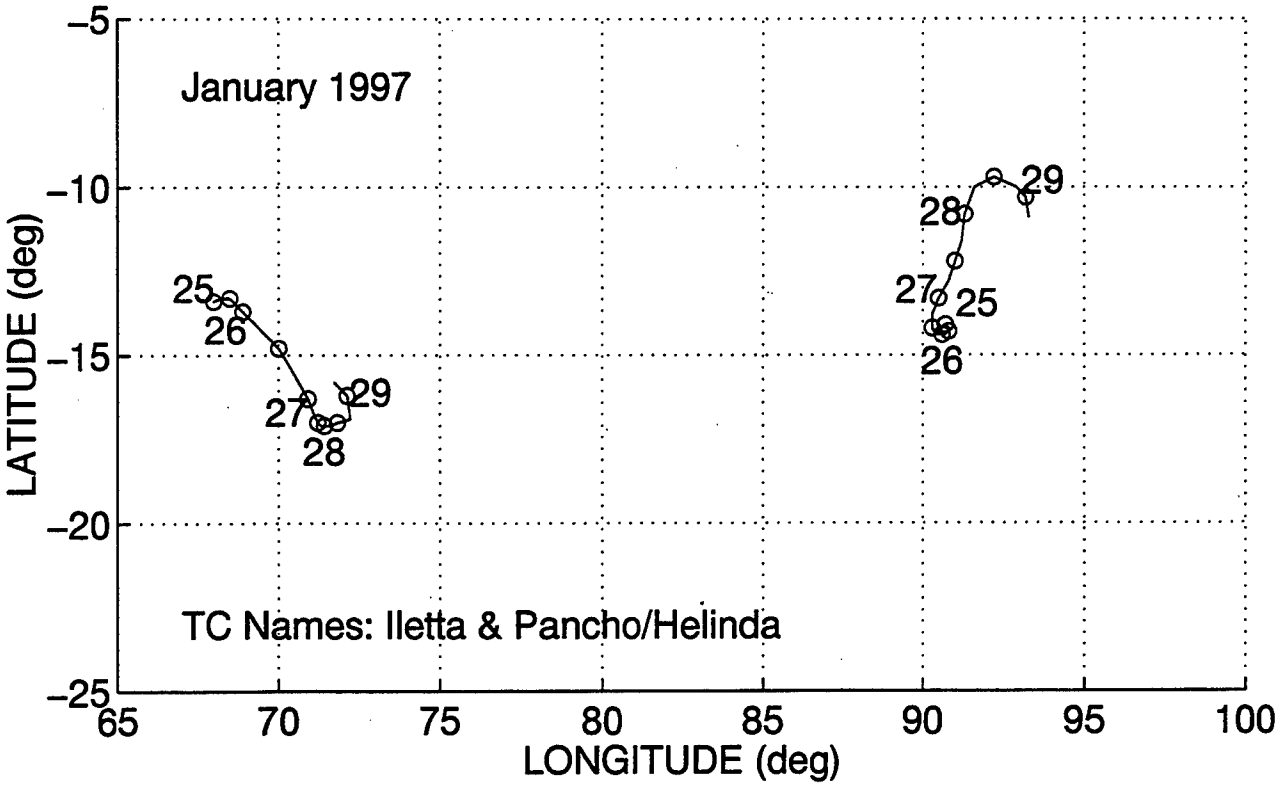

Figure 27. Tracks as in Fig. 25 of TCs 2197 (Iletta) and 1997 (Pancho/Helinda) during 12 UTC 23 January to 00 UTC 29 January 1997 with circles each 12 h.

strong midlatitude wave activity (Fig. 28a-d). At 00 UTC 26 March (Fig 28a), a midlatitude trough to the southeast of Iletta has penetrated the subtropical anticyclone and imposed a poleward environmental flow over Iletta, as indicated by the isotach maximum immediately northeast of Illeta. Generation of a beta-induced anticyclone to the east of Iletta imposes an equatorward steering across Pancho/Helinda, which is consistent with the presence of a 20-kt isotach maximum to the northwest of Pancho/Helinda. On the 27th and 28th (Figs. 28b-c), the ITIE pattern of TC/intervening ridge/TC is readily apparent. During this period, Pancho/Helinda moves strongly equatorward under the influence of the peripheral anticyclone being generated by Iletta, which has intensified from 50 kt at 00 UTC 25 January to 75 kt at 00 UTC 27 January. After 27 January, Iletta rapidly dissipates, which is expected to remove the source of the intervening of the anticyclone that has been driving Pancho/Helinda equatorward. Accordingly, the NOGAPS analyses on 28 and 29 January (Fig. 28c-d) indicate a weakening of the anticyclone between the two TCs. The concomitant poleward turn of Pancho/Helinda during 28 January (Fig. 27) is precisely what one would expect in response to the dissipation of the peripheral anticyclone from Iletta and the persistent deep midlatitude trough to the south. As in the case of Mariola above, the poleward turn by Pancho/Helinda is also supported by an increase in the size of the TC circulation and the development of a peripheral anticyclone to the northeast of Pancho/Helinda

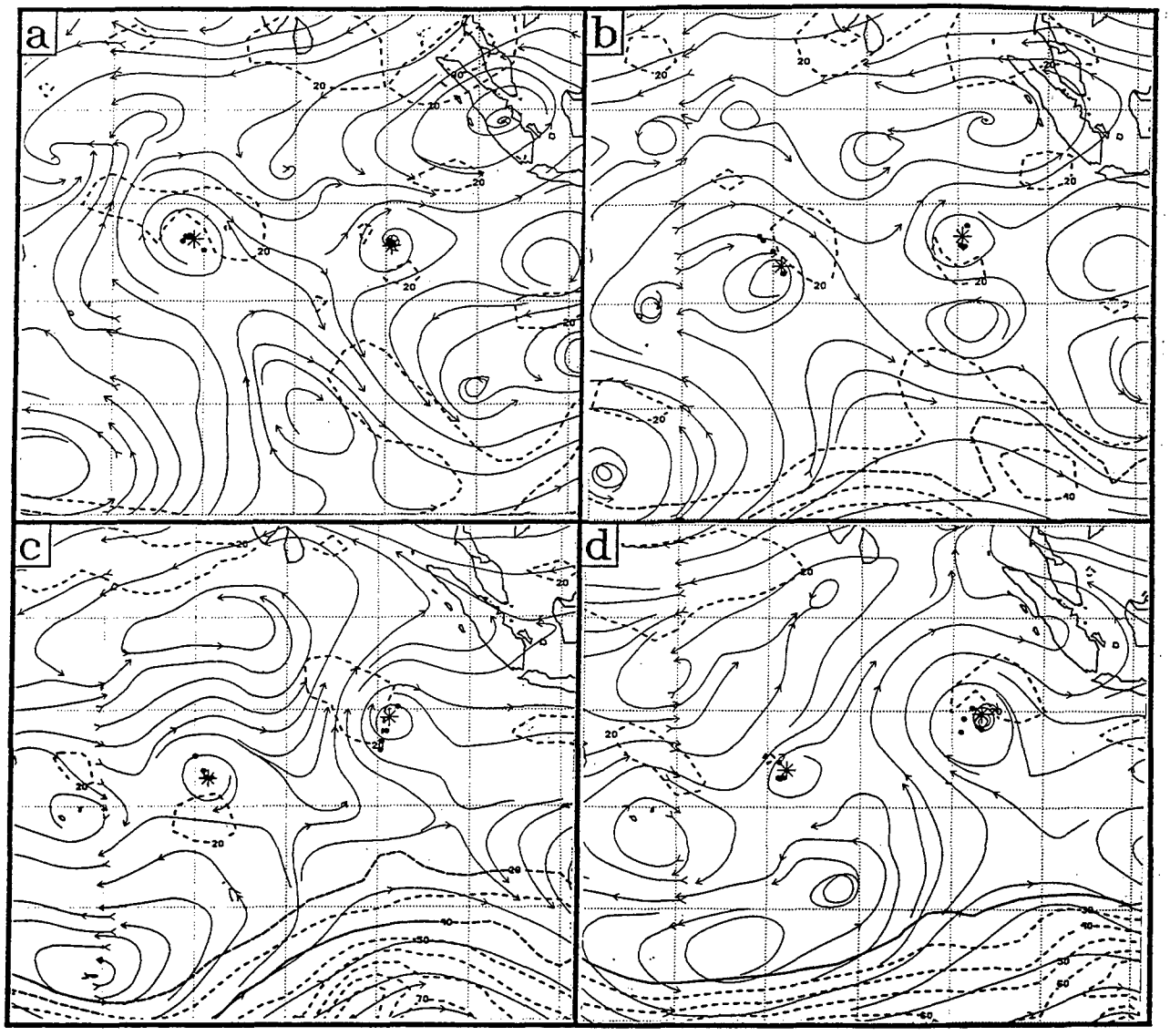

Figure 28. NOGAPS 500-mb analyses as in Fig. 7, except at 00 UTC on (a) 26, (b) 27, (c) 28, and (d) 29 January 1997. The western (eastern) TC is Iletta (Pancho/Helinda).

(compare Figs. 28a and 28d). The apparent growth of Pancho/Helinda may have also contributed to the concomitant weakening of the intervening anticyclone (which would be an example of the ITIW phenomenon), but this is difficult to establish independently of the weakening expected as a result of the dissipation of Iletta.

The above two illustrations of the ITIE phenomena in the Southern Hemisphere are a stereotypical sequence of track changes that the forecaster should be cognizant of whenever conditions for an ITIE scenario are present. First, the beta-induced dispersion of energy eastward and equatorward of a western TC (Litanne and Iletta in the above cases) generates a peripheral anticyclone that produces an equatorward steering on the eastern TC, as well as a tendency to promote cyclone development in that location (for a NH simulation of this see Fig. 12c of Carr and Elsberry 1997a). If a TC develops or moves into this eastern region (Mariola and Pancho/Helinda in the above cases), the TC will tend to move equatorward and also grow. The growth of the eastern TC in turn tends to generate a beta-induced anticyclone eastward and equatorward of the eastern TC. The poleward steering from this second anticyclone in turn tends to drive the eastern TC poleward, which usually overcomes the ITIE effect from the western TC, particularly if the western TC begins to weaken for any reason (e.g., landfall, vertical wind shear, etc.). In addition, the cyclonic vorticity advection to the southwest of the eastern TC can result in sufficient erosion of the beta-induced anticyclone from the western TC to cause the western TC to turn from a poleward track to a more equatorward track, particularly if the subtropical ridge poleward of the western TC is reasonably strong or is building. This behavior is termed ITIW and regularly occurs in the western North Pacific (see Carr *et al.* 1997a, Fig. 18 and related discussion). As mentioned at the beginning of this section, a definitive example of the ITIW phenomenon was not observed in this four-year database. In view of the comparatively small size of the database, Southern Hemisphere forecasters should not rule out the possibility of ITIW.

In the above two examples, the NOGAPS analyses depicted reasonably well the intervening beta-induced anticyclone from a western TC that explains the period of equatorward motion of the eastern TC. In the following two examples, a temporary period of equatorward motion of an eastern TC occurs that is consistent with the location and development of another TC to the west. Although the track changes are consistent with an ITIE event, an intervening anticyclone may not be readily evident in the NOGAPS analysis. This example illustrates how judicious use of the ITIE conceptual model may enable forecasters to anticipate a complex TC motion scenario that may not be well depicted in the numerical guidance. The case has practical utility since it occurs near the coastline of northern Australia under circumstances in which the ITIE phenomenon appears to have significantly influenced the track, and also the development trend of the affected TC.

During 30 December 1996 to 2 January 1997, the eastern TC Rachel moved in a non-climatological northwest direction, while the western TC Phil followed a sinuous west-southwestward track (Fig. 29). On 30 December, the precursor disturbance that will become Rachel is depicted in the NOGAPS analysis (Fig. 30a) as a comparatively small circulation that has just made landfall on the western shore of the Gulf of Carpentaria. By contrast, Phil is a 70-kt

system near 17°S, 117°E that is depicted as having a large cyclonic circulation. Given the large size of Phil, a significant peripheral anticyclone should be generated that would account for the equatorward motion of Rachel. However, such a feature is not readily evident in the NOGAPS analysis. The absence of the peripheral anticyclone in the NOGAPS analysis may be due to a lack of data, or because Phil and Rachael are only about 18° lat. apart. (less than average separation for ITIE cases), which may be insufficient room for a model of NOGAPS resolution to analyze the anticyclone. Although Rachel contines to move equatorward for the next two days, the corresponding NOGAPS analyses (Figs. 30b-c) do not have an obvious anticyclone between Rachel and Phil, although an equatorward steering adjacent to Rachel and a small isotach maximum to the west are evident in Fig. 30c. The fact that Rachel turns poleward during 2 February (Fig. 29) when Phil undergoes significant weakening provides some circumstantial evidence for the weakening of an unanalyzed beta-induced anticyclone.

Inference of an ITIE influence from Phil may also be found in the development of Rachel, which eventually moved offshore and significant intensification (eventually to 80 kt) occurred. As in the cases of Mariola and Pancho/Helinda described above, the circulation of Rachel increases dramatically in size and generates a prominent beta-induced peripheral anticyclone in subsequent NOGAPS analyses (Fig. 31a-b). This beta-induced anticyclone in turn may have contributed to an equatorward extension of the subtropical anticyclone to the southwest of TC Drena near 15°S, 164°E, which experiences a temporary equatorward turn. This would be an example of an ITIE influence at a separation distance of just over 30° lat., which appears to be a rough limit for the phenomenon in both the Southern and Northern Hemispheres. Interestingly, Drena intensified significantly and subsequently developed a strong peripheral anticyclone that contributed to a sharp poleward turn (not shown). The implication of this sequence from Phil-Rachel to Drena is that the Rossby wave train may contribute to an equatorward track deflection, and a size increase, of the eastern TC, and then the sequence may be extended to a third TC. Such a sequence of ITIE events has occurred with Caitlin/Doug, Doug/Ellie, and Ellie/Fred in the western North Pacific (see 1994 ATCR).

During 10 to 13 February 1994, TC Ivy (1694) had a period of equatorward motion while TC Hollanda (1594) to the southwest was moving increasingly poleward (Fig. 32). At 00 UTC 10 and ll February (Fig. 33a-b), the NOGAPS analyses have almost no peripheral anticyclone between Ivy and Hollanda. In view of the weakness of the subtropical anticyclone south of Ivy, the proposed explanation for the equatorward motion of Ivy during this period is that an un-analyzed peripheral anticyclone must actually have been present. In support of this supposition, Hollanda was an intense TC at this time (Fig. 32), although this does not prove that a significant peripheral anticyclone should be present. Additionally, the weakening of Hollanda that commences on 11 February as the TC approaches the subtropical ridge axis coincides well with the resumption of poleward movement by Ivy (Fig. 32), which is consistent with the view that a beta-induced anticyclone previous generated by Hollanda was responsible for the equatorward excursion of Ivy. Finally, notice that by 00 UTC 13 February (Fig. 33d) the size of Ivy depicted by NOGAPS has increased significantly, and a beta-induced anticyclone has formed to the northeast of Ivy. As discussed above, these changes to the circulation size and environment

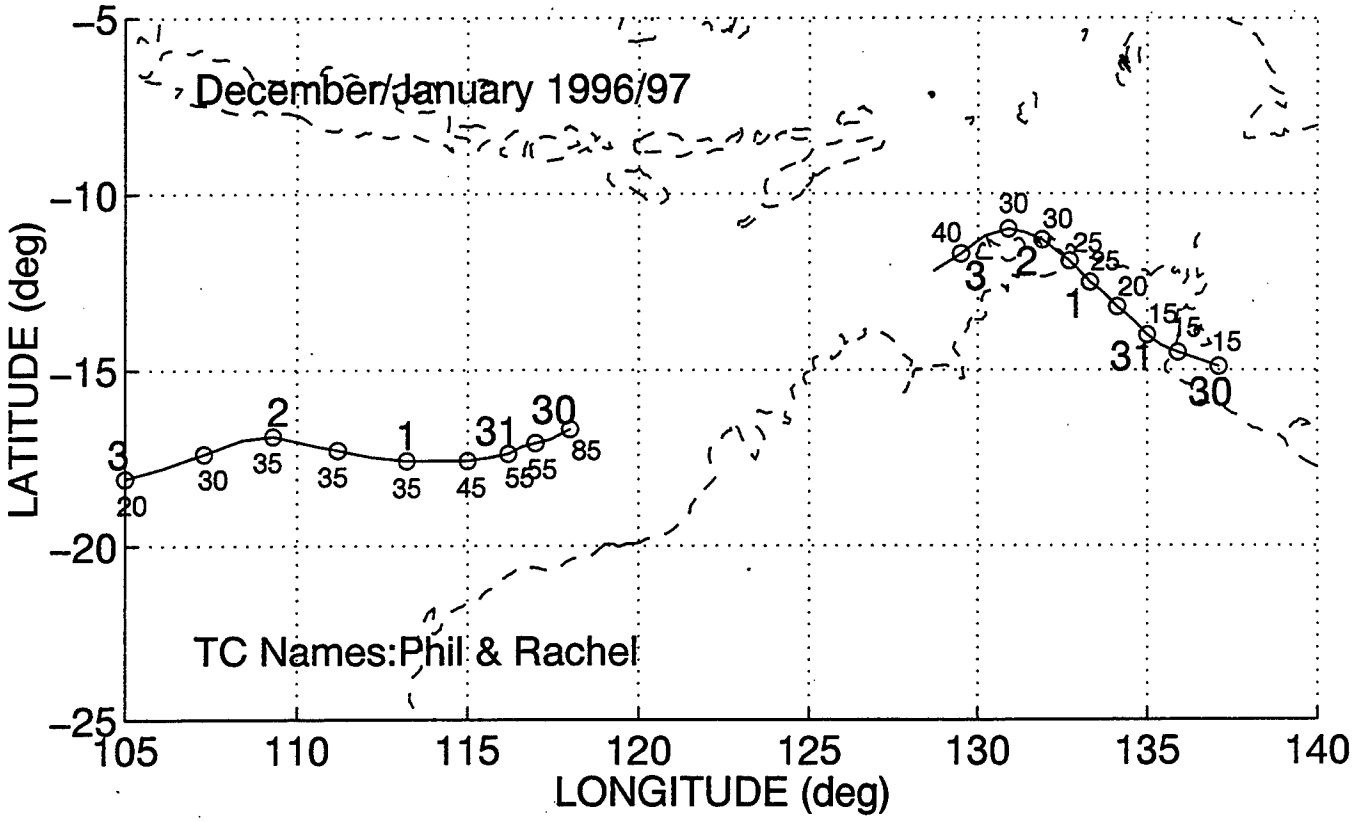

Figure 29. Tracks as in Fig. 25 of TCs 1297 (Phil) and 1597 (Rachel) during 00 UTC 30 December 1996 to 00 UTC 3 January 1997 with circles each 12 h.

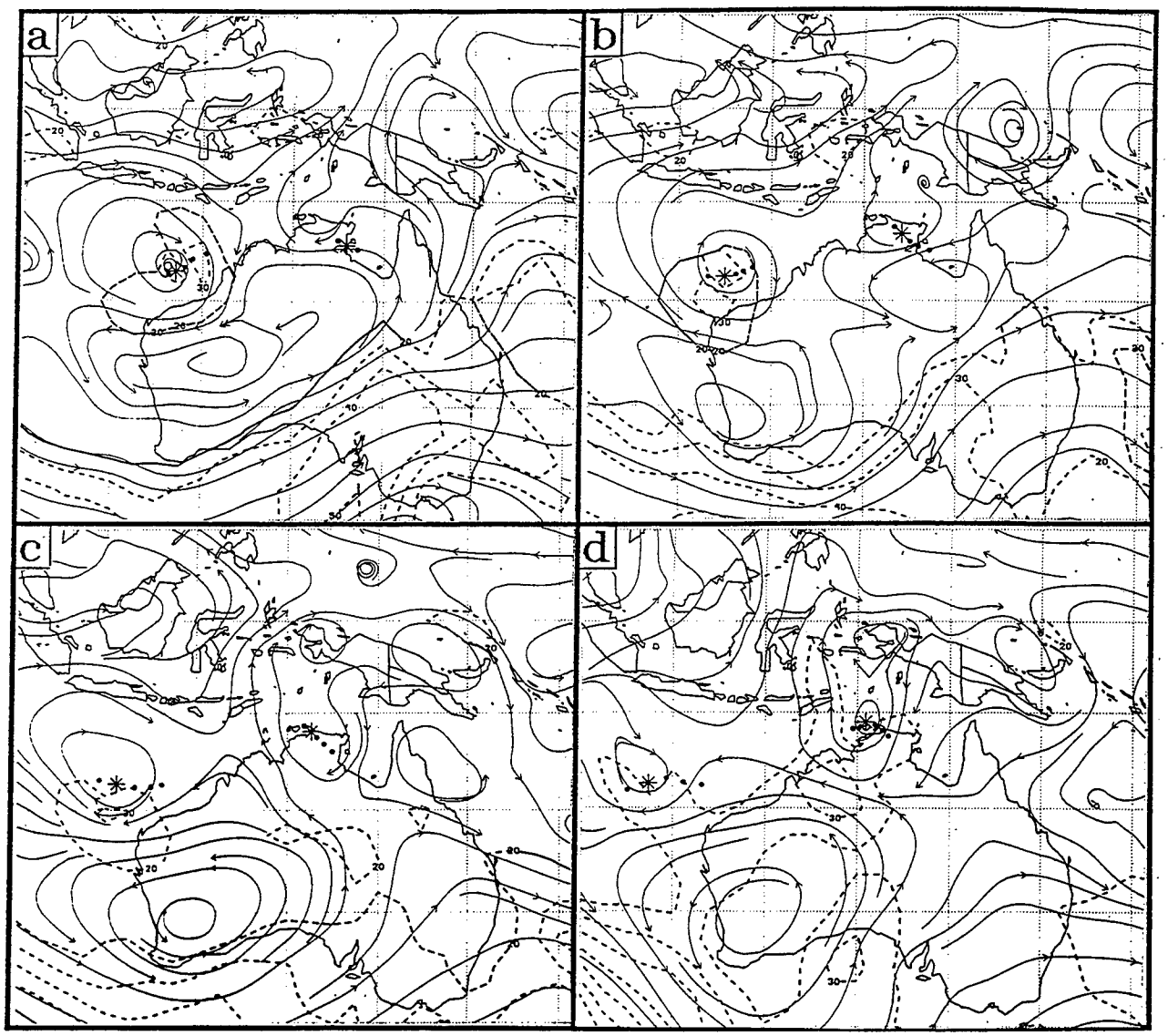

Figure 30. NOGAPS 500-mb analyses as in Fig. 7, except at 12 UTC on (a) 30 and (b) 31 December 1996, and (c) 1, and (d) 2 January 1997. The western (eastern) TC is Phil (Rachel).

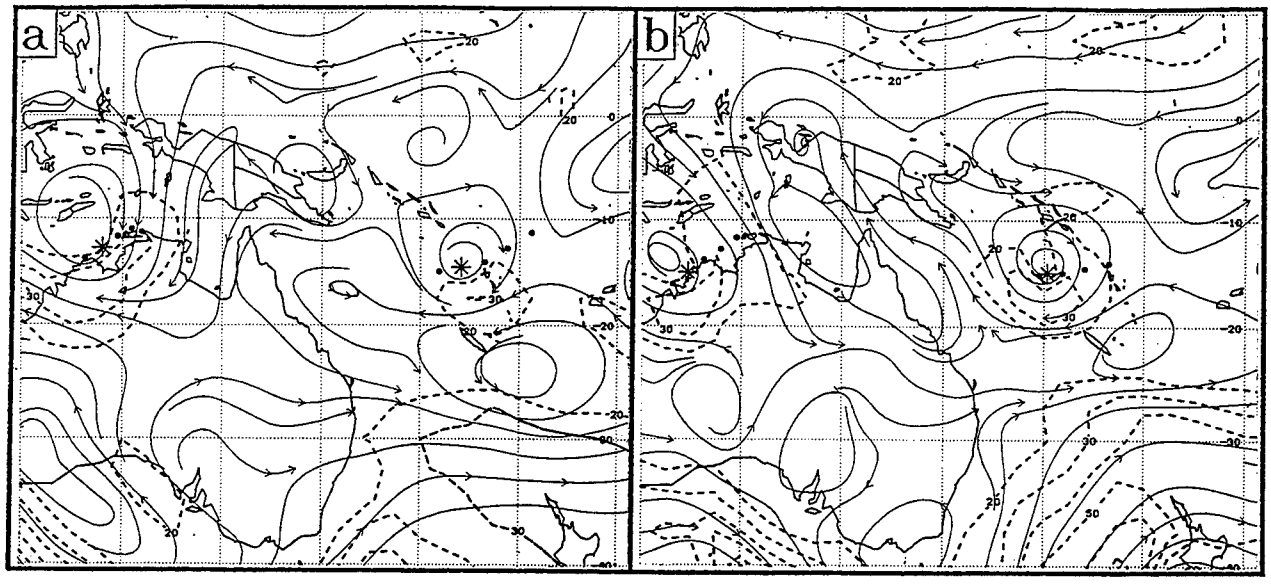

Figure 31. NOGAPS 500-mb analyses continued from Fig. 30 at 12 UTC on (a) 3 and (b) 4 January 1997. The western (eastern) TC is Rachel (Drena).

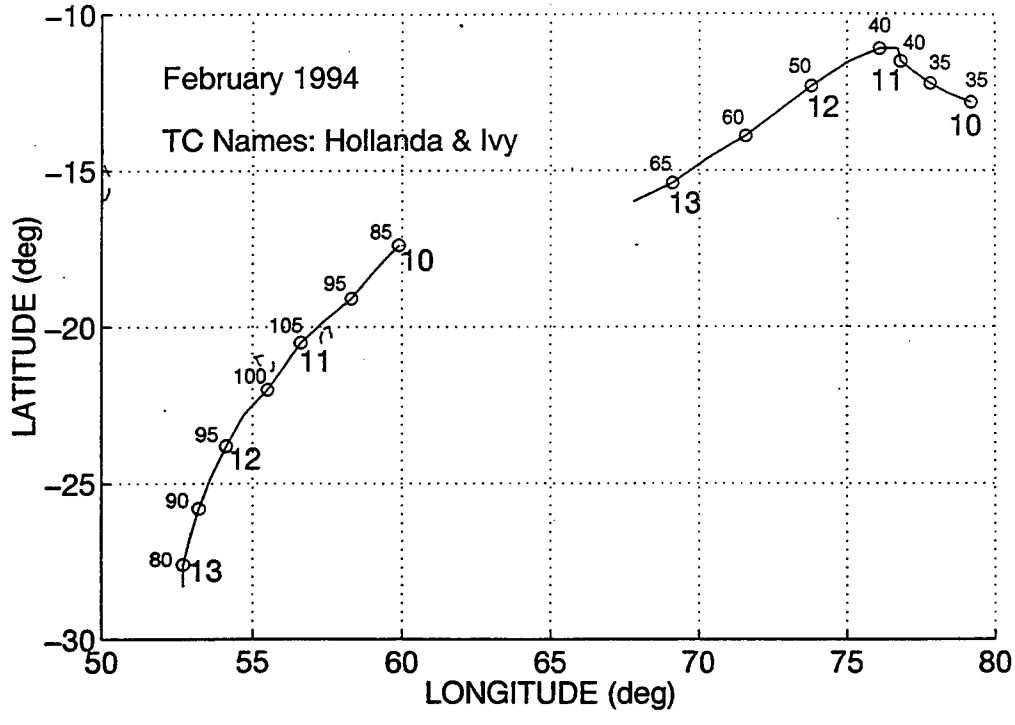

Figure 32. Tracks as in Fig. 25 of TCs Ivy (eastern) and Hollanda (western) during 00 UTC 10 February 1994 to 00 UTC 13 February with circles each 12 h.

structure of an eastern TC (i.e., Ivy) are to be expected if a beta-induced wave train has been emanating from a TC to the southwest (i.e., Hollanda). Thus, the provisional conclusion is that the period of equatorward motion of Ivy may be explained by the ITIE mechanism.

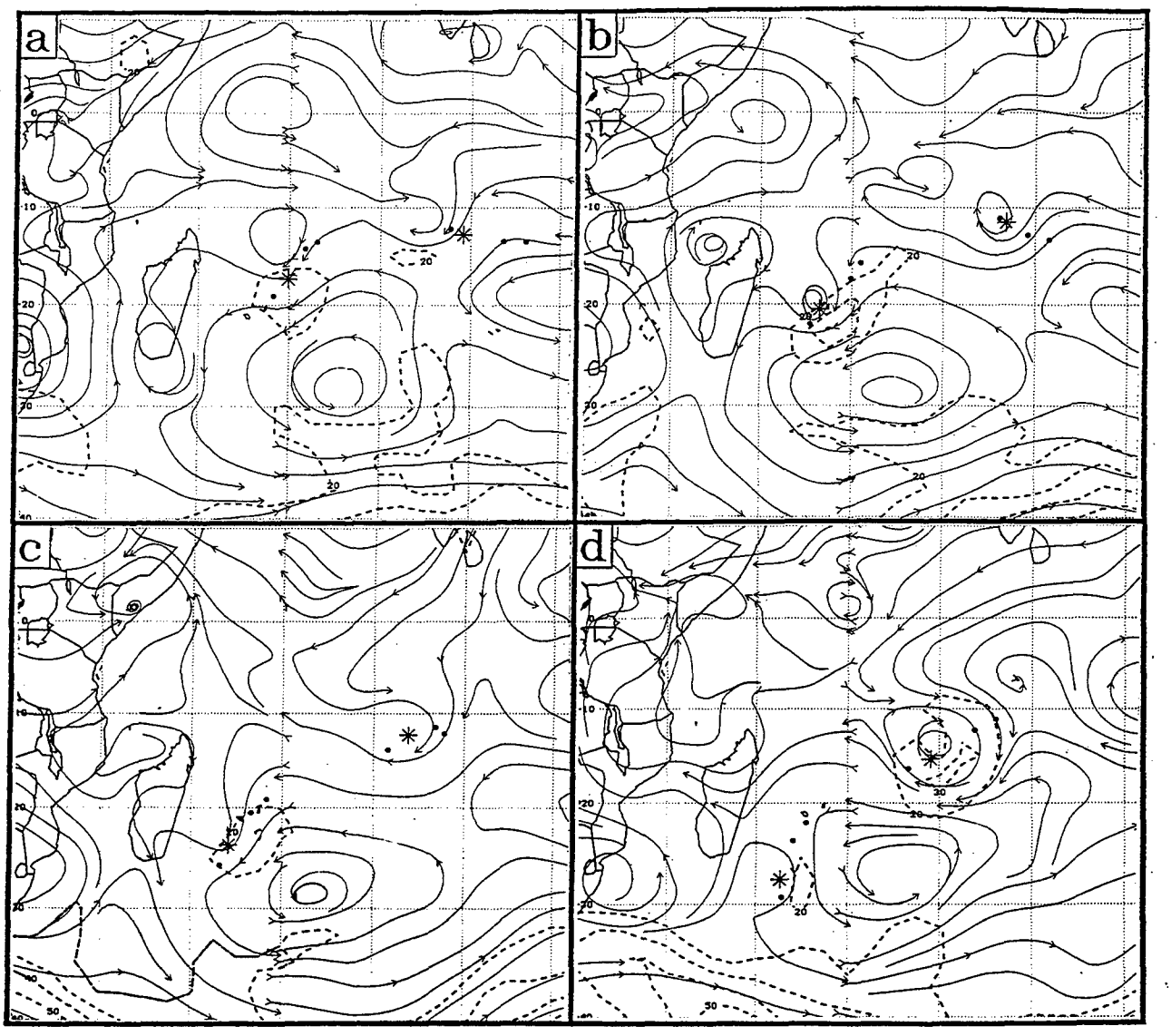

Figure 33. NOGAPS 500-mb analyses as in Fig. 7, except for 00 UTC on (a) 10, (b) 11, (c) 12, and (d) 13 February 1994.

6. ENVIRONMENT STRUCTURE TRANSITIONS

As illustrated in the conceptual models in Figs. 6, 9, 13, and 19 and in the tracks in Figs. 8, 11, 18, and 21, as long as a TC remains in the steering flow associated with a particular synoptic pattern and region, the motion of the TC will tend to fall within a certain range of directions and speeds, i.e., in a characteristic track. It is possible for a TC to remain in the same pattern/region combination throughout its existence, with the most common case being "straight running" TCs that remain in the tradewind easterlies equatorward of the subtropical ridge; that is, in the S/DR pattern/region. However, the majority of TCs in any basin follow more complex tracks owing to changes in the environment structure in the vicinity of the TC. The Systematic Approach meteorological knowledge base treats these changes as "transitions" from one pattern/region combination to another. Mechanisms that act to change the environment structure of the TC are called transitional mechanisms (see list in Fig. 1).

An overview of the frequency of environment transitions and associated transitional mechanisms during the period of the study is presented in this section. Then, a series of mini-case studies are presented that use JTWC best tracks and NOGAPS analyses to illustrate the more frequently occurring transitions. (Note: Readers that desire more discussion of the various transitional mechanisms listed in Fig. 1 and the associated environment structure transitions are referred to Carr *et al.* (1997b), which develops each conceptual model in a Northern Hemisphere context, and provides illustrative case studies using examples from the western North Pacific basin.)

a. *Frequency.*

The entire set of Southern Hemisphere TCs during January 1994 - June 1997 experienced a total of 156 recurring (more than two occurrences) transitions of environment structure that affected the tracks of the 111 TCs (Fig. 34). That is, on average about seven transitions will occur for every five TCs. A similar average number of transitions is found for the South Indian Ocean TCs (Fig. 35a). However, only about one transition per TC is found in the western South Pacific despite defining a recurring transition as being more than one transition (Fig. 35b). This difference may be related to the Indian Ocean TCs persisting longer than South Pacific TCs, which allows more time for transitions in environment structure to occur.

The most frequent transition is from a S/DR to a P/PO pattern/region, which usually is associated with the generation of a beta-induced anticyclone to the east and north via the Ridge Modification by a TC (RMT) transitional mechanism when only one TC is present, or the Reverse Trough Formation (RTF), which involves the favorable superposition of peripheral anticyclones of two adjacent TCs. Notice also that a significant number of reverse transitions from P/PO to S/DR occur. These transitions arise from: (i) a weakening of the beta-induced peripheral anticyclone of the TC (often a result of TC weakening/dissipation); (ii) superposition of a midlatitude ridge poleward of the TC, which is called Subtropical Ridge Modification by a Ridge (SRMR); or (iii) a combination of (i) and (ii).

Environment Structure Transitions
SOUTHERN HEMISPHERE
1994 – 1997

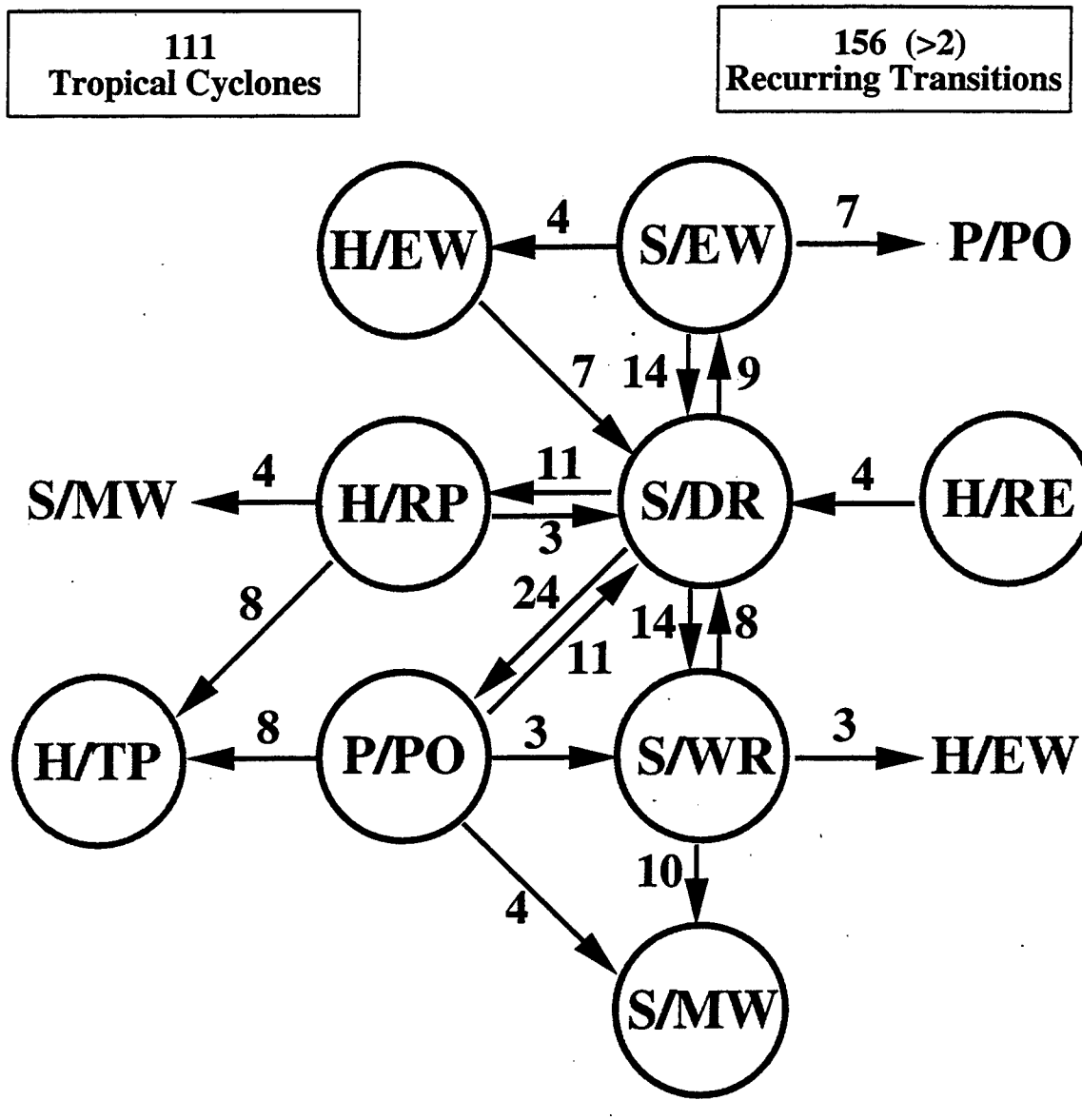

Figure 34. Environment structure transition occurrences for the 111 TCs in the SH during January 1994 to June 1997, where the synoptic pattern/region designators are defined in Fig. 1, and described in Section 3. Only "recurring" transitions that occurred more than two times during the period are included, with a total of 156 transitions.

Environment Structure Transitions

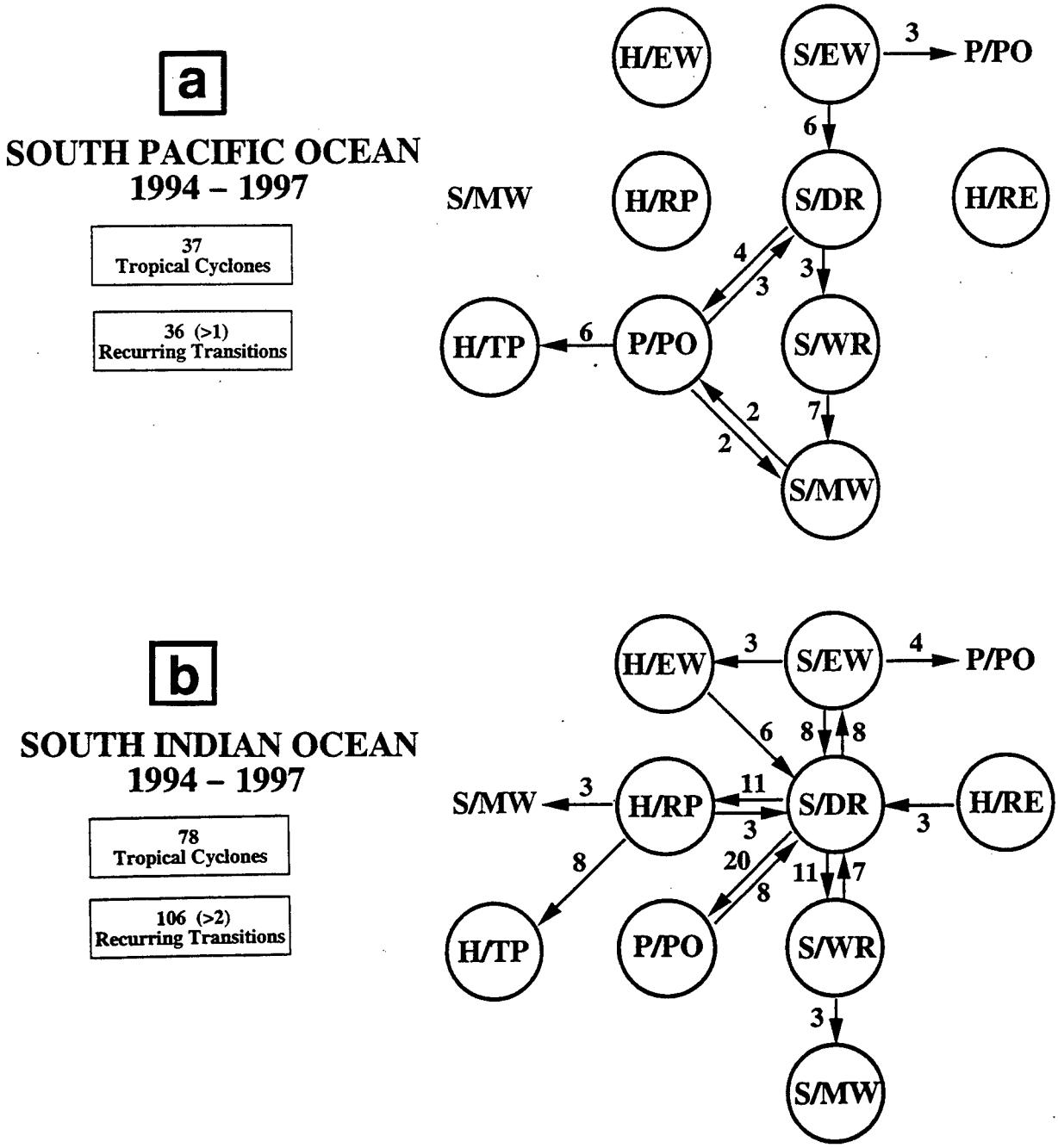

Figure 35. Recurring environment structure transitions as in Fig. 34, except for (a) 37 TCs in the South Pacific Ocean separately from the (b) 78 TCs in the South Indian Ocean. The definition of recurring was greater than one for the South Pacific.

Transitions among the regions of the S pattern are a significant fraction of the total. Transitions between the S/EW and S/DR regions are roughly equal and usually result from fluctuations in the competing influences of the equatorial westerlies and tradewind easterlies. Increases in the equatorial westerlies, which tend to promote a S/DR to S/EW transition, may arise from a cross-equatorial "surge," or may be associated with multiple SH TCs at low latitudes in proximity, or "twin" TC developments in both hemispheres at similar longitudes. Increases in the tradewind easterlies, which tend to promote a S/EW to S/DR transition, are usually a result of increased amplitude of the subtropical ridge. This amplification may occur owing to large-scale circulation changes, or as a result of midlatitude ridging tendencies poleward of the subtropical ridge in the vicinity of the TC.

Transitions within the S pattern that result in poleward motion of the TC (i.e., S/DR to S/WR, and S/WR to S/MW) into and through a pre-existing or developing subtropical ridge weakness may occur as a result of the southwestward beta-effect TC propagation (BEP), which is proportional to TC size, or the Subtropical Ridge Modification by a Trough (SRMT) mechanism. Conversely, the equatorward track change associated with the S/WR to S/DR transition usually results from a building of the subtropical ridge poleward of the TC via the SRMR mechanism that overcomes the persistent property (validated by theory, modeling, and observational studies) of TCs to propagate poleward.

Since the H pattern is by definition associated with midlatitude troughs and ridges of comparatively high amplitude, transition to (from) the H pattern is always the result of: (i) increased (decreased) modulation of the subtropical ridge (SRM) by amplifying (weakening) midlatitude wave activity in the vicinity of the TC; (ii) movement of pre-existing high-amplitude wave activity into the vicinity of the TC; or (iii) some combination of (i) and (ii).

b. *Transitions within the S Pattern*

1. TC Beti (2396) case. During 24-38 March 1996, the track of Beti changes from west-southwestward motion to southeastward motion, with recurvature at about 00 UTC 26 March (Fig. 36). As described below, this track corresponds to the following sequence of transitions: S/DR to S/WR to S/MW.

At 12 UTC 24 March (Fig. 37a) Beti is equatorward of a thin primarily zonally-oriented subtropical anticyclone. Notice that Beti has recently turned westward from a more poleward track, which is consistent with the recent passage of a midlatitude trough and approach of a midlatitude ridge to the south. By 1200 UTC 25 March (Fig. 37b), the subtropical anticyclone orientation has become more zonal in response to the decreased amplitude of the midlatitude waves to the south. The ridge structure, isotach maximum south-southeast of Beti's position, and the structure of the subtropical anticyclone are all consistent with a S/DR pattern/region classification (Fig. 6). By 1200 UTC 26 March (Fig. 37c), Beti has slowed and is tracking poleward, and the TC is at the anticyclone axis with an isotach maximum to the east, which is consistent with poleward steering. Thus, the environment structure is changed to the

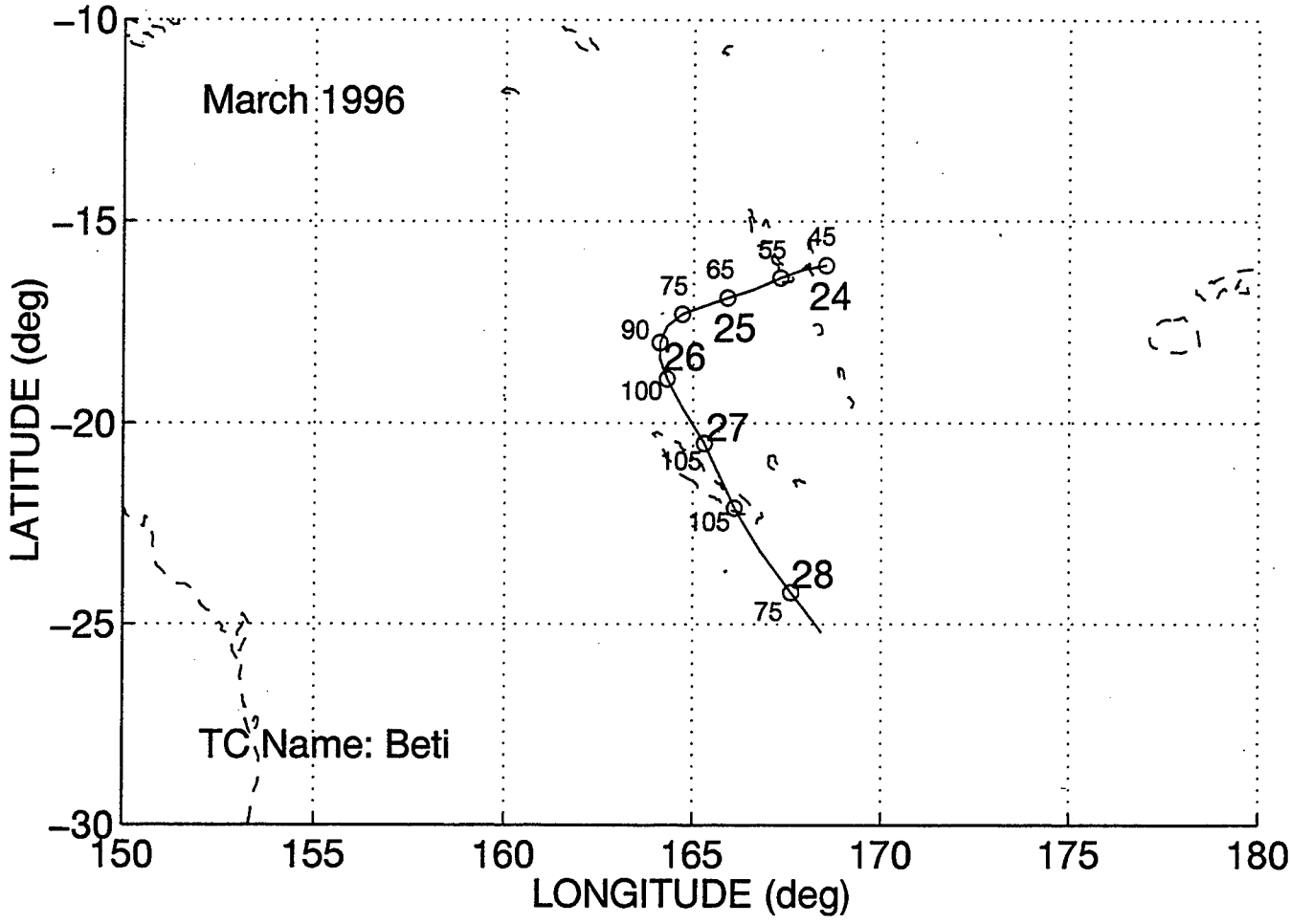

Figure 36. Track as in Fig. 25 of TC Beti during 00 UTC 24 March to 00 UTC 28 March 1996 with circles each 12 h.

S/WR as in Fig. 6. Beti passes the weakness in the subtropical anticyclone despite the approach of a midlatitude ridge to the south (the SRMR mechanism) that would tend to inhibit poleward motion by the TC. Thus, the movement is consistent with significant beta-effect propagation of Beti, which in satellite imagery appears to have a somewhat larger than average size (not shown). However, the interaction of Beti's circulation with the environment has not generated a significant beta-induced wave train to the northeast of Beti, which would be required to classify Beti's environment as having transitioned to P/PO via the RMT transitional mechanism. (Note: See the case of Drena below for an example of a transition of a P/PO by another intense TC in nearly the same location). By 1200 UTC 27 March (Fig. 37d), Beti is accelerating to the southeast, and Beti is moving around the subtropical anticyclone to the east, which is consistent with the S/MW pattern as in Fig. 6.

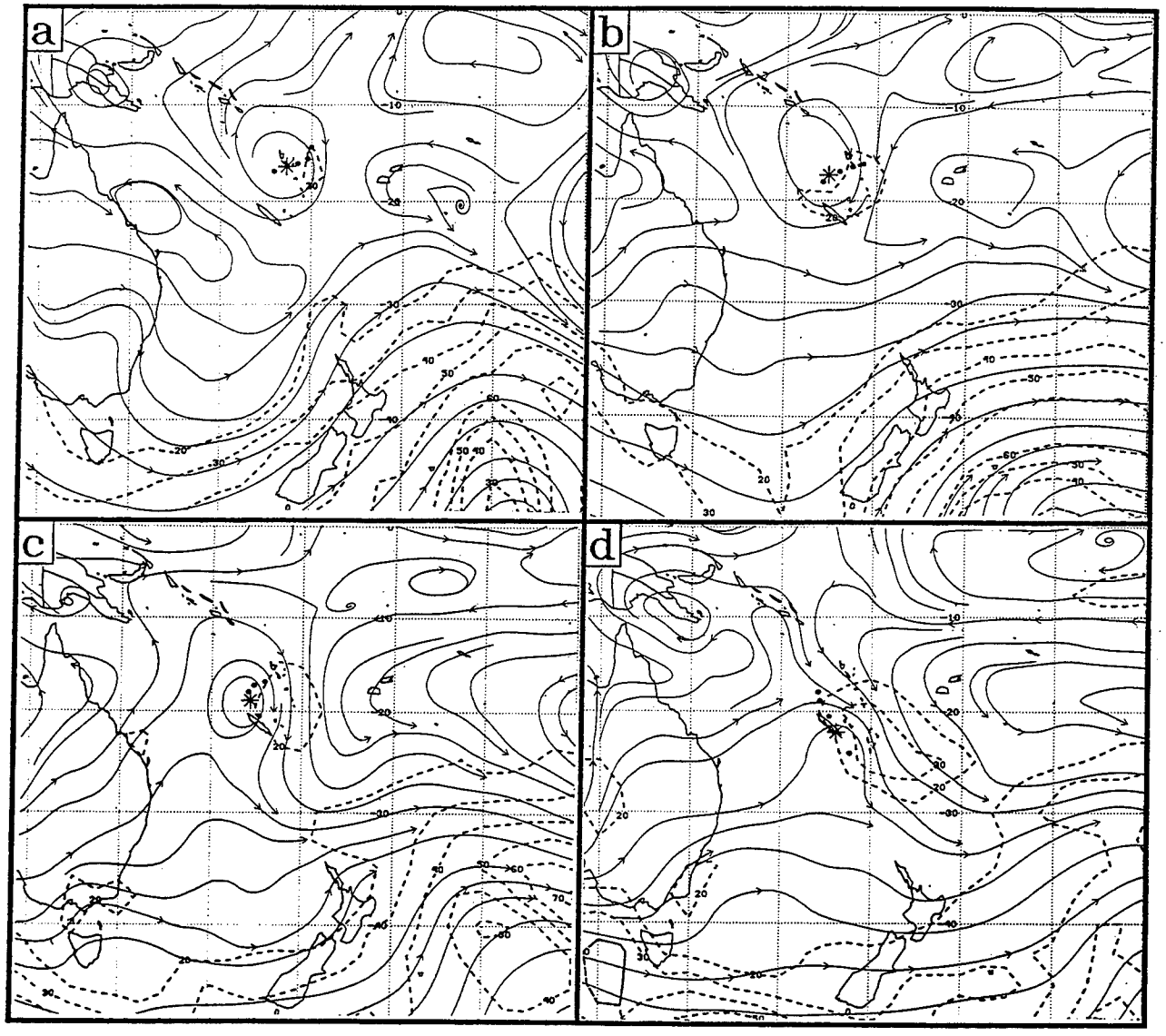

Figure 37. NOGAPS 500-mb analyses as in Fig. 7, except for 12 UTC on (a) 24, (b) 25, (c) 26, and (d) 27 March 1996.

2. TC Daryl/Agnielle (0196) case. During 16 to 25 November 1995, Daryl/Agnielle (hereafter Daryl) followed a complex track that began with south-southeast motion at very low latitude, then had a sharp westward turn, and poleward turn (Fig. 38). As described below, this track results from the following sequence of synoptic pattern/region transitions: S/EW to S/DR; S/DR to S/WR; and S/WR to S/DR.

At 1200 UTC 16 November (Fig. 39a), an extensive region of equatorial westerlies at 500 mb is analyzed to the west-northwest of Daryl. Notice that the track of Daryl over the past 36 h is consistent with the steering effect after the turning of these equatorial westerlies into northwesterlies. Only a thin, zonally-oriented subtropical ridge extends east-west just poleward of Daryl. Thus, the synoptic situation and past motion of Daryl are consistent with the S/EW portion of Fig. 6. During 17 to 19 March (Fig. 39b-d), Daryl turns from a poleward track onto a nearly westward track (Fig. 38), presumably due to the increasing influence of the tradewind easterlies equatorward of the thin subtropical ridge. This turn reflects a transition in environment structure from S/EW to S/DR as depicted in the upper right of Fig. 6. Perhaps coincidentally, this turn occurs as a weak ridge in the midlatitude westerlies passes to the south, which may suggest that weak SRMR helps to strengthen the subtropical anticyclone poleward of Daryl, and thus may have been a contributing factor to the transition. At 12 UTC 21 and 22 November (Fig. 40a-b), the approach of a relatively weak midlatitude trough appears to weaken the thin subtropical ridge (i.e., a SRMT) to the southwest of Daryl. Concomitantly, Daryl slows and turns onto a poleward track (Fig. 38), which is consistent with a transition from S/DR to S/WR as in Fig. 6. Subsequently, the midlatitude trough moves eastward and is replaced by a ridge in the NOGAPS analyses for 23 and 24 November (Fig. 40c-d). The track of Daryl turns back onto a westward heading, presumably due to the restoration (via SRMR) of a unbroken subtropical ridge to the south of Daryl that may not be well-depicted in the NOGAPS analysis. This last turn and associated large-scale flow changes are consistent with a S/WR to S/DR transition in Fig. 6. Notice in Fig. 38 that the intensity of Daryl decreases rapidly as the second westward turn occurs, which suggests that a vertical wind shear-related lowering of the effective steering level for Daryl may have played a role in the environment structure transition and associated turn.

Given only Fig. 40b without reference to the preceding and following analyses, the forecaster might be tempted to believe that a deep trough from the midlatitudes has penetrated nearly to the equator just west of Daryl. That is, a H pattern may seem to exist at 12 UTC 22 November. However, this appearance only applies to Fig. 40b, since ridging is clearly evident west of Daryl in preceding and subsequent analyses (Figs. 40a and c, respectively). As will be described later in the case studies of transitions to and from the H pattern, deep midlatitude troughs do not develop and weaken this rapidly. Rather, a possible explanation is that the "appearance" of a deep trough is an under-representation in the NOGAPS analysis of the thin subtropical anticyclone to the west-southwest of Daryl (notice the weak ridge superposed on the apparent deep trough). Owing to data sparsity, this small feature is difficult to analyze between the cyclonic circulation of the midlatitude trough and Daryl. This instance is a good example of the challenge that confronts forecasters in attempting to discern the actual environmental

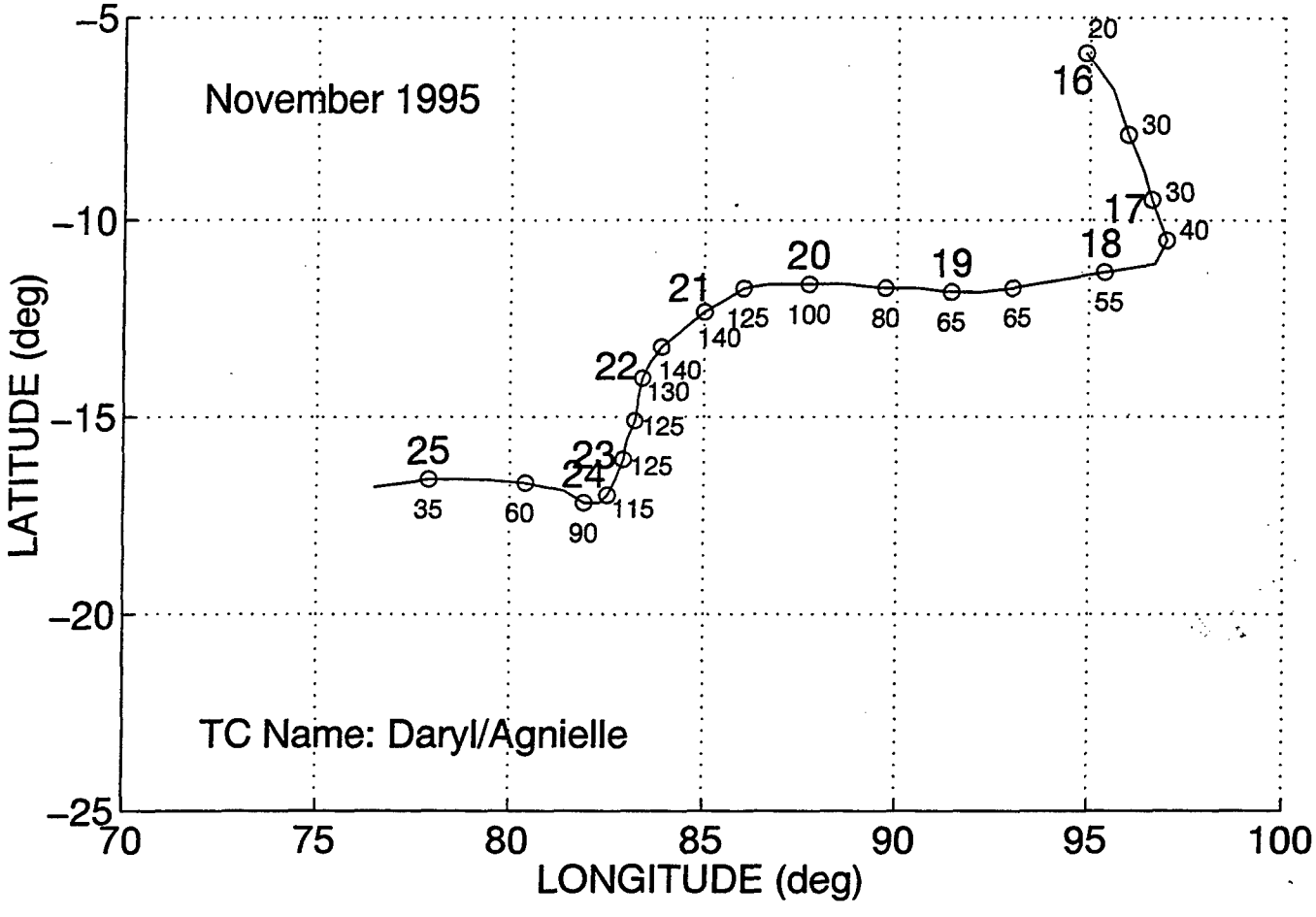

Figure 38. Track as in Fig. 25 of TC Daryl/Agnielle during 00 UTC 16 November 1995 to 00 UTC 25 November with circles each 12 h.

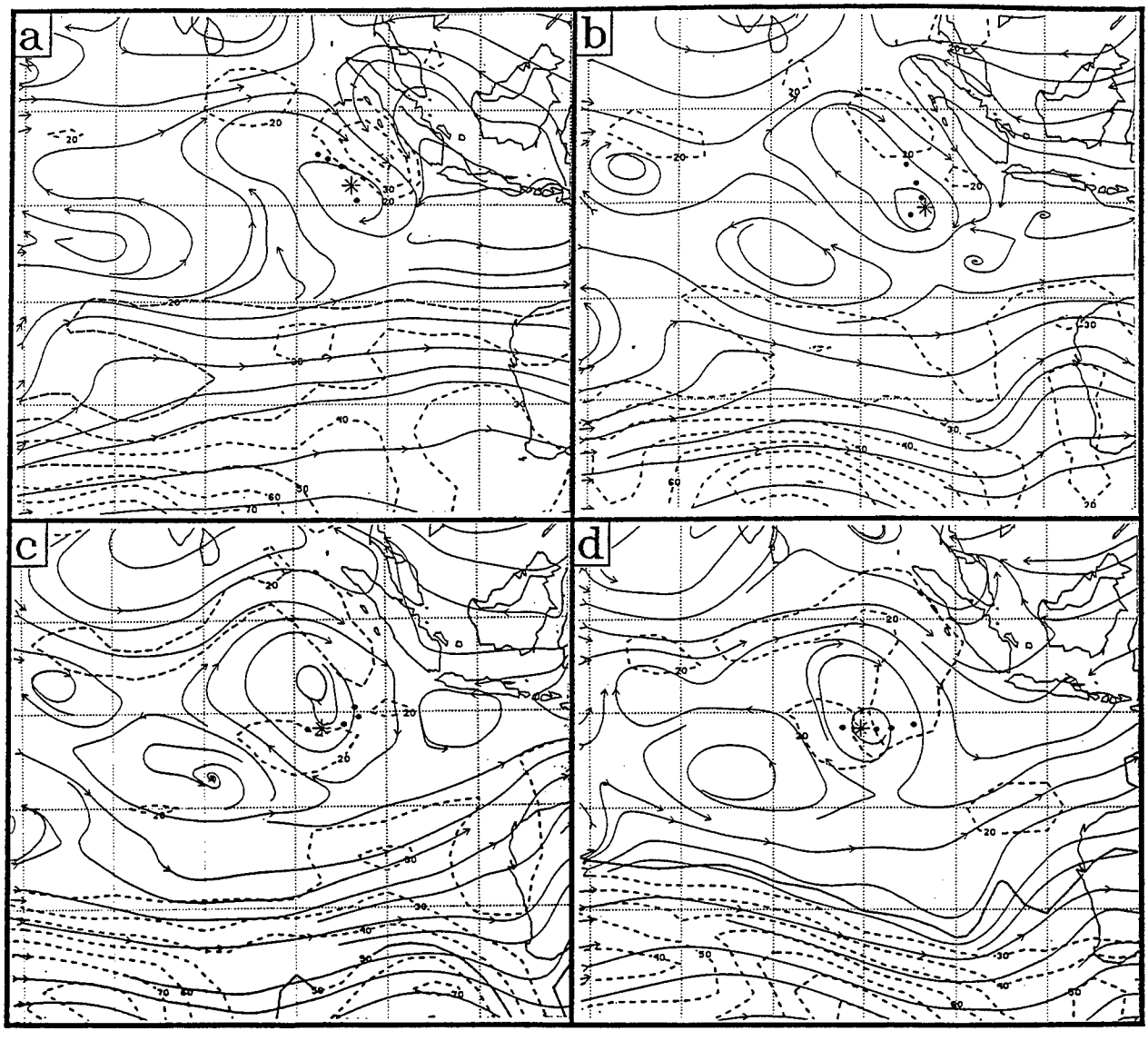

Figure 39. NOGAPS 500-mb analyses as in Fig. 7, except at 12 UTC for (a) 17, (b) 18, (c) 19, and (d) 20 November 1995.

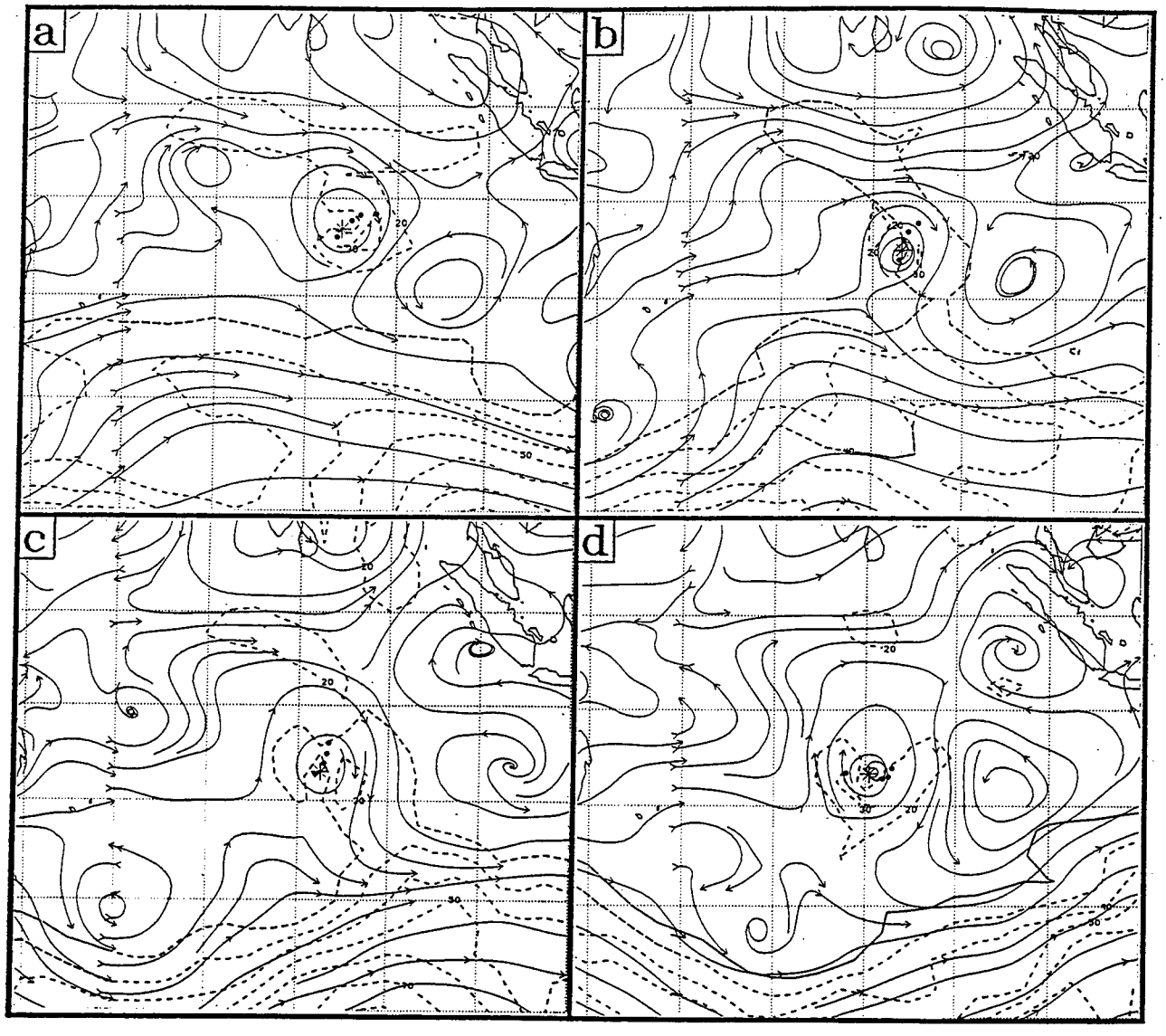

Figure 40. NOGAPS 500-mb analyses as in Fig. 7, except at 12 UTC for (a) 21, (b) 22, (c) 23, and (d) 24 November 1995.

situation affecting TC motion using operational analyses that necessarily suffer from a lack of data in the mid-troposphere.

c. *Transitions to/from P Pattern*

1. TC Ivy (1694) case. During 13 to 18 February 1994 (Fig. 41), the track of Ivy turned from west-southwestward to a sinuous poleward track. Notice also that Ivy intensified quite significantly after turning poleward. As described below, this track change occurs during a transition from a S/DR to a P/PO environment structure classification.

At 00 UTC 13 February 1994 (Fig. 42a), Ivy is depicted in the NOGAPS analysis as being equatorward of a prominent subtropical anticyclone that has a east-northeast to west-southwest orientation. Although a prominent peripheral anticyclone appears to the northeast of Ivy, the isotach maximum to the southeast confirms that steering from the subtropical anticyclone is primarily responsible for the southwestward motion (Fig. 41). When the tilt of the subtropical anticyclone is taken into account, the environment structure in the vicinity of Ivy conforms well to the eastern TC in the S/DR region in Fig. 6 for which a beta-induced anticyclone is depicted. Although such a peripheral anticyclone to the northeast is present in Fig. 42a, its contribution to the environmental steering of Ivy depends on the relative strengths of the subtropical anticyclone and the beta-induced anticyclone as time progresses. Notice also that TC Hollanda (1594) is southwest of Ivy and is passing through recurvature at a latitude of about 28°S, which is the approximate latitude of the subtropical anticyclone axis.

At 00 UTC 14 February (Fig.42b), the isotach maximum has shifted to the east of Ivy as the subtropical anticyclone has weakened and the peripheral anticyclone has built. By 00 UTC 15 February (Fig. 42c), the isotach maximum has shifted to the northeast of Ivy and Ivy has slowed and is about to turn poleward. At this time, the structure of the environment of Ivy is in a transitional state between the S and Poleward (P) patterns, which will be denoted as S/DR|P/PO. By 00 UTC 16 February (Fig. 42d), Ivy is moving poleward in response to beta-induced anticyclone to the northeast, which indicates that the transition to the P/PO pattern/region has occurred. Although a trough appears in the midlatitudes to the south of Ivy, this is a reflection of the remnants of the recurved Hollanda, and is not a deep midlatitude trough to which the poleward turn of Ivy can be attributed. This evolution can be confirmed in Fig. 42c, which still shows the circulation of Hollanda as distinct from the essentially zonal midlatitude westerlies farther south.

Notice that Ivy turned poleward at a latitude of only 20°S, which is well equatorward of the latitude of the subtropical anticyclone axis at which Hollanda recurved earlier (see Fig. 42a). This poleward turn at a latitude significantly equatorward to the pre-existing subtropical anticyclone axis is a common characteristics of a transition from S/DR to P/PO. Because a TC is still in the P/PO pattern/region equatorward of the high vertical wind shear associated with the midlatitude westerlies, significant intensification after a transition to P/PO is a common occurrence.

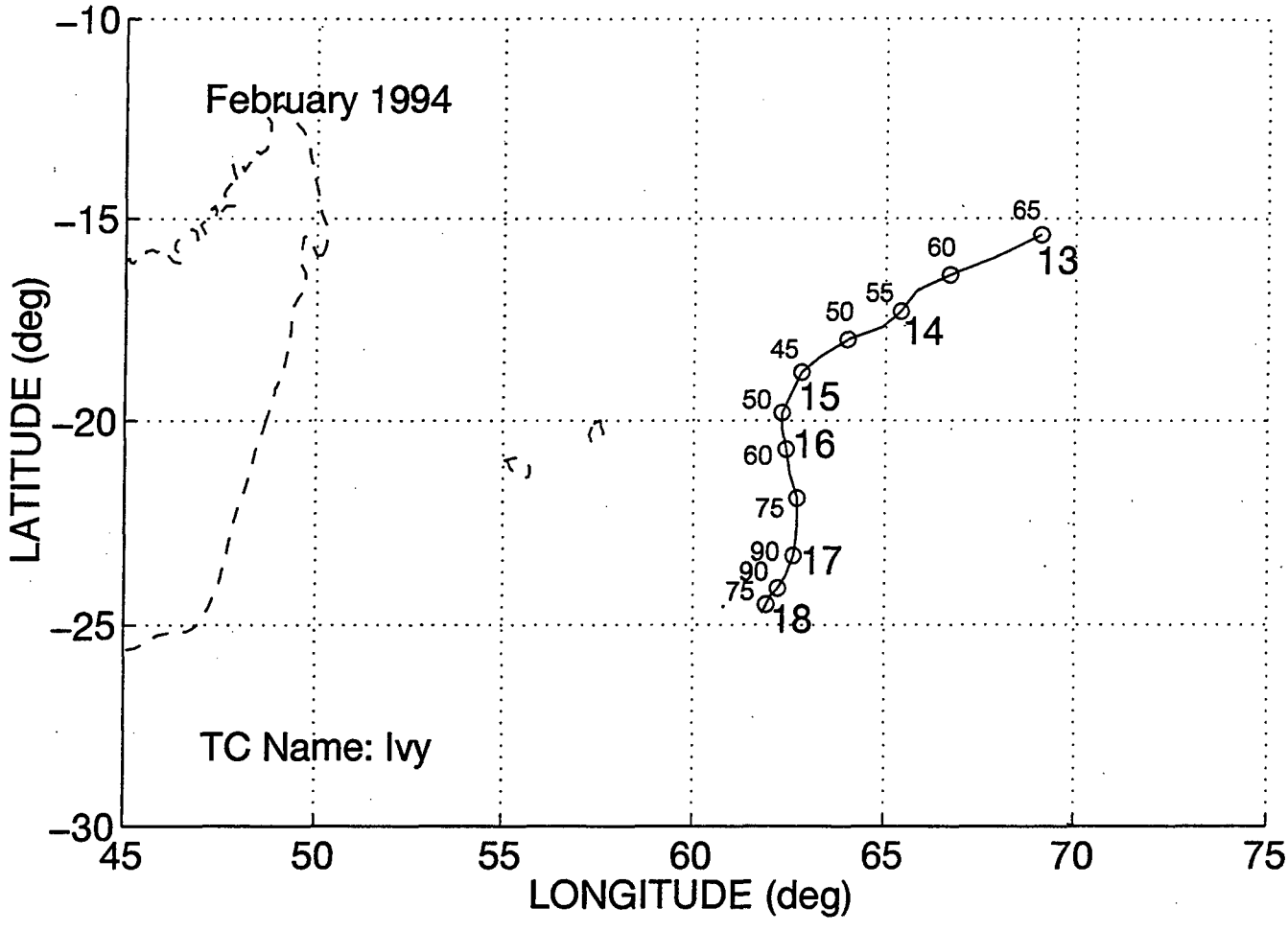

Fig 41. Track as in Fig. 25 of TC Ivy during 00 UTC 13 February 1994 to 00 UTC 18 February with circles each 12 h.

2. TC Drena (1697) case. During 3 to 8 January 1997, Drena underwent a turn from a west-southwestward to a southeastward direction of movement (Fig. 43) that is very similar to that of Beti (Fig. 36) described above. Whereas, the Beti track is a reflection of a transition from S/DR to S/WR to S/MW, the environment structure transition for Drena is from S/DR to P/PO. In this case, the influence of the beta-induced anticyclone is accompanied by significant midlatitude wave activity (SRM) that influences the character of the track change and the accompanying intensity change.

At 00 UTC 3 January 1997 (Fig. 44a), the track of Drena is west-southwestward equatorward (Fig. 43) of a subtropical anticyclone. Although a significant midlatitude trough appears to be modulating the subtropical anticyclone poleward of Drena, the anticyclone is more zonal than meridional. At this time, the environment structure of Drena is characterized as being S/DR. During the next two days (Figs. 44b-c), the subtropical anticyclone is weakened as

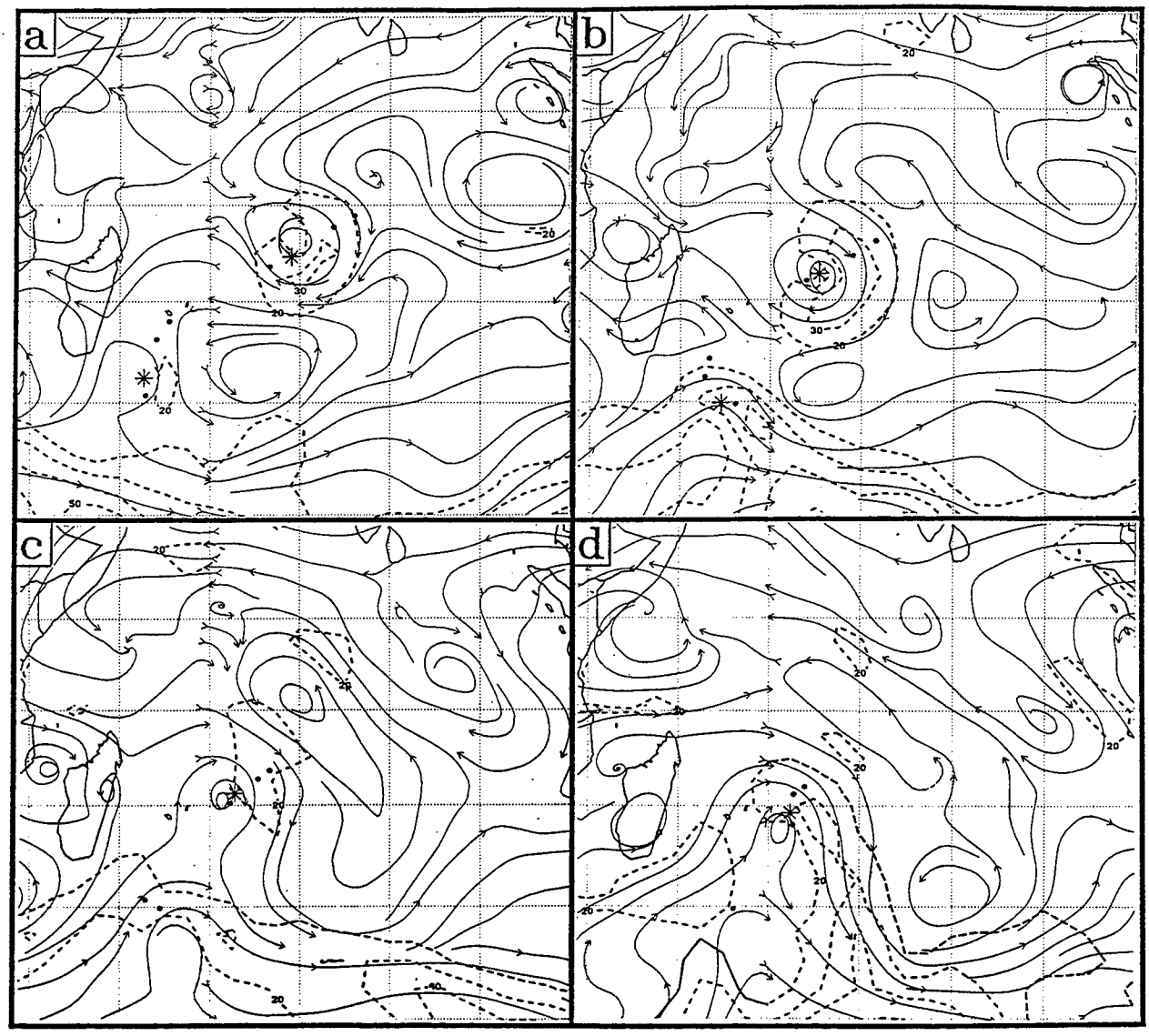

Fig. 42. NOGAPS 500-mb analysis as in Fig. 7, except at 00 UTC on (a) 13, (b) 14, (c) 15, and (d) 16 February 1994. TC Ivy (Hollanda) is the eastern (western) storm.

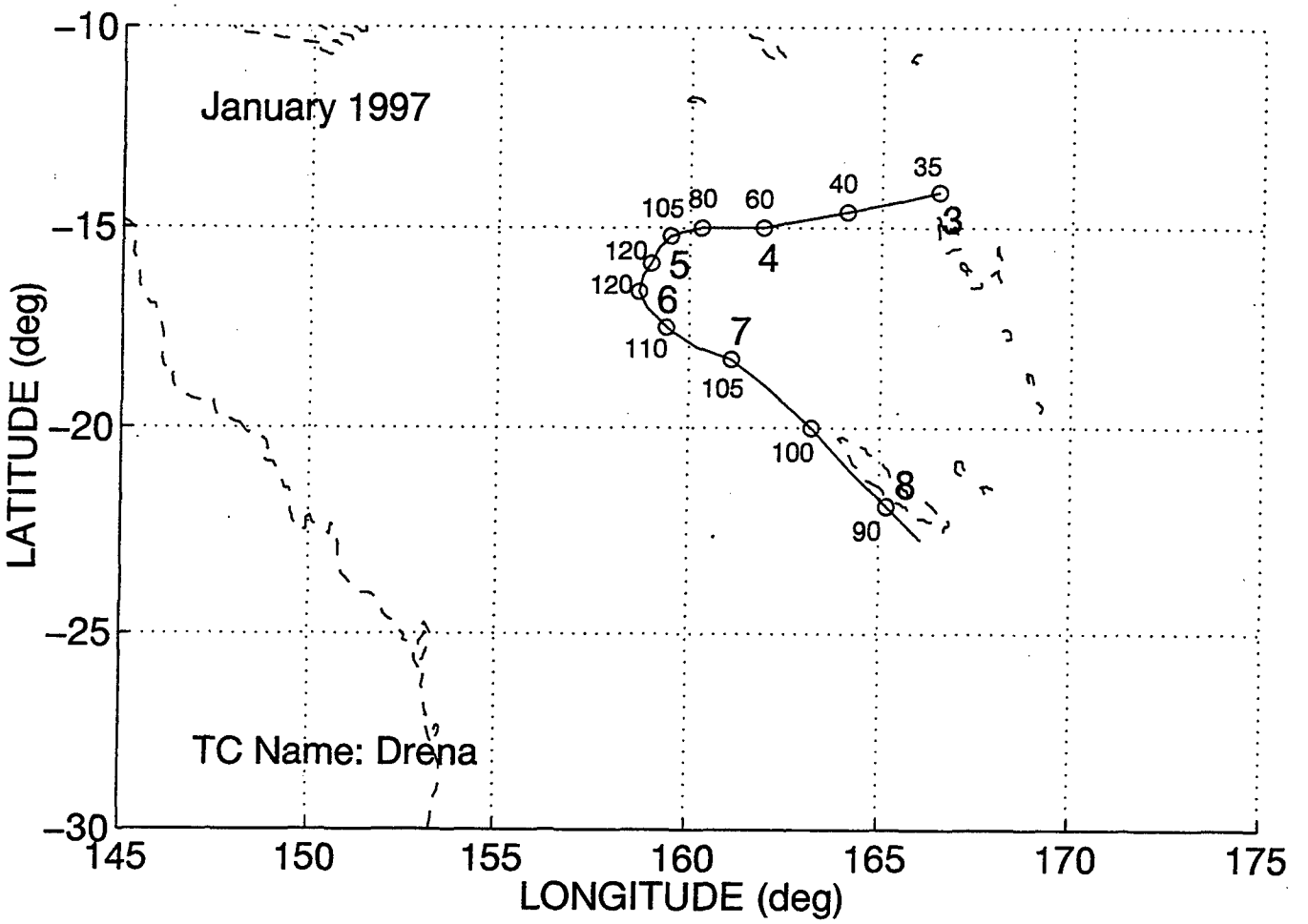

Figure 43. Track as in Fig. 25 of TC Drena during 00 UTC 3 January 1997 to 00 UTC 8 January with circles each 12 h.

the midlatitude trough digs equatorward. If this trough breaks the ridge to the west of Drena (i.e., SRMT), a recurvature via S/WR and S/MW would be expected. However, the midlatitude ridge is also amplified and approaches from the southwest. This is designated as a SRMR because it rebuilds the subtropical ridge to the south of Drena. The crescent-shaped isotach maximum poleward of Drena at 00 UTC 5 January (Fig. 44c) confirms that the subtropical anticyclone circulation is still determining the environmental steering. However, a separate isotach maximum to the northeast of Drena is a manifestation of a growing beta-induced anticyclone. The steering from this peripheral anticyclone is beginning to offset that from the subtropical anticyclone, which is consistent with a recent decrease in translation speed of Drena (Fig. 43).

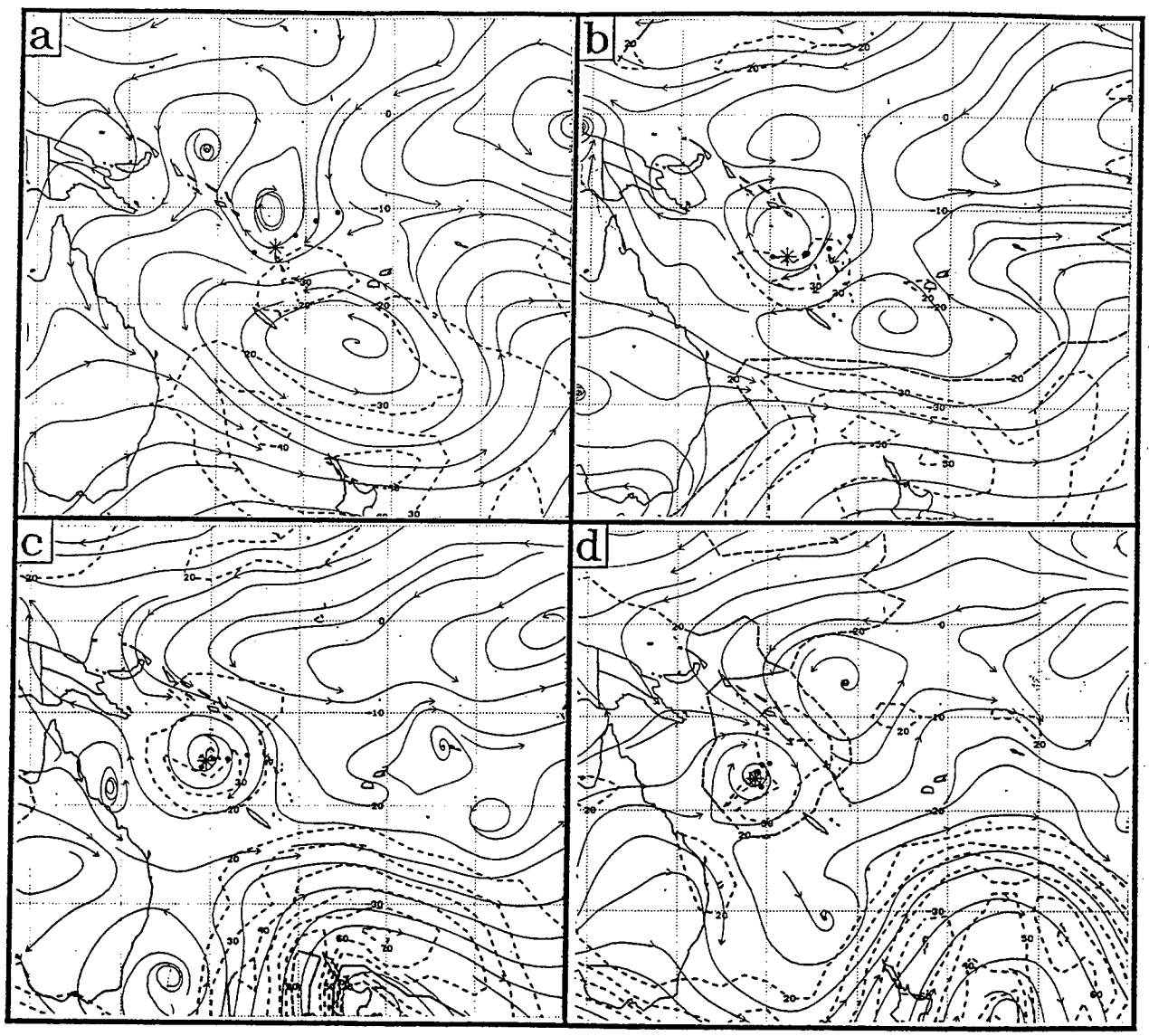

Figure 44. NOGAPS 500-mb analysis as in Fig. 7, except at 00 UTC on (a) 3, (b) 4, (c) 5, and (d) 6 January 1997.

By 0000 UTC 6 January (Fig. 44d), the peripheral anticyclone to the northeast has a more prominent appearance in the NOGAPS analysis, and the 30-kt isotach maximum to the northeast is significantly larger than its counterpart poleward of Drena. Since Drena has now turned onto a poleward heading (Fig. 43), the environment structure of Drena has changed to P/PO as in Fig. 9. One difference from this conceptual model is the presence of midlatitude westerly flow impinging on the TC (Fig. 44d). In contrast to the Ivy case discussed above, this impinging flow is expected to subject the TC to more vertical wind shear. Thus, it is not surprising that Drena does not intensify as it moves poleward in the P/PO region. However, the slow weakening of Drena by 20 kt in 2 days as it moves poleward (Fig. 43) implies that the vertical wind shear (not shown) is still not very high, as might be expected when a TC recurves primarily due to the influence of a prominent midlatitude trough and more rapid weakening is observed.

3. TC Lisette (3097) case. During 26 February to 2 March 1997, the track of Lisette underwent a turn from poleward to westward while in the Mozambique Channel (Fig. 45). This case is an example of an environmental structure transition from P/PO to S/DR owing to a midlatitude wave-induced strengthening of the subtropical ridge poleward of the TC (i.e., SRMR).

At 00 UTC 27 February 1997, Lisette is tracking strongly poleward (Fig. 45) in response to a well defined peripheral anticyclone to the east and north (Fig. 46a) which is consistent with the PO portion of Fig. 9. By 00 UTC 28 February (Fig. 46b), the anticyclone to the northeast appears to have weakened, 20-kt isotach maxima appear on both the east and west sides of Lisette, the translation speed has slowed, and a turn to the west is about to take place (see +12 h position). All of these changes indicate that the environment structure of Lisette is in process of a transition from P/PO. By 00 UTC 1 March (Fig. 46c), the subtropical anticyclone is building over southern Africa, presumably in response to passing of a midlatitude ridge farther south (i.e., SRMR). Lisette is now tracking due westward (Fig. 45), and will continue on a west-northwest track that will take it ashore as the midlatitude ridge passes by to the south (Fig. 46d). Notice also in Fig. 46c that an isotach maximum has appeared to the south-southwest of Lisette, which indicates that the subtropical anticyclone to the southwest is steering the TC.

The evolution of environment structure that has caused this track change by Lisette is a transition from a P/PO to a S/DR pattern/region, owing to the SRMR-induced building of the subtropical anticyclone to the south of Lisette. The west-northwestward motion of Lisette suggests the strength of the subtropical anticyclone is adequate to "dominate" the steering flow of Lisette. The small meridional scale of the subtropical anticyclone and a lack of mid-level data are possible reasons why this anticyclone evolution in the NOGAPS analyses does not seem to be well resolved. Alternately, the NOGAPS (at this time with T159 resolution) analysis may actually be a proper representation of the thin anticyclone, but the presence of Lisette's circulation is contributing to what merely "appears" to be a weak anticyclone.

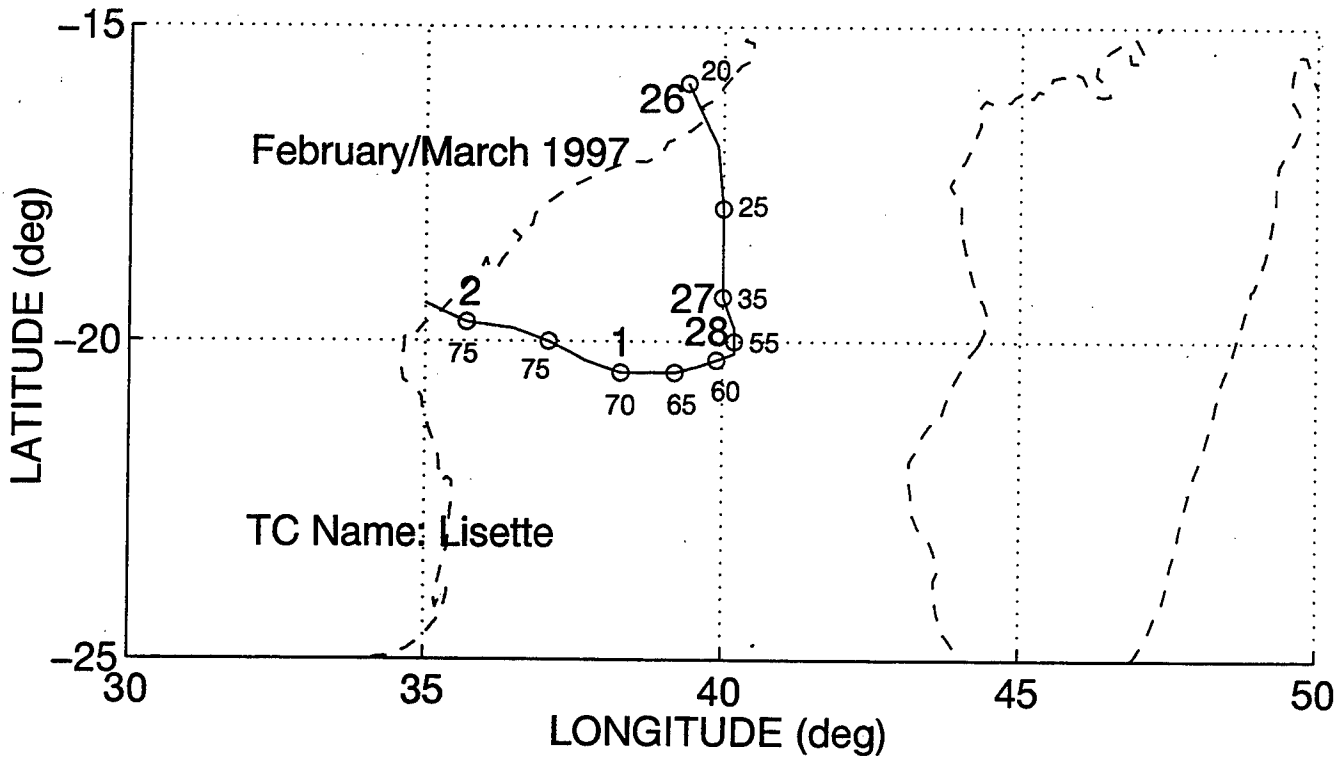

Figure 45. Track as in Fig. 25 of TC Lisette during 00 UTC 26 February 1997 to 00 UTC 2 March 1997 with circles each 12 h.

It is emphasized that the transition from a P/PO to a S/DR environment structure took place while Lisette was a severe TC and was intensifying (Fig. 45). Thus, it is unlikely that an vertical wind shear-induced change of steering level as the mechanism for this track change. Pending an in-depth evaluation of situation-specific TC forecast model traits in the Southern Hemisphere, it is expected that a SRMR-related S/DR to P/PO transition should be relatively well-forecast by a dynamical model that has synthetic TC observations to define the outer wind structure. The reasons for this expectation are: (i) the structure and movement of the midlatitude ridge that is hypothesized to be responsible for the transition should be relatively well-analyzed by NOGAPS, and easy to discern by the TC forecaster; and (ii) the TC is assumed to be adequately represented in a model such as NOGAPS for the purpose of responding to environmental steering, as long as synthetic TC observations are being inserted during the data assimilation cycle.

4. TC Sharon (2294) case. During 13 to 18 March 1994, Sharon followed a sinuous track (Fig. 47) that included a poleward turn on the 13th that will be shown to be associated with an environment structure transition from S/DR to P/PO, and then a westward turn on the 16th that corresponded to the onset of significant weakening of Sharon. In contrast to the Lisette case discussed above, this is an example of an environment structure transition from S/DR to P/PO that arises from a significant change in TC steering level as vertical wind shear weakens the TC.

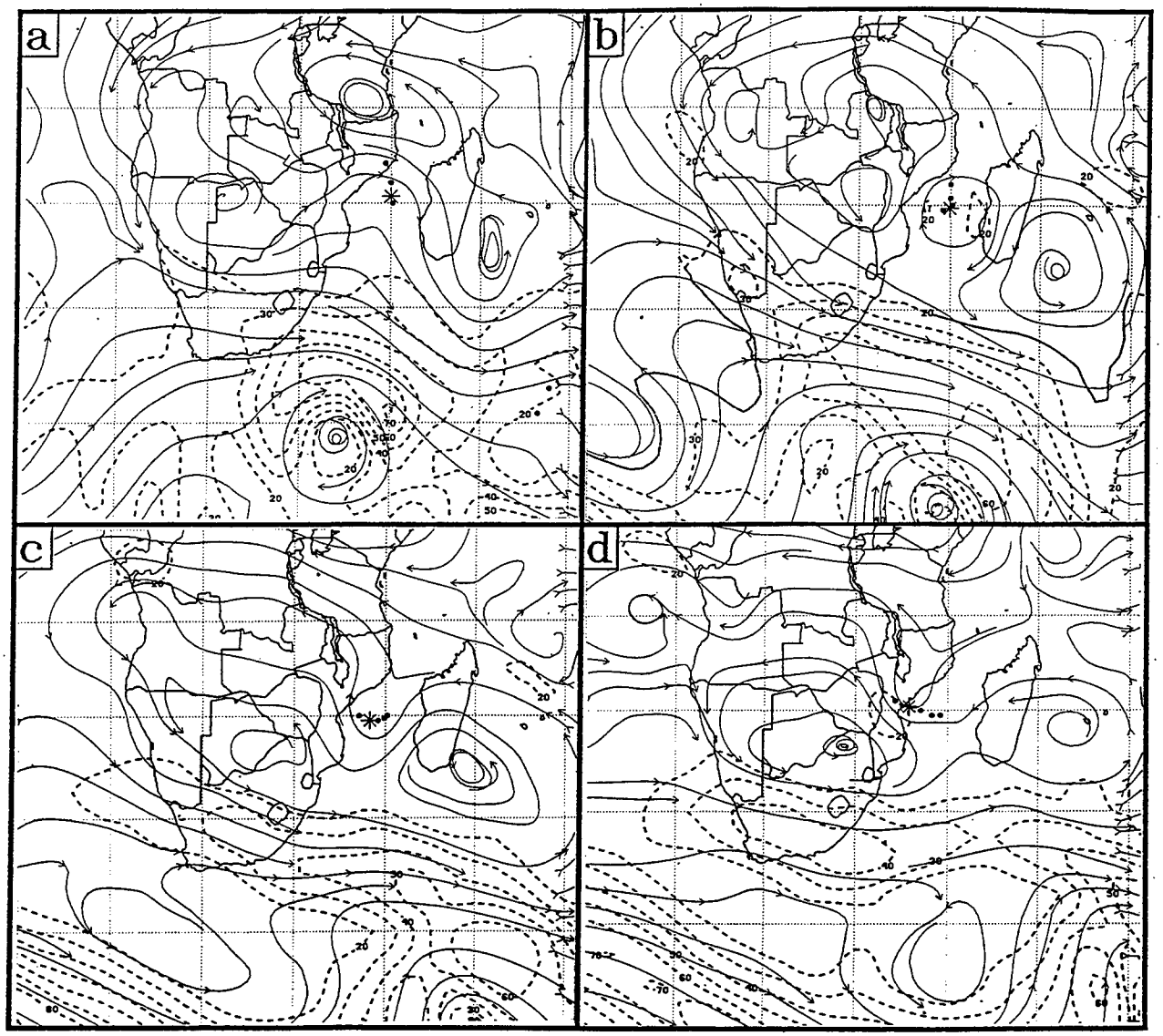

Figure 46. NOGAPS 500-mb analyses as in Fig. 7, except at 00 UTC on (a) 27, (b) 28 February, and (c) 1, and (d) 2 March 1997.

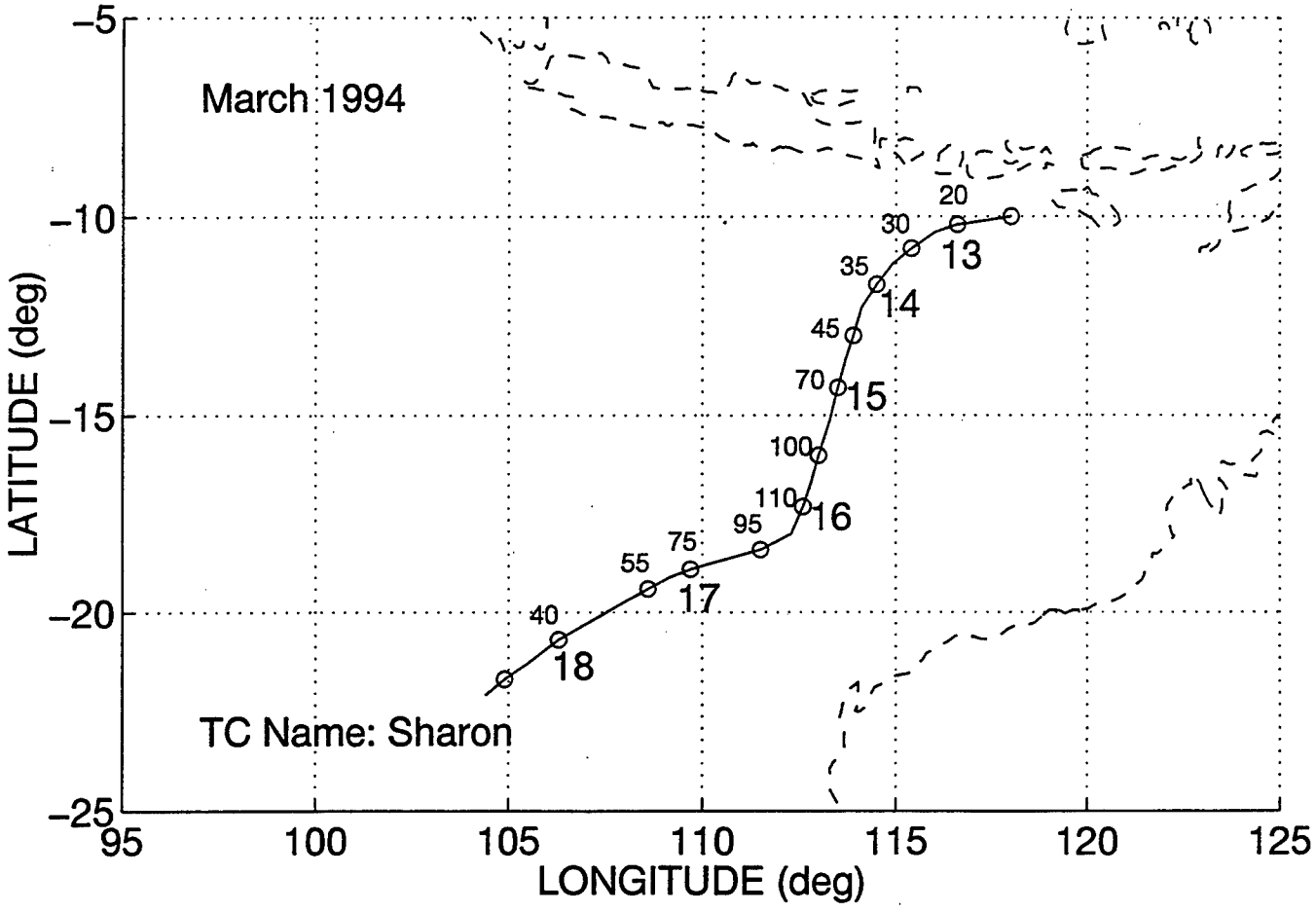

Figure 47. Track as in Fig. 25 of TC Sharon from 12 UTC 12 March 1994 to 12 UTC 18 March with circles each 12 h.

At 00 UTC on 15 and 16 March (Fig. 48a-b), Sharon is tracking strongly poleward (Fig. 47) despite a subtropical anticyclone to the south that slopes from east-southeast to west-northwest. The interpretation here is that Sharon is moving poleward in association with a well-defined, beta-induced anticyclone to the east and north that is generating poleward steering. This steering is consistent with the isotach maximum between Sharon and the peripheral anticyclone to the northeast. By 00 UTC 18 March (Fig. 48d), the subtropical anticyclone poleward of Sharon appears to have been completely eroded. The peripheral anticyclone is still present, albeit weakened. Thus, the environment structure at 500 mb still has a P pattern structure that should continue to drive the TC poleward. Instead, Sharon has turned westward.

A comparison of the NOGAPS 500-mb analyses on 16 and 18 March (Fig. 48b and d) with the corresponding 850-mb analyses (Fig. 49a-b) provides an explanation for the westward track change of Sharon. Notice the south-southwest motion of Sharon at 00 UTC 16 March is more consistent with the steering implied in the 500-mb analysis than in the 850-mb analysis (Fig. 49a), when Sharon is at 110 kt intensity and therefore is a deep circulation for which 500 mb represents a good steering level. By contrast, the southwestward turn of Sharon at 00 UTC 18 March is more consistent with the steering in 850-mb analysis (Fig. 49b) than with the 500-mb analysis. As Sharon is transformed by vertical wind shear into a weaker and shallower circulation, the 850-mb is a better steering level. Visible imagery of Sharon at 0300 UTC on 17 and 19 March (Figs. 50a and b, respectively) confirm the vertical shear explanation. Notice that the low-level circulation of Sharon separates from the convective cloud mass in response to the vertical wind shear that is implied by the cirrus streamers toward the southeast. It is proposed that had Sharon remained a vertically-coupled and deep circulation as it weakened, it would have continued turning poleward and then eastward. In that scenario, landfall would have occurred in the vicinity of the Northwest Cape of Western Australia.

Pending an in-depth evaluation of situation-specific TC forecast model traits in the Southern Hemisphere, it is proposed that vertical wind shear-related S/DR to P/PO transition may be poorly forecast by numerical models. The reasons for this expectation are: (i) the cumulus parameterization schemes presently used in dynamical models may not provide thermodynamic maintenance of the model TC circulation in the same way that actual convective processes maintain real TCs against vertical shear; and (ii) the actual vertical wind shear of the TC environment may not be represented with sufficient accuracy in numerical models to capture the very sensitive response of real TCs. This problem may arise from lack of observations with sufficient vertical resolution to reflect the depth-dependent nature of the vertical wind shear, or from inherent errors in the wind data that are available. As a minimum, the forecaster may ensure accurate nowcasts of the response of the TC to the vertical wind shear event by: (i) being thoroughly familiar with the two possible outcomes (alternate scenarios) of the vertical wind shear situation; (ii) having a dynamically-based understanding of the physical processes involved; (iii) diligently monitoring the structure evolution of the TC via satellite imagery; and (iv) discerning changes in the level at which the TC seems to be steering based on objective analyses.

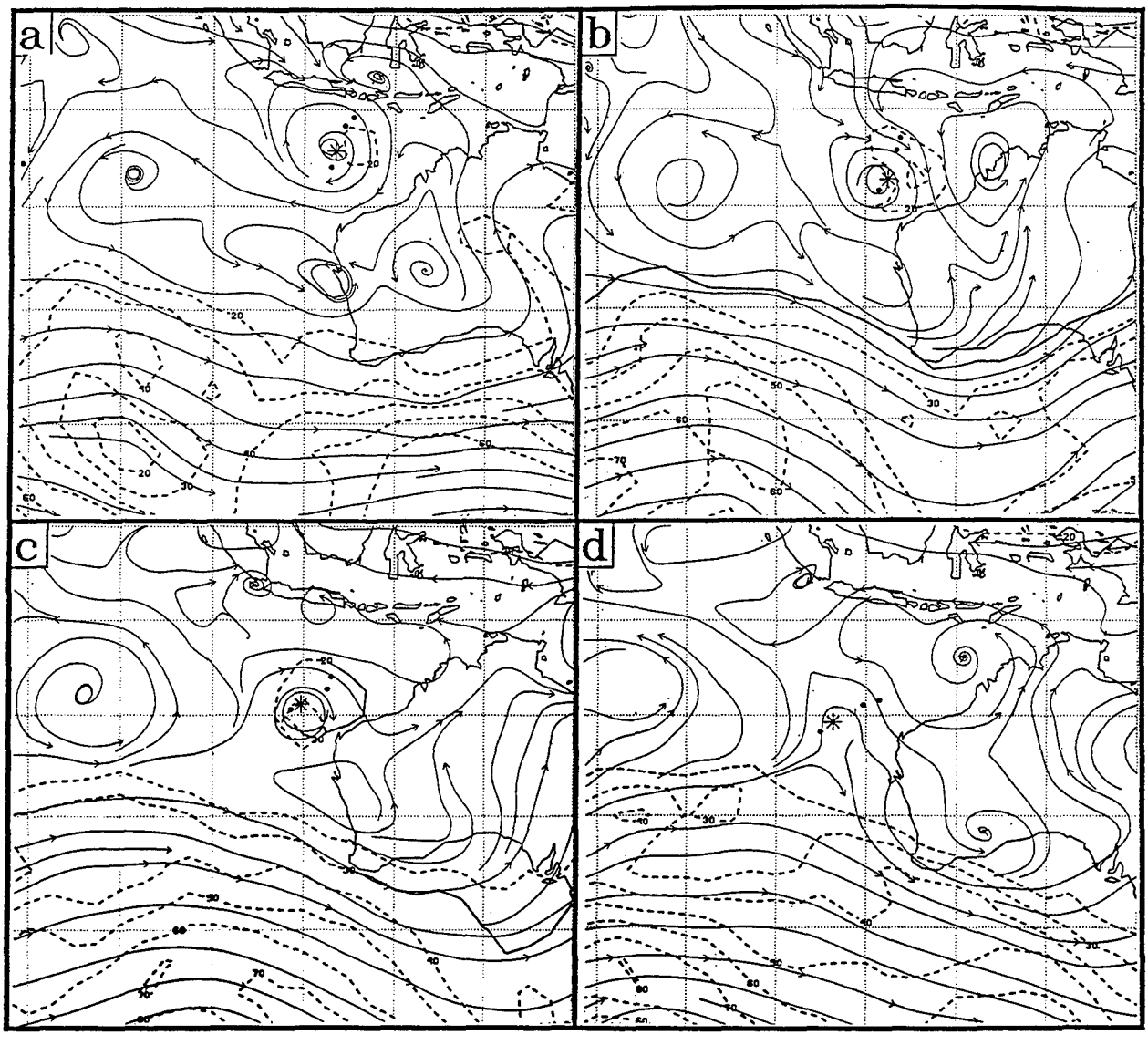

Figure 48. NOGAPS 500-mb analyses as in Fig. 7, except at 00 UTC on (a) 15, (b) 16, (c) 17, and (d) 18 March 1994.

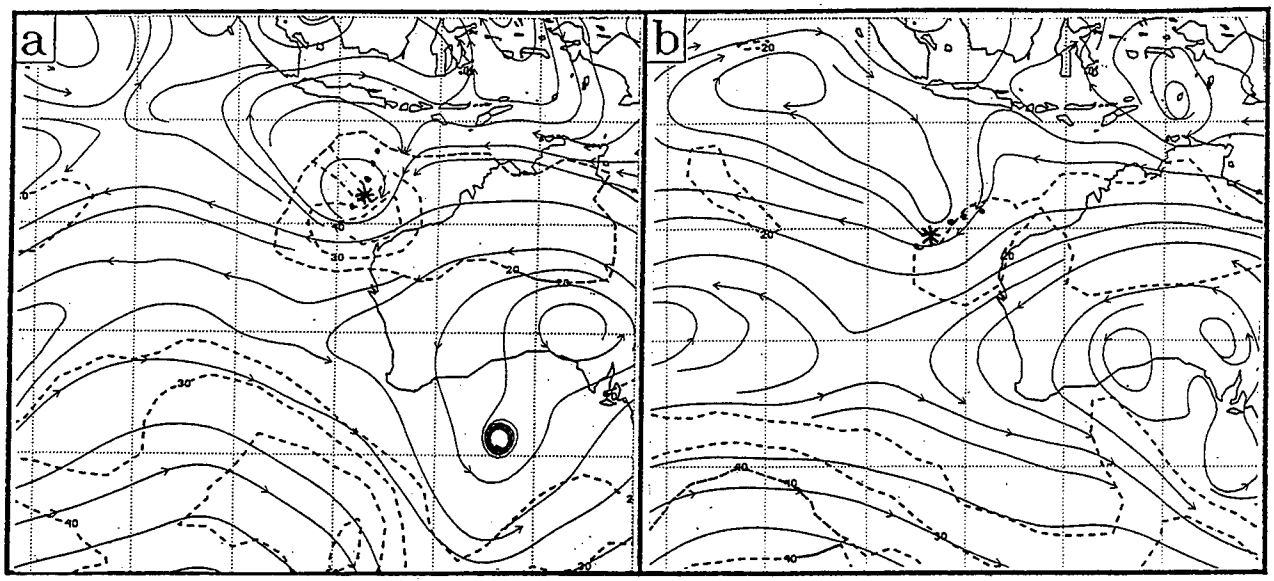

Figure 49. NOGAPS analyses as in Fig. 7, except at 850 mb and at 00 UTC on (a) 16 and (b) 18 March 1994.

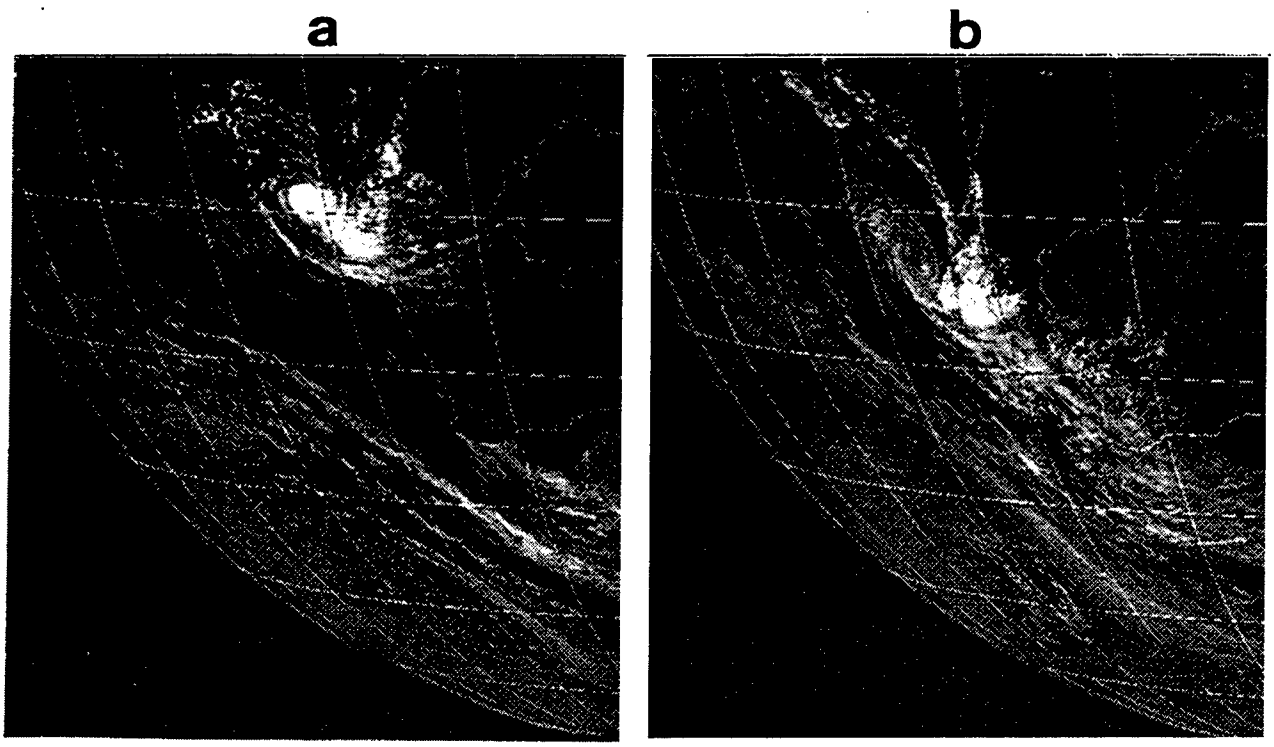

Figure 50 . Infrared imagery of TC Sharon at 0300 UTC on (a) 17 and (b) 19 March 1994.

d. *Transition to/from the H Pattern*

1. TCs Elvina (0997), Nicholas (1097), and Ophelia (1197) case. During 11 to 17 December 1996, TCs Elvina, Nicholas, and Ophelia all underwent a poleward turn from an initially westward direction of motion (Fig. 51a and b). As will be discussed below, in each case the turn resulted from a transition of the environment structure from the S pattern to the H pattern (Fig. 13) as a result of the formation of high-amplitude midlatitude waves.

At 1200 UTC 11 December 1996 (Fig. 52a), TCs Nicholas (east) and Elvina (west) are tracking to the west equatorward of a zonally-oriented, and characteristically thin (for the Southern Hemisphere) subtropical anticyclone. At this time, both TCs are in an S/DR environment. A midlatitude trough to the south-southwest of Nicholas seems to be weakening the subtropical ridge via the SRMT mechanism, which may account for the somewhat more poleward track of Nicholas compared to Elvina. During the subsequent 72-h period (Fig. 52b-d), the persistent influence of a high-amplitude trough/ridge southwest of Australia has transformed the previously thin subtropical ridge into two large, and quasi-circular anticyclones, with the eastern one to the southeast of Elvina, and the other southeast of Nicholas. The presence of these meridional circulations and the more poleward tracks of both TCs is consistent with the H/RP portion of Fig. 13. Thus, the environment structure of each TC has experienced a transition from S/DR to H/RP.

A cursory evaluation of Fig. 52c might tempt the forecaster to conclude that a deep trough has formed west of Nicholas that is consistent with the H/TP portion of Fig. 13. As with the case of Daryl discussed earlier, a single analysis with a deep trough may only be an "apparent" feature comprised of the developed circulation of the third TC Ophelia at about 10°S, 109°E, and an under-representation of the thin subtropical anticyclone directly south of Ophelia. The fact that Ophelia moves slowly westward until 12 UTC 14 December (Fig. 51b) indicates that a weak subtropical anticyclone is still present during this period, and thus that environmental structure of Ophelia is best described as a S/DR pattern/region.

By 00 UTC 15 December (Fig. 53a), the midlatitude trough south of Ophelia and Nicholas has amplified sufficiently to completely break the subtropical anticyclone over an extensive area of the South Indian Ocean west of Australia. Notice that Ophelia has not turned sharply onto a southeastward track, and that Nicholas is also turning southeastward as it makes landfall (Fig. 51b). The appearance of the large-scale environment in Fig. 53a and the motion of the two associated TCs are consistent with the deeper trough portion of Fig. 13, after allowance is made that the axis of the real trough is tilted northwest-southeast. It seems clear that the environment structure of Nicholas has changed from H/RP to H/TP via strong SRMT. Perhaps the environment structure of Ophelia at the equatorial end of the trough may be said to have transitioned from S/DR to H/EW via strong SRMT. An alternate scenario is that the equatorial westerlies have also increased in strength as the midlatitude trough has interacted with the monsoon trough (Fig. 53b). Consequently, the environment structure might also be characterized as S/EW. Whether H/EW or S/EW, the TC motion will be eastward, and the key is

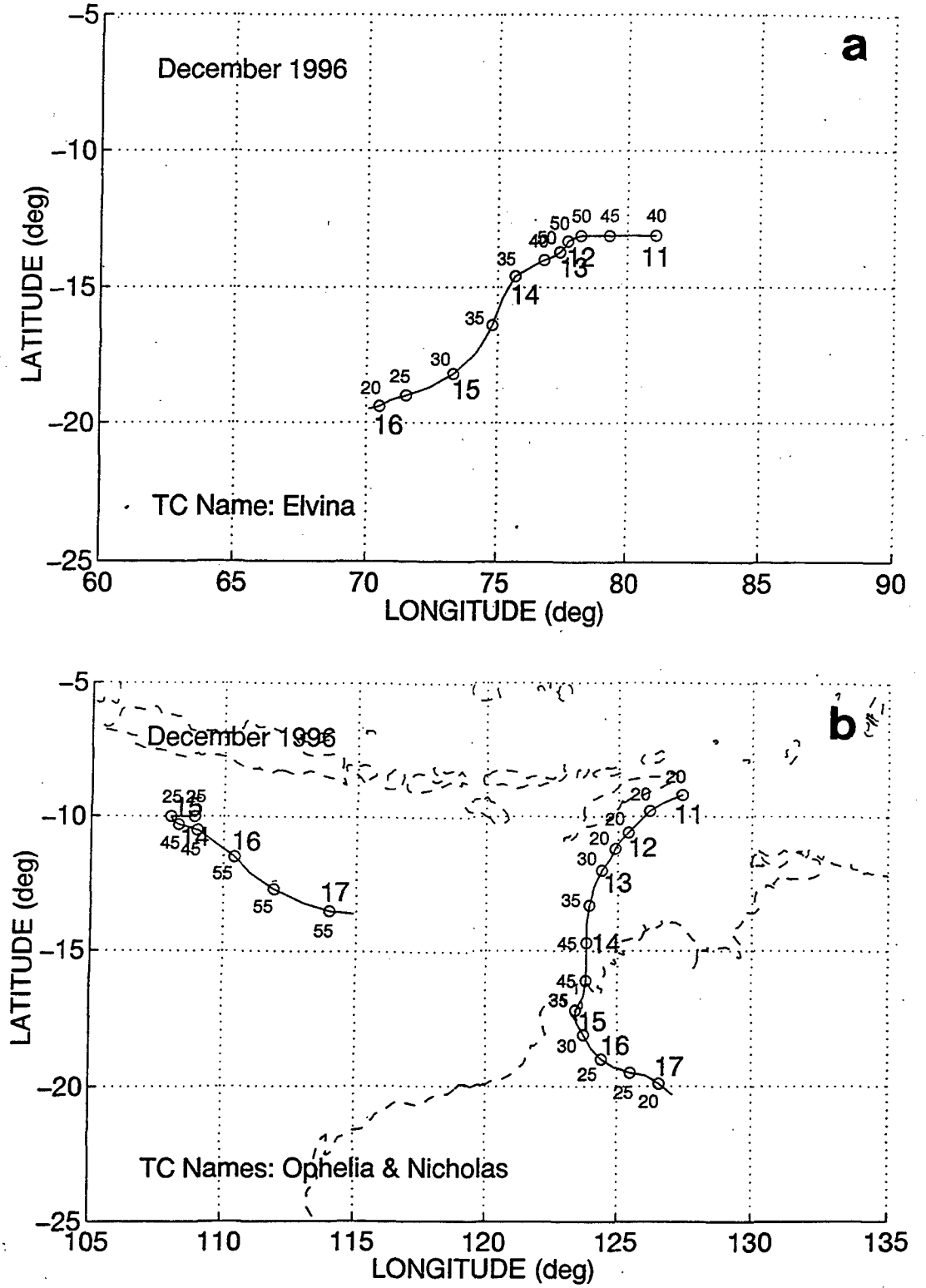

Figure 51. Tracks of (a) TC Elvina from 00 UTC 11 December 1996 to 00 UTC 16 December, and (b) TC Nicholas (eastern) from 00 UTC 11 December to 00 UTC 17 December and Ophelia (western) from 00 UTC 14 to 00 UTC 17 December with circles each 12 h.

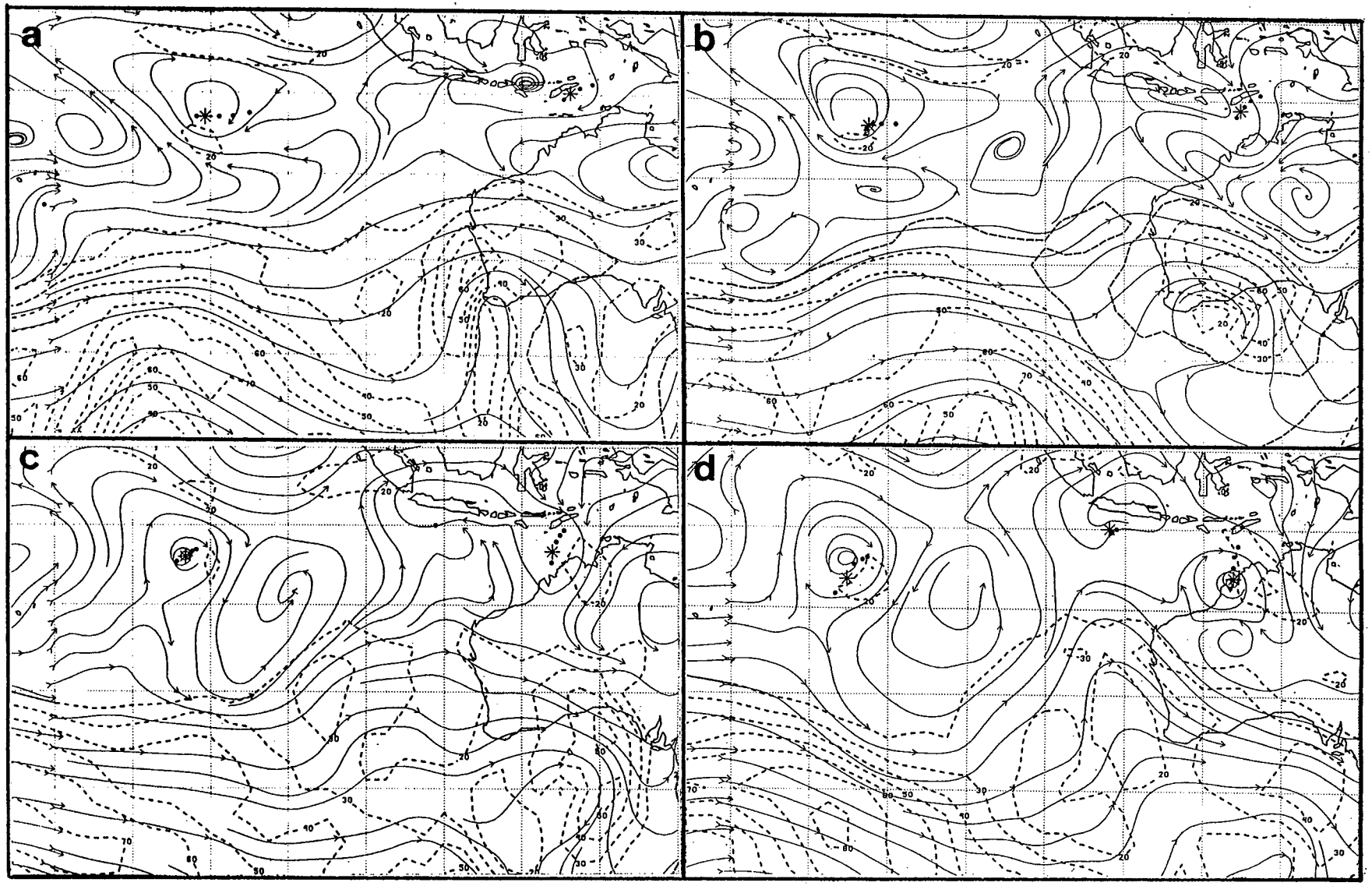

Figure 52. NOGAPS 500-mb analysis as in Fig. 7, except at 12 UTC on (a) 11, (b) 12, (c) 13, and (d) 14 December 1996.

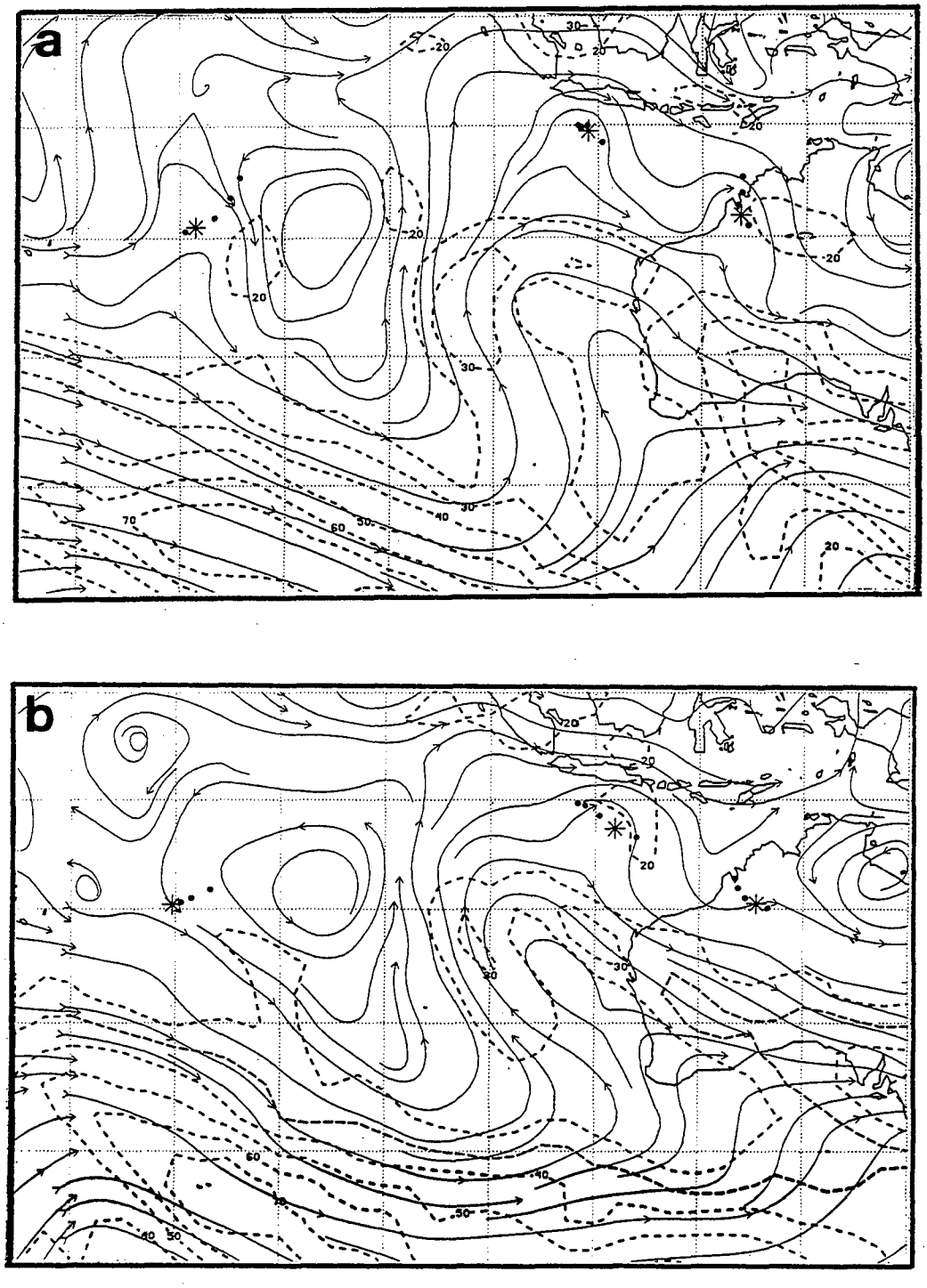

Figure 53. NOGAPS 500-mb analyses as in Fig. 7, except at 12 UTC on (a) 15 and (b) 16 December 1996.

whether the monsoon trough-related or midlatitude trough-related environmental steering is more important. Notice that Ophelia actually intensifies significantly after its turn to the southeast, which indicates an absence of significant vertical wind shear in the vicinity of this very deep midlatitude trough intrusion. As low vertical wind shear is also found in the next case to be discussed, the provisional conclusion is that the equatorial end of very deep midlatitude trough intrusions may be a favorable region for TC intensification.

The environmental steering of Ophelia and Nicholas continues to be similar to the previous day at 12 UTC 26 December (Fig. 53b). However, Elvina is not moving in a west-southwest direction that is inconsistent with the environmental steering implied by the 500-mb level. As with the Sharon case discussed earlier, vertical wind shear has significantly weakened the intensity of Elvina (see Fig. 51a), which is expected to result in a lowering of the effecting steering level. Thus, Elvina is now moving in response to easterly steering at low levels, and its environment structure may be said to have changed from H/RP to S/DR.

It is instructive to note that the transition of Nicholas' environment structure from H/RP to H/TP in conjunction with the deepening of the midlatitude trough may make it seem as if the TC position has jumped from the west portion to the east portion of the H pattern conceptual model (Fig. 13). However, the trough/ridge amplitudes and the positions of the TC in the conceptual model must be adjusted as the environment of the real TC evolves with time. It should not be inferred that a TC has been advected from the RP region to the TP region via the midlatitude westerlies in a persistent H pattern.

2. TC Kelli (3897) case. During 8 to 13 June 1997, TC Kelli initially moved anticyclonically, executed a small cyclonic loop, and then proceeded in a southeastward direction (Fig. 54). Similar to cases discussed above, this case is an example of a transition from the S to H pattern. However, this transition does not result from the *in situ* amplification of a midlatitude trough, but rather is the result of the eastward movement of a midlatitude trough with nearly rather constant amplitude into the vicinity of the TC.

At 12 UTC 8 June (Fig. 55a), Kelli is tracking slowly westward (Fig. 54) equatorward of a zonally oriented thin subtropical anticyclone that is a common characteristic in the Southern Hemisphere. Thus, Kelli is in S/DR pattern/region albeit with very weak easterlies. Notice that a deep trough is present to the west that extends equatorward along the east coast of Australia all the way to the Equator. Over the subsequent five days (Fig. 55c-d), the trough migrates eastward into the vicinity of Kelli, which completely erodes the subtropical ridge. Thus, the direction of the steering flow for Kelli changes from westward to southeastward. Notice the shift of the most prominent isotach near Kelli from south of the TC on 00 UTC 10 June (Fig. 55b) to northeast of the TC at 12 UTC 13 June (Fig. 55d). Thus, the track change of Kelli may be characterized as being due to a transition in environment structure from S/DR to H/TP with perhaps a brief period of H/EW as Kelli undergoes the cyclonic loop. As in the case of Ophelia above, Kelli intensifies significantly (Fig. 54), which indicates that region near the equatorial end of the deep trough has

low vertical wind shear.

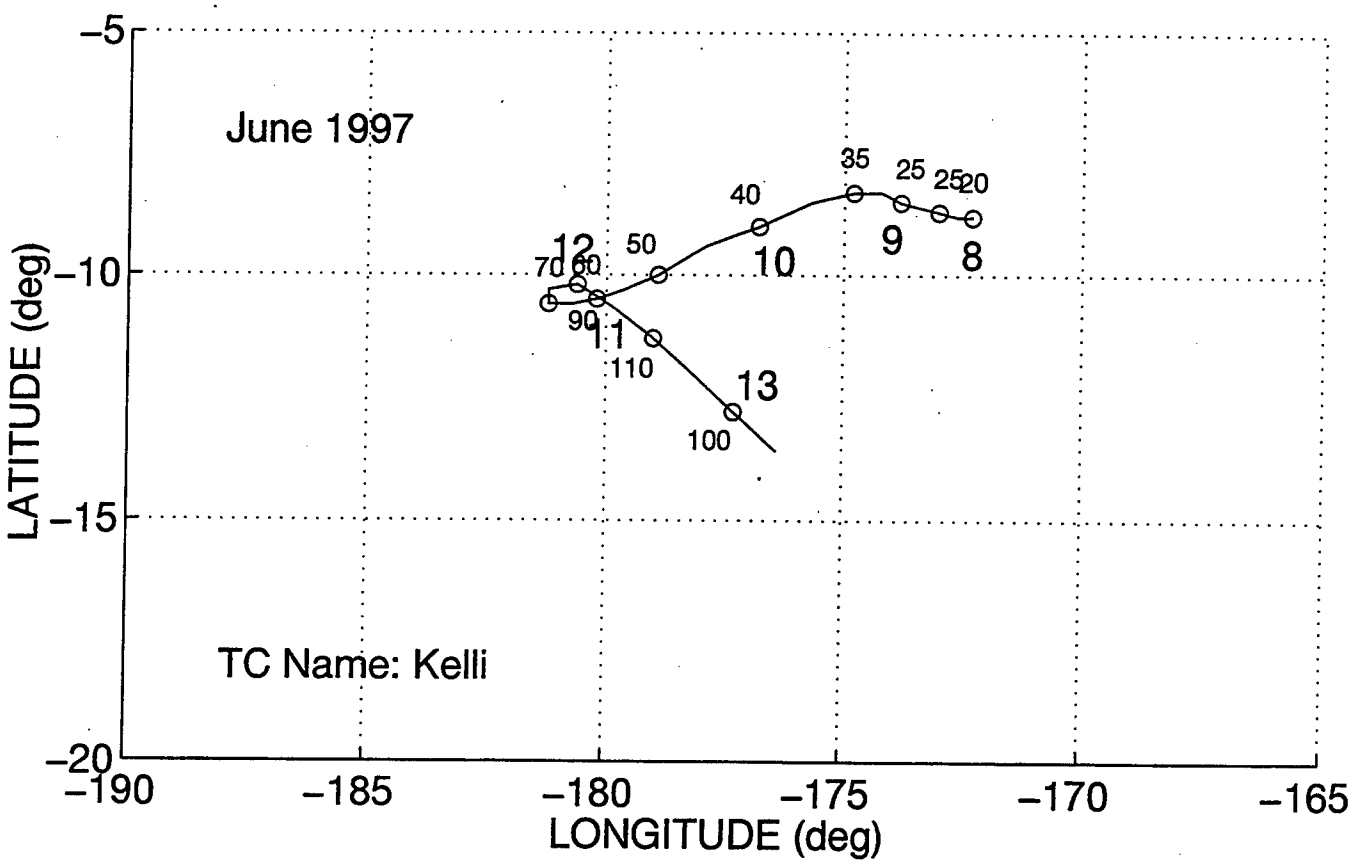

Figure 54. Track of TC Kelli from 00 UTC 8 June 1997 to 00 UTC 13 June with circles each 12 h.

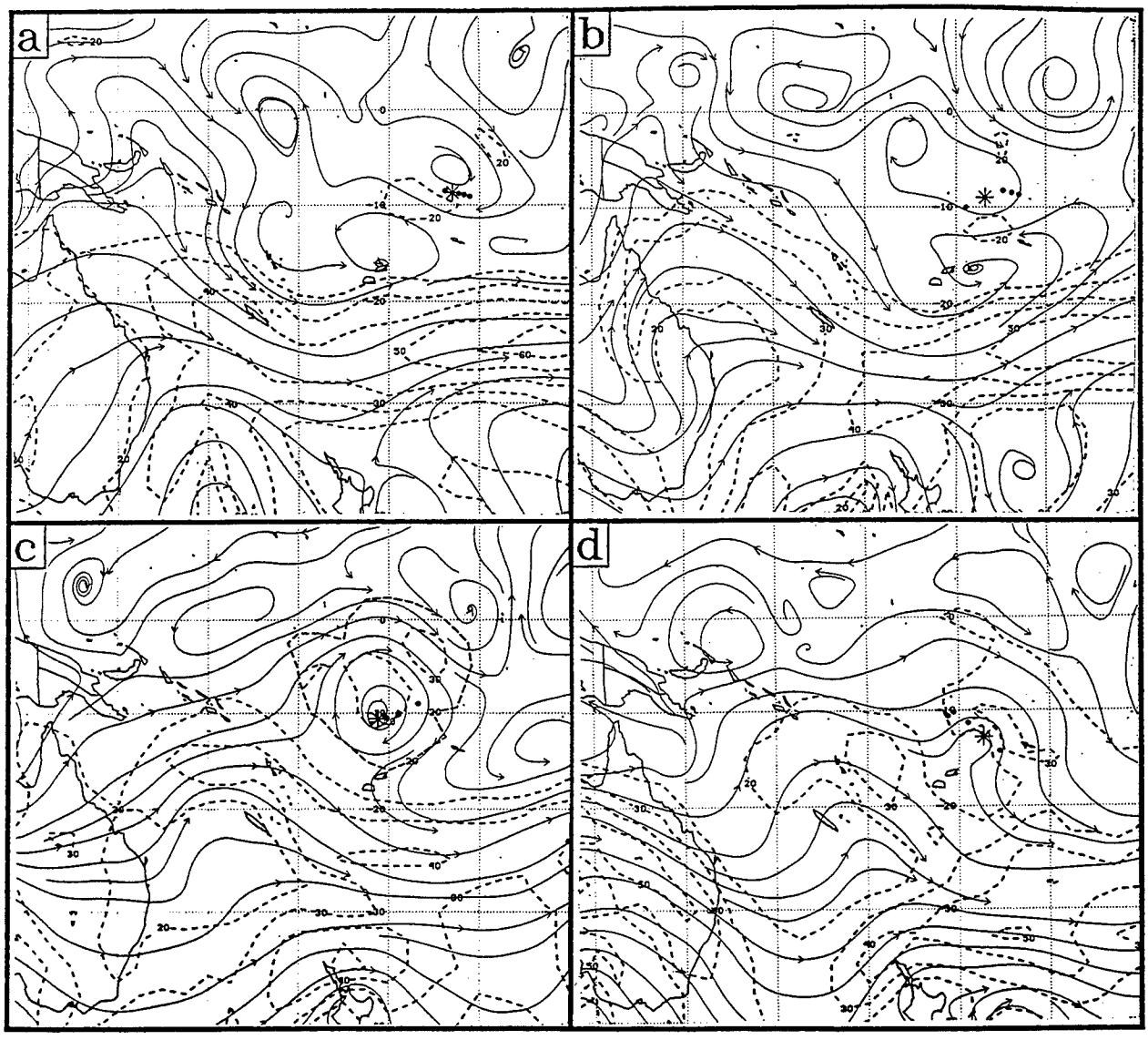

Fig. 55. NOGAPS 500-mb analyses as in Fig. 7, except at (a) 12 UTC 8 June, (b) 00 UTC 10 June, (c) 12 UTC 11 June, and (d) 00 UTC 13 June 1997.

7. CONCLUSIONS

The greatest limitation of the present study is that this meteorological knowledge base is derived from only January 1994 through June 1997. Clearly, the statistics on occurrences and numbers of transitions must be regarded as preliminary. Another limitation has been the absence of satellite imagery west of the GMS coverage. An inherent limitation of any dynamical model analysis such as NOGAPS is the data sparcity in the Southern Hemisphere. Whereas post-season (best track -- in this case from JTWC) tracks have been used here, the real-time tracks will be more noisy. For those slow-moving or weaker TCs, inaccuracies in the fix positions, almost exclusively from satellites, contribute to greater uncertainties in track direction that are important in applying the meteorological knowledge basis of the Systematic Approach.

The most important conclusion is that a limited set of four synoptic patterns with 11 synoptic regions is adequate to describe all 1592 cases during the January 1994-June 1997 period. These synoptic patterns and regions are generally defined in terms of 500-mb analyses -- in this case, the NOGAPS analyses, except in weak storms or vertically sheared cases that have an environmental steering at lower levels. Given the benefit of retrospective analysis, a "storyline" could be developed to explain every case. Development of such a storyline will of course be more difficult in real time. Nevertheless, the environment structure conceptual models of synoptic patterns and regions appear to be useful for the SH forecaster to develop a coherent, time-consistent evaluation of the present scenario. Given an understanding of the physical mechanisms determining the recent past motion can allow a more informed assessment by the forecaster of the model guidance, and especially to assess whether or not the same physical mechanisms will continue to control the motion.

A number of similarities with the original Systematic Approach (Carr and Elsberry 1994) for the western North Pacific are found. One of the more important track changes from westward to poleward associated with the change from Standard (S)/Dominant Ridge (DR) pattern/region to Poleward (P)/Poleward Oriented (PO) pattern/region occurs frequently in the SH. That is, the Ridge Modification by a TC (RMT) transformation initiated by Rossby wave dispersion leads to a peripheral anticyclone to the south and east of the TC in the SH. One difference in this transformation in the SH is that the peripheral anticyclone does not have to have as large amplitude because of the relative weakness of the subtropical anticyclones that are governing the environmental steering in the S/DR pattern/region. Thus, smaller TCs may generate a smaller amplitude anticyclone that will become the dominant steering effect and change the track direction to poleward. One of the interesting features of the P/PO pattern/region is that the TC may be sustained far to the south, presumably because the vertical wind shear is not large. Thus, a significant fraction of the TCs at high latitudes in the SH originate in the P/PO pattern/region.

As described in Section 2e, the three TC interaction modes of Carr *et al.* (1997a) were adapted for the SH as in Fig. 5. Of course, not as many binary TC situations occur in the SH as in the western North Pacific. However, all three TC interactions do occur. Whereas the Direct or Semi-direct TC interactions are less frequent than in the western North Pacific, the number of

Indirect TC interactions per year involving the eastern TC is similar to that in the NH. These ITIE events result in an equatorward steering flow that can result in non-climatological tracks. Although tested with a limited data base, the adaptation of the objective NH criteria for ITIE in the SH appears to be useful. Some false alarms are found, so the forecaster will have to check the actual conditions.

The most important new feature of the adaptation of the Systematic Approach meteorological data base to the SH has been the addition of the High-amplitude (H) synoptic pattern with five associated synoptic regions. The deep intrusions of midlatitude troughs into the tropics is a unique characteristic of the SH upper-tropospheric circulations. In association with meridionally oriented (and often tilted SE-NW) subtropical anticyclone cells, these circulations can affect TC formation and motion. Two synoptic regions of poleward steering flow -- one dominated by the trough (TP), and one dominated by the ridge (RP) circulation, are found in this pattern. In the TP synoptic region, the TC can move rapidly poleward to high latitudes.

A larger number of eastward-moving TCs in low latitudes are found in the SH than were identified in the western North Pacific. This led to introduction of an explicit monsoon trough and an Equatorial Westerlies (EW) synoptic region in the Standard (S) synoptic pattern. Perhaps a surprising aspect of the deep midlatitude trough intrusions is that TCs can form at the equatorward end of the trough, and then move eastward in the EW region of the H pattern.

As mentioned above, the subtropical anticyclone in the South Indian Ocean and western South Pacific Ocean is more mobile, has a smaller meridional extent, and is more transient than in the western North Pacific region. It is not clear whether this is due to large-scale general circulation processes, or is somehow related to the vigorous midlatitude intrusions through the subtropical anticyclone region and deep into the tropics. In addition to the special aspects of the High-amplitude (H) pattern, the relatively weaker subtropical anticyclone and the so-called Dominant Ridge (DR) region is more susceptible to transformation, especially the RMT transformation mentioned above. That is, relatively subtle circulation changes can lead to a change from westward steering flow in the S/DR pattern/region to poleward steering in the P/PO pattern/region. One of the challenges of forecasting in the SH is the deficiency of observations to define these subtle circulation changes.

8. FUTURE WORK

Whereas this test demonstrates the potential applicability of the Systematic Approach meteorological knowledge basis in the Southern Hemisphere, a larger data base is required. Additional cases during the 1989-90 and 1990-91 seasons are available in the NPS archives. However, the procedures for inserting TC synthetic observations in the NOGAPS analyses were not implemented until June 1990 and were still being modified during the 1990-91 season. Although subjective analyses from the Darwin office are available for earlier seasons, they do not cover the entire domain of this study. It is not clear how reliable the subjective 500-mb analyses are given that most of the data for tropical analyses are in either the lower troposphere or in the upper troposphere. The dynamical model-based analyses link these two primary data levels in a way that may not be done consistently by subjective analysts.

Thus, future additions to the data base will probably come from the 1997-98 season and subsequent seasons. An introduction of these conceptual models is planned for JTWC to obtain feedback from the forecasters. An evaluation by the Perth BM office during this season is also anticipated. The McIDas system available in the BM offices provides displays of streamlines and isotachs from the Tropical Analysis Prediction System, which should be comparable to those used in this study.

Given the synoptic pattern/region climatology developed in this study, a number of extensions are possible following the applications developed for the western North Pacific TCs. It is known (Pike and Neumann 1985) that the western South Pacific TCs are the most difficult to forecast of any basin. However, the degree of difficulty has been found to vary with the synoptic pattern/region, each of which has been shown to have characteristic tracks. This characteristic track property has allowed the development of a simple statistical-synoptic track prediction technique for the S/DR and P/PO pattern/regions in the western North Pacific that has skill relative to the operational CLImatology-PERsistence (CLIPER) technique. Such a statistical-synoptic track prediction technique should be successful in the SH as well.

One of the useful benefits of a synoptic pattern/region climatology is to assess the accuracy of the official forecasts and of the guidance tools. Since the JTWC issues forecasts for the entire domain of this study, and an archive of these forecasts and the guidance is available, this extension will be relatively straight-forward. The interpretation of when to use or not use the guidance in different synoptic pattern/region scenarios will be more difficult, but it is a primary objective of the Systematic Approach.

Should the above studies prove favorable, development of an expert system module analogous to that being developed for the western North Pacific region may follow. The objective TC interaction technique described in Sections 2e and 5a is being provided to JTWC for evaluation. This is just one module of an expected system, which is expected to assist forecasters in assessing each scenario, evaluating the track guidance, and providing a more accurate and time-consistent forecast that will improve warnings of SH tropical cyclones.

REFERENCES

Black, P. G., and G. J. Holland, 1995: The boundary layer of tropical cyclone Kerry (1979). *Mon. Wea. Rev.*, **123**, 2007-2028.

Boothe, M. A., 1997: Extension of systematic approach to tropical cyclone track forecasting in the eastern and central Pacific. M. S. Thesis, Naval Postgraduate School, Monterey, CA 93943-5114, (in press).

Boothe, M. A., L. E. Carr, III, and R. L. Elsberry, 1997: Extension of systematic approach to tropical cyclone track forecasting in the Eastern and Central Pacific. *Preprints*, 22nd Conf. Hurr. Trop. Meteor., Amer. Meteor. Soc., Boston, MA 02108.

Carr, L. E., III, and R. L. Elsberry, 1994: Systematic and integrated approach to tropical cyclone track forecasting. Part I. Approach overview and description of meteorological basis. Tech. Rep. NPS-MR-94-002, Naval Postgraduate School, Monterey, CA 93943-5114, 273 pp.

Carr, L. E., III, and R. L. Elsberry, 1995: Monsoonal interactions leading to sudden tropical cyclone track changes. *Mon. Wea. Rev.*, **123**, 265-289.

Carr, L. E., III, and R. L. Elsberry, 1997a: Models of tropical cyclone wind distribution and beta effect propagation for application to tropical cyclone track forecasting. *Mon. Wea. Rev.*, **125**, 3190-3209.

Carr, L. E., III, and R. L. Elsberry, 1997b: Objective diagnosis of binary tropical cyclone interaction for the western North Pacific Basin. *Mon. Wea. Rev.*, (accepted).

Carr, L. E., III, M. A. Boothe, S. R. White, C. S. Kent, and R. L. Elsberry, 1995: Systematic and integrated approach to tropical cyclone track forecasting. Part II. Climatology, reproducibility, and refinement of meteorological knowledge base. Tech. Rep. NPS-MR-95-001, Naval Postgraduate School, Monterey, CA 93943, 96 pp.

Carr, L. E., III, M. A. Boothe, and R. L. Elsberry, 1997a: Observational evidence for alternate modes of track-altering binary tropical cyclone scenarios. *Mon. Wea. Rev.*, **125**, 2094-2111.

Carr, L.E., III, R. L. Elsberry, and M. A. Boothe, 1997b: Condensed and updated version of the systematic approach meteorological knowledge base -- Western North Pacific. Tech. Rep. Naval Postgraduate School (in press).

Kent, C. S. T., 1995: Systematic and integrated approach to tropical cyclone track forecasting in the North Atlantic. M. S. Thesis, Naval Postgraduate School, Monterey, CA 93943, 76 pp.

Pike, A. C., and C. J. Neumann, 1987: The variation of track forecasting difficulty among tropical cyclone basins. *Wea. Forecasting*, **2**, 237-241.

White, S. R., 1995: Systematic and integrated approach to tropical cyclone track forecasting in the eastern and central North Pacific. M. S. Thesis, Naval Postgraduate School, Monterey, CA 93943, 79 pp.

APPENDIX

Annual summaries of the synoptic pattern/region assignments for each storm during January 1994 through June 1997 are provided on the following pages. Each entry in the main part of the table shows the number of synoptic times (0000 and 1200 UTC) that the identified TC was classified as being in each of the particular pattern/region combinations appearing at the top of the table. If at a particular time the environment of the TC was considered to be in a transitional state between two pattern/region combinations, each combination was assigned a value of 0.5. This convention accounts for appearance of non-integer values in the tables. The total number of synoptic times for each TC appears in the far right column labeled DTG. Summary statistics for that year and for the entire four-year database are provided at the bottom of each table.

1993-94		S				P	H				M		
#	STORM	EW	DR	WR	MW	PO	RP	RE	EW	TP	EF	PF	DTG
1S	Alexina												
2S	Bettina												
3S	Cecilia												
4S	Naomi												
5P	Rewa		2	1.5	10.5	8.5		8		5.5	3		39
6S	Oscar		2.5				5.5						8
7P	07P				1.5							1.5	3
8S	Daisy		9.5						2.5				12
9S	Pearl		15.5		1		3.5						20
10S	Edema	0.5	3		2	7.5							13
11P	Sarah		8.5			12.5							21
12S	Quenton		9	2									11
13S	Geralda		18			1							19
14P	Sadie					6							6
15S	Hollanda		10	3	2.5	2.5							18
16S	Ivy		15			11							26
17S	17S		2				6						8
18P	Theodore	1	1						3	6			11
19S	Kelvina					10							10
20S	Litanne		21			5							26
21S	Mariola		20										20
22S	Sharon		5.5			5.5							11
23S	Nadia		14.5		9	0.5							24
24P	Tomas		4.5			6.5				1			12
25P	Usha	2.5				8.5							11
26S	Odille		23	2.5	0.5	7							33
27S	Tim		8										8
28S	Vivienne		11			1.5				3.5			16
29P	29P		2		2								4
30S	Willy		1.5			7.5							9
31													
32													
33													
34													
35													
36													
37													
38													
93-94	REGIONS	4	207	9	29	101	15	8	5.5	16	3	1.5	399
	%	1	51.9	2.3	7.3	25.3	3.8	2	1.4	4	0.8	0.4	100
	PATTERNS		249			101		44.5			4.5		
	%		62.4			25.3		11.2			1.1		
94-97	REGIONS	103	681	73	108.5	353	60.5	21	64.5	95.5	13	19.5	1592
	%	6.5	42.8	4.6	6.8	22.2	3.8	1.3	4.1	6	0.8	1.2	100
	PATTERNS		965.5			353		241.5			32		
	%		60.6			22.2		15.2			2		

1994-95		S				P	H				M		
#	STORM	EW	DR	WR	MW	PO	RP	RE	EW	TP	EF	PF	DTG
1P	Vania		2.5			8.5							11
2S	Albertine		5.5	6.5		10							22
3S	Annette					15							15
4P	04P									4			4
5P	William					4.5				3.5			8
6S	Bentha		3.5			6.5							10
7S	Christelle	1				1							2
8S	Donna		11	6.5			0.5						18
9S	Fodah				1.5	7.5							9
10S	Gail		8			2.5				3.5			14
11S	Heida		7.5									1.5	9
12S	Bobby		4.5		0.5	9							14
13S	Ingrid		4			5							9
14P	Violet												
15P	Warren												
16S	Josta								6				6
17S	Kylie	1.5	2				4			2.5		1	11
18P	18P									2			2
19S	Marlene		5.5	9		4			5.5				24
20S	20S		1.5									2.5	4
21S	Chloe		2.5			7.5							10
22P	Agnes	7	7										14
23													
24													
25													
26													
27													
28													
29													
30													
31													
32													
33													
34													
35													
36													
37													
38													
94-95	REGIONS	9.5	65	22	2	81	4.5		11.5	15.5		5	216
	%	4.4	30.1	10.2	0.9	37.5	2.1		5.3	7.2		2.3	100
	PATTERNS		98.5			81			31.5			5	
	%		45.6			37.5			14.6			2.3	
94-97	REGIONS	103	681	73	108.5	353	60.5	21	64.5	95.5	13	19.5	1592
	%	6.5	42.8	4.6	6.8	22.2	3.8	1.3	4.1	6	0.8	1.2	100
	PATTERNS		965.5			353			241.5			32	
	%		60.6			22.2			15.2			2	

1995-96		S				P	H				M		
#	STORM	EW	DR	WR	MW	PO	RP	RE	EW	TP	EF	PF	DTG
1S	Daryl/Agnielle	2.5	11.5	5									19
2S	Emma	8	7.5						4.5				20
3S	Frank	0.5			2.5	4	4.5			2.5			14
4S	Gertie												
5P	Barry					5.5			2.5				8
6S	Bonita	2	22										24
7S	Hubert/Coryna		9										9
8S	Yasi				5								5
9P	Celeste			2	9								11
10P	Jacob		21.5	0.5		2							24
11S	Isobel		3.5			5.5							9
12S	12S		2	2									4
13P	Dennis	2.5	2.5					4	8				17
14S	Doloresse		7.5			6.5							14
15S	15S		0.5				3			1.5			5
16S	Edwige		6			5.5	2	2			4.5		20
17S	Flossy		3			6						6	15
18S	Kirsty	2	3			5							10
19P	Ethel	5.5	4		4		1.5						15
20P	Zaka					3				2			5
21P	Atu					5.5				2.5			8
22S	Guylianne		5.5			6.5							12
23P	Beti		4	7.5	7.5								19
24S	Hansella		11		3.5		2.5	1					18
25S	Olivia		9			2.5				3.5			15
26S	Itelle		21										21
27S	27S		10.5				2			1.5			14
28S	Jenna	2.5					6			3.5			12
29													
30													
31													
32													
33													
34													
35													
36													
37													
38													
95-96	REGIONS	25.5	164.5	17	31.5	57.5	21.5	7	15	17	4.5	6	367
	%	6.9	44.8	4.6	8.6	15.7	5.9	1.9	4.1	4.6	1.2	1.6	100
	PATTERNS		238.5			57.5		60.5			10.5		
	%		65			15.7		16.5			2.9		
94-97	REGIONS	103	681	73	108.5	353	60.5	21	64.5	95.5	13	19.5	1592
	%	6.5	42.8	4.6	6.8	22.2	3.8	1.3	4.1	6	0.8	1.2	100
	PATTERNS		965.5			353		241.5			32		
	%		60.6			22.2		15.2			2		

1996-97		S				P	H				M		
#	STORM	EW	DR	WR	MW	PO	RP	RE	EW	TP	EF	PF	DTG
1S	Lindsay		0.5	2.5	6								9
2S	02S		1			7		0.5	4.5				13
3S	03S		4										4
4S	Antoinette		15										15
5S	Melanie/Bellamine	1.5	18	3			2			3.5			28
6P	Cyril			1.5	7	6.5							15
7S	Chantelle	1	13										14
8S	Daniella		5	1.5		9.5							16
9S	Elvina		9.5	1.5			4						15
10S	Nicholas						4			2.5		1.5	8
11S	Ophelia	5	14						8				27
12P	Phil	3.5	22.5						4				30
13P	Fergus			2.5		8.5		0.5	3.5				15
14S	Fabriola		7	1									8
15S	Rachel		5.5			12		2.5					20
16P	Drena		7.5			6				5.5			19
17P	Evan					3							3
18S	18S			1.5								5.5	7
19S	Pancho/Helinda	10	27			9							46
20S	Grettelle		16	1.5	1.5	0.5				4.5			24
21S	Iletta		5.5	2		2			5.5				15
22P	22P			1.5	5.5	6							13
23S	Josie	5.5	10			11.5							27
24P	Gillian		2.5			2.5							5
25S	Karlette		17				3			4			24
26P	Harold				3.5	5.5	4						13
27S	27S	5.5	6				2.5		3				17
28P	Ita	1	2										3
29P	29P		1			5				4			10
30S	Lisette		5.5			3.5							9
31P	Gavin	6.5			4	4.5				7			22
32P	Justin	11.5	18.5	2	5.5			2.5			5		45
33P	Hina	4	1.5		4.5	4							14
34P	Ian				4.5	4.5							9
35P	June	9	3										12
36S	Rhonda					2.5			4	8.5			15
37P	37P			3	4								7
38P	Kelli		6.5							7.5			14
96-97	REGIONS	64	244.5	25	46	113.5	19.5	6	32.5	47	5	7	610
	%	10.5	40.1	4.1	7.5	18.6	3.2	1	5.3	7.7	0.8	1.1	100
	PATTERNS		379.5			113.5			105			12	
	%		62.2			18.6			17.2			2	
94-97	REGIONS	103	681	73	108.5	353	60.5	21	64.5	95.5	13	19.5	1592
	%	6.5	42.8	4.6	6.8	22.2	3.8	1.3	4.1	6	0.8	1.2	100
	PATTERNS		965.5			353			241.5			32	
	%		60.6			22.2			15.2			2	

DISTRIBUTION LIST

Space and Naval Warfare Systems Command PMW 185 4301 Pacific Highway San Diego, CA 92110-3127	5
Dr. Carlyle H. Wash, Chairman Department of Meteorology, MR/Wx Naval Postgraduate School 589 Dyer Rd., Room 254 Monterey, CA 93943-5114	1
Dr. Russell L. Elsberry Department of Meteorology, MR/Es Naval Postgraduate School 589 Dyer Rd., Room 254 Monterey, CA 93943-5114	80
Library, Code 0142 Naval Postgraduate School Monterey, CA 93943	2
Dean of Research, Code 09 Naval Postgraduate School Monterey, CA 93943	1
Defense Technical Information Center Cameron Station Alexandria, VA 22304-6145	2